A NOVEL PCR BASED DNA MICROANALYZER SYSTEM FOR DETECTION OF VIRAL GENOME

A Dissertation
presented to the Faculty of the Graduate School
University of Missouri-Columbia

In Partial Fulfillment
of the Requirements for the Degree

Doctor Of Philosophy

---

by

SHANTANU BHATTACHARYA

Dr. Shubhra Gangopadhyay and Dr. Sheila A. Grant, Dissertation Supervisors

AUGUST 2006

The undersigned, appointed by the Dean of Graduate School,
have examined the dissertation entitled

A NOVEL PCR BASED DNA MICROANALYZER SYSTEM FOR DETECTION OF VIRAL GENOME

Presented by Shantanu Bhattacharya

A candidate for the degree of Doctor of Philosophy

And hereby certify that in their opinion it is worthy of acceptance.

Dr. Shubhra Gangopadhyay (Co-Advisor),
Department of Electrical and Computer Engineering

Dr. Sheila A. Grant (Co-Advisor),
Department of Biological Engineering

Dr. Steven B. Kleiboeker,
College of Veterinary Medicine

Dr. Lela K. Riley
College of Veterinary medicine

Dr. Mark Haidekker
Department of Biological Engineering

Dr. Xudong Fan,
Department of Biological Engineering

ACKNOWLEDGEMENTS

This project would not have been possible without the help and guidance of several individuals. I would like to specially acknowledge Dr. Shubhra Gangopadhyay and Dr. Sheila Grant, my dissertation co-advisors for their help, inputs, support and effective guidance at all stages of my research work. I would also like to specially acknowledge Dr. Keshab Gangopadhyay for his constant support, motivation and guidance at all steps of my research. My special thanks to my thesis committee members Dr. Steven Kleiboeker, Dr. Mark Haidekker, Dr. Lela Riley and Dr. Xudong Fan for their constant interaction and valuable suggestions throughout my graduate school at Missouri. I would further like to thank my laboratory seniors Dr. Rajesh Shende, Dr. Maruf Hussain, Dr. Shameem Hassan and Dr. Nripen Chanda (Chemistry Department) their valuable encouragement and guidance. Special acknowledgements to my peers Yuanfang Gao, Venumadhav Korampally, Maslina Othaman, Ravindran Ramasamy, Rosalynn Manor, Steve Apperson and Mike Kraus who have helped me tremendously in my research. I acknowledge the valuable inputs received from Darcy Lichlyter and Sunny Troxell for my project. My special thanks to Deb Gangopadhyay, Damien Von Schoenberg and Paul Koch , high school summer interns, who participated in this project and made some valuable contributions. My special acknowledgements to the graduate school for financially supporting my education by providing me a prestigious Huggins G. Ellsworth fellowship. Finally, I would like to thank my parents who have brought me to this stage of life through their constant support and guidance and have inculcated in me the basic values of life which has helped me to succeed in all my endeavors. I dedicate this dissertation to them.

TABLE OF CONTENTS

ACKNOWLEDGEMENTS----------ii

LIST OF FIGURES----------ix

LIST OF TABLES----------xii

ABSTRACT----------xiii

Chapter1. INTRODUCTION & OBJECTIVES----------1

1.1 Introduction----------1

1.1.1 Hybridization----------3

1.1.2 Polymerase chain reaction----------4

1.1.3 Electrophoresis----------6

1.1.4 Microsystems and micro-fluidics----------9

1.1.5 Processing using photolithography, contact printing and replica molding----12

1.1.6 Wafer level bonding techniques----------14

1.1.6.1 Field assisted bonding----------14

1.1.6.2 Bonding with an intermediate layer----------15

1.1.6.3 Direct Bonding----------15

1.2 Objectives----------17

1.3 PCR assay for testing the devices----------17

1.4 Summary of accomplishments----------18

1.4.1 Use of SOG for multi-level wafer bonding ----------18

1.4.2 Micro-fabricated PCR platform ----------19

1.4.3 Micro-fabricated capillary electrophoresis systems and novel nano-composite materials for sieving matrices ----------23

1.5 References----------25

1.6 Figures----------37

Chapter 2. MECHANICS OF PLASMA EXPOSED SOG (SPIN-ON-GLASS) AND PDMS (POLYDIMETHYLSILOXANE)SURFACES AND THEIR IMPACT ON BOND STRENGTH----------39

2.1 Abstract----------39

2.2 Introduction----------40

2.3 Experimental----------42

2.3.1 Fabrication of blisters in PDMS for bond strength between irreversibly sealed SOG coated wafers and PDMS surfaces----------42

2.3.2 Description of plasma tool----------42

2.3.3 Contact angle measurement----------43

2.3.4 ATR-FTIR characterization of post exposed SOG surface----------43

2.4 Results and discussion----------44

2.4.1 Change of contact angle of SOG surface with time----------44

2.4.2 Correlation between bond strength and surface hydroxyl group----------46

2.4.3 Surface modification studies of SOG----------46

2.4.4 Universal curve for bond strength and contact angle----------47

2.5 Conclusion----------48

2.6 Acknowledgements----------49

2.7 References----------50

2.8 Figures----------53

Chapter 3 OPTIMIZATION OF DESIGN AND FABRICATION PROCESS FOR REALIZATION OF A PDMS-SOG-SILICON DNA AMPLIFICATION CHIP----------58

3.1 Abstract----------58

3.2 Introduction----------59

3.3 Design and optimization----------61

3.3.1 Design of PCR chamber----------61

3.3.2 Design of heaters----------62

3.4 Experimental----------63

3.4.1 Fabrication of the device----------63

3.4.2 Thermal cycling system----------63

3.4.3 PCR reaction----------64

3.5 Results and discussions----------65

3.5.1 Efficiency of serpentine heater design----------65

3.5.2 Surface wettability studies of SOG----------66

3.5.3 Change of contact angle of SOG surface with time----------67

3.5.4 Non-specific binding of DNA to channel and chamber walls (fluorescence studies with labeled DNA)----------68

3.5.5 Polymerase chain reaction using the chip----------69

3.6 Conclusions and future work----------72

3.7 Acknowledgements----------73

3.8 References----------74

3.9 Figures----------79

Chapter 4 HIGH CONDUCTIVITY AGAROSE NANO-PLATINUM COMPOSITE---86

4.1 Abstract----------86

4.2 Introduction----------86

4.3 Experimental----------88

4.3.1 Preparation of platinum colloids via reduction with sodium boro-hydride----88

4.3.2 Preparation of agarose platinum mix----------89

4.3.3 I-V characterization for measurement of conductivity----------89

4.3.4 Characterization of the nano-particles and doped films----------90

4.3.5 DNA mobility studies----------90

4.4 Results----------91

4.4.1 Preparation of the platinum hydrosol----------91

4.4.2 Agarose platinum mix----------91

4.4.3 IV- characteristics----------92

4.4.4 Increased DNA mobility in the new material----------95

4.5 Discussion----------96

4.6 Conclusion----------97

4.7 Acknowledgements----------98

4.8 References----------99

4.9 Figures----------103

Chapter 5 A NOVEL MICRO-FABRICATED CAPILLARY BASE ELECTROPHORESIS SYSTEM----------109

5.1 Abstract----------109

5.2 Introduction----------109

5.3 Experimental----------112
5.3.1 Fabrication of micro-capillaries with PDMS----------112
5.3.2 Capillary electrophoresis in micro-channels----------112
5.3.3 Synthesis of pluronic gels----------113
5.3.4 Fluorescence and absorption studies of different gels----------114
5.4 Results and discussion----------114
5.4.1 Capillary electrophoresis using agarose----------114
5.4.2 Limit of resolution of agarose gels using slab gel electrophoresis----------115
5.4.3 Pluronic gels----------116
5.4.4 Fluorescent and absorption studies of gels----------117
5.4.5 Comparative mobility studies of F127 and agarose gels----------118
5.5 Conclusions----------119
5.6 Acknowledgements----------119
5.7 References----------120
5.8 Figures----------124
Chapter 6 CONCLUSION AND FUTURE DIRECTIONS----------134
6.1 Conclusions and future directions----------134
6.2 Figure----------136
VITA----------137

LIST OF FIGURES

Figure Page

1.1 Basic DNA structure----------37

1.2 Hybridization assay----------37

1.3 Three step polymerase chain reaction process----------38

1.4 Apparatus for anodic bonding of silicon to glass----------38

2.1 (a) Blown-up view of adobe illustrator mask for blister----------53

2.1 (b)Schematic of a blister assembly----------53

2.2 Contact angle photographs of post exposed SOG surface with relaxation time-54

2.3(a) Gaussian fit ATR-FTIR spectra of methyl group for untreated SOG after plasma treatment (immediately after exposure 1hour and 5hours)
(b)Gaussian fit ATR-FTIR spectra of OH absorption band for untreated SOG after plasma treatment
(immediately after exposure, 1 hour and 5hour)----------55

2.4 Total area under Gaussian curve in arbitrary units of CH and OH region for untreated, immediately after treatment, 1hour and 5 hours----------56

2.5 Comparison between SOG and SiO2 surfaces immediately after plasma exposure. (Area under the OH peak for SOG= 27,745 (AU), Area under the OH peak for SiO2= 2045 (AU)----------56

2.6 Universal curve for SOG-PDMS bonding----------57

3.1 (a) Schematic of the Silicon PDMS cassette. (b) Image of a typical device----79

3.2(a) Mask for Platinum heaters. (b) Magnified view of the heaters with description of the boundary condition and X-Y scale----------80

3.3 Temperature distribution with “X” spacing varying from 0-75 microns---------80

3.4 Fabrication process flow chart----------81

3.5 (a) Power MOSFET driven circuit acting as a current controller (b) Real time plot of temperature time data plotted by labview----------82

3.6 (a) Serpentine versus thin film continuous heaters wire bonded to copper connections on the microelectronic packaging (b) Comparison of temperature ramp-up and ramp-down time between continuous thin film heater in a 3mm X 3mm area for 12 cycles----------83

3.7 (a) Reduction in fluorescent intensity with time (b) Background fluorescence of the buffer solution and residual fluorescence left over in the micro-chamber----------84

3.8 (a) Slab gel image for the first on-chip amplification (b) Slab gel image for the second on-chip amplification----------85

3.9 (a) Slab gel image of a 100000:1 dilution of the initial template by amplifying on the chip (b) Slab gel image of an amplified product without template DNA on a test chip after washing off the PCR products from the pervious run----------85

4.1 (a) TEM image of platinum nano-particles----------103

4.1 (b) Particle size distribution----------103

4.2 (a) Array of platinum nano-particles at 10K in agarose matrix and snapshot of a single particle at 60 Kmagnification----------104

4.2 (b) EDS spectra of the platinum nano-particle taken at 30KV accelerating voltage (NoPtCl peak at 2.62 Kev indicating full reduction of chloro-platinate salt)----------104

4.3 TEM image of an agarose membrane doped with platinum nano-particle-----105

4.4 Plot between current density (amp./sq.m.) and electric field (V/m)----------105

4.5 Comparison of dielectric constant of agarose and platinum doped agarose---106

4.6 Absorption spectra of platinized and plain agarose----------106

4.7 Images of fluorescent band in plain and doped agarose take at different for times 200V applied voltage----------107

4.8 Mobility plots for plain and doped agarose----------107

4.9 Image of a 100-1000bp gene marker electrophoresced in a platinum doped agarose gel----------108

5.1 Mask for micro-channel electrophoresis----------124

5.2 Glass PDMS micro-channel structures for capillary electrophoresis----------124

5.3 (a) sample loading from port 1a. (b) port 1a and b pressurized and agarose melt loaded from 2a (c) agarose melt injected from port 2b and sample buried in the room cooling of the microchannel----------125

5.4 Capillary loaded with agarose burying the sample----------125

5.5 Bubbles entrapped in capillaries----------126

5.6 (a) Movement of a 100-1000 bp gene marker captured in an UV detection setup after 25 secs.(b) electrophoresis of gene marker between 45 and 50 secs.(300 V DC is applied)----------126

5.7: Limit of detection of agarose gel using EtBr (10ng of DNA)----------127

5.8 Micelle formation of Pluronic molecules in 1XTBE buffer----------127

5.9 Phase transition curve for F127 molecules----------128

5.10 Mechanical stability of F127 gels. (22% onwards the gel is able to retain its deformation)----------128

5.11 Absorption spectra of EtBr in 1X TAE buffer (absorption peak at 480nm)-129

5.12 Emission peak of EtBr (emission maxima at 620nm)----------129

5.13 Emission acquisition of agarose with EtBr at 480nm excitation (Plateauing observed due to high scattering and background fluorescence)-130

5.14 Absorption spectra of EtBr doped agarose, synergel, sea-plaque and F127 using UV-Vis. Note the high scattering of agarose and its different versions in comparison to F127----------130

5.15 Fluorescence spectra of EtBr in agarose, synergel, sea-plaque and F127----131

5.16 Gel images at times(a)0, (b)15, (c)30, (d)45, (e)60, (f)75, (g)90, (h)105 minutes respectively using F127 as sieving media at an operating voltage of 200V----------132

6.1 Plan view and side elevation of the DNA micro-analyzer----------136

LIST OF TABLES

Table Page

2.1 Contact angle and bond strength data for various chamber pressures, RIE powers and time of exposure values----------57

5.1 Absorption wavelengths of various gel materials----------133

5.2 Mobility calculations in agarose and F127----------133

A NOVEL PCR BASED DNA MICROANALYZER SYSTEM FOR DETECTION OF VIRAL GENOME

Shantanu Bhattacharya

Dr. Shubhra Gangopadhyay, Dr. Sheila A. Grant, Dissertation Supervisors

ABSTRACT

A micro-fluidic assay to quickly analyze microscopic samples of DNA is being developed for field applications. It consists of a micro-PCR chamber, micropumps, and micro-heaters. Additional components of the device include gel electrophoresis micro-channels and solid core waveguide fluorescence collectors. The intended analyzer is a micro-fluidic platform that is principally based on the three-step polymerase chain reaction (PCR) mechanism. It is fabricated using standardized microelectronic fabrication techniques on easily available materials like silicon and poly (dimethyl) siloxane (PDMS) etc. The fluid handling on chip is realized by a set of discreet peristaltic pumps. Currently, a labview code is used to run a proportional, integral, differential (PID) controller for programmed operation of thermal cycling. The micro-pumps, PCR chamber and capillary electrophoresis system have been designed fabricated and tested. For fabrication of the device, a regime has been developed for bonding PDMS surfaces to a variety of substrates (silicon in the present case). The unique heater design formulated for thermal cycling of the PCR micro-chamber has extremely short ramp-up and down times at a low operating power of 6-watts. We have successfully achieved a compression in the cycle time by a factor of ten from the conventional PCR system. Our chip can effectively amplify positive samples with a pico-gram concentration of DNA which is very close to the clinical samples. A novel coating has

been developed on the walls of the micro-chamber which in non-inhibitive to the PCR process. The confirmation of surface dynamics with attenuated total reflection fourier transform infrared spectroscopy (ATR FTIR) has revealed the temporal transition of the coating surface from hydrophilic (immediately after oxygen plasma exposure) to hydrophobic nature. This is indicated by a gradual methylation and dehyroxylation with post exposure relaxation time. Fluorescent studies indicate negligible non-specific binding to our chip which has been a major problem in earlier assays. We have already electrophoresed a 100-1000 bp gene marker using PDMS capillaries filled with agarose. We obtained a time reduction of $1/40^{th}$ from the time of conventional gel electrophoresis. A new gel material with extremely low background and high signal to noise ratio has been developed. We are currently involved in stain detection across capillaries loaded with this novel gel material using optical fibers. The new gel has an additional property of changing phase between gel to liquid and vice versa with temperature and concentration. This will make our test chip reusable. One requirement of the DNA assay posed by its intended field applicability is the need for operating at low powers. One problem with the current capillary electrophoresis systems is the use of extraordinarily high DC voltages for obtaining sample separation. We have achieved electrophoresis at a lower voltage by doping different gel materials with conducting nanoparticles. We have been successfully able to decrease the gel resistivity of agarose by a factor of five using this method. The stain resolution does not get altered due to the dopant and the sample mobility increases two folds at low electric field values (16 V/cm).

The successful development of our lab-on-a-chip device will have several advantages over conventional bench top systems, which primarily include an overall reduction in size,

reduced use of reagents, decreased power requirements, increased speed and accuracy of analysis, and increased portability for field use. We envision this assay as a highly sensitive field deployable analyzer tool with a capability to pick-up trace samples.

Chapter 1

INTRODUCTION AND OBJECTIVES

1.1 Introduction

DNA is, arguably, the most interesting of all molecules. Some of the well known features of this unique molecule are its relatively regular structure consisting of a sequence of four different kinds of nitrogenous bases (Adenine, Guanine, Cytosine and Thymine), its high charge density (negative charge), the intense specificity of base pairing (with hydrogen bonds) and the existence of a biological machinery to duplicate and copy it into RNA [Figure 1.1]. These features have necessitated a strong urge of chemical manipulation of nucleic acids some of which are sequence detection techniques, purification of detected sequences, and sometimes immortalizing them. The analysis of genetic material has been one of the most important facets of molecular biology, health sciences (specially diagnosis of diseases) and forensics. The three major techniques forming the foundation of DNA analysis are Hybridization, Polymerase Chain Reaction (PCR) and Electrophoresis. In hybridization, a specific DNA sequence is used to identify its complement, usually among a complex mixture of components (a technique commonly used for sequence identification) [1]. In PCR and other related amplification schemes, short DNA segments of known sequence are used to prime the synthesis of adjacent DNA where the remaining part of the sequence need not be known in advance. This allows formation of unlimited amounts of any relatively short DNA molecule of interest with bits of known sequences of DNA primers [2]. In electrophoresis, DNA molecules are separated on the basis of molecular sizes by passing them through different

media. It is a basic tool used for DNA sequencing and purifications. Quite often, these three basic techniques are combined to get a complete picture of the DNA such as the electro-phoretic analysis of PCR systems or the use of PCR systems to speed up the rate of subsequent hybridization analysis etc.

DNA technology has advanced tremendously, with some of the most dramatic advances occurring within the past five to ten years. Analysis that used to require large volumes and longer times can be now be performed in pico-liter sized volumes using extremely short durations of time. The fundamental pathway through which all these advances have evolved has been microelectronic fabrication to transport and process extremely small fluidic samples of genetic materials in chip-based architectures [3]. Apart for reducing the times and sample volumes these new techniques also reduce or eliminate external sample contamination. The concept of integrated genetic analysis systems came into limelight with the fabrication of micro-channels capable of conducting liquids for IC or solid-state MEMS [3]. Subsequently, an integrated approach combining heaters, temperature detectors, optical components, active on-chip fluidic control structures such as pumps, valves etc. were realized on a single or multiple chips. The field of integrated gene analysis systems is in active phase of research and continues to expand at a rapid rate [4]. Although a lot of such miniaturizations have been developed and tried, they do not target a full scale integration. For example, PCR- capillary electrophoresis (CE) combination is evaluated by using external excitation and detection [5]. In this combination, a 5 micro-liter PCR sample was amplified within a micro-chamber and was electro-kinetically injected directly into the glass CE micro-channel. Anderson et. al. [6] demonstrated a PCR device integrated with hybridization array technology for DNA and

RNA analysis. This technology involved the used of multiple laminated polycarbonate sheets to form micro-channels, the analysis chamber, and micro-valves. Water et. al. [7] demonstrated a series of glass PCR-CE systems that were capable of thermal cell lysis, amplification of several targets and subsequent separation on a single CE channel. In addition, the same group has presented enzymatic digestion of nucleic acids followed by micro-channel CE. Unfortunately these initial monolithic glass systems required placing the entire device on a thermal cycling block, removing some of the advantages of conducting micro-scale PCR. Burns et. al. [8] has demonstrated individual working parts of a fully integrated DNA analysis system although a fully integrated functionality was not demonstrated [3]. We have envisioned an assay which uses a combination of PCR, CE and optical detection all on a same chip to perform complete gene analysis for detection of gene signatures of different viral genome. We have successfully developed an on-chip thermo-cycler, a capillary electrophoresis system, a set of micro-pumps which utilizes the discreet peristalsis effect and a novel gel material with low scattering and low background fluorescence. We have further doped agarose with conducting nano-particles and demonstrated electrophoresis in thin 225 micron deep capillaries, at low voltages to make it a field applicable assay. We further plan to integrate waveguides and off chip spectrometer to make it a portable complete gene analysis system.

1.1.1 Hybridization

DNA molecules themselves are perfect set of reagents to identify particular DNA sequences. This is because of the strong sequence specific base pairing between complementary DNA strands [9]. Here one strand of the DNA is considered as the

sample and the other is the probe. The analysis of a particular DNA sequence consists in asking whether a probe can find its target in the sample of interest. If the probe does so, a double stranded DNA complex is formed. The process is called hybridization, and information of the sequence can be extracted by this method on the basis of the knowledge of the initial single stranded material [10]. The earliest hybridization experiments were carried out in homogenous solutions [11]. The hybridization was allowed to proceed for a fixed time period and then, a physical separation was performed to capture double stranded material by using columns filled with Hydroxyapatite [9]. The amount of double stranded material could be confirmed by using a radio-isotopic label on the probe or the target [11]. Modern hybridization protocols involve the immobilization of the probe or the target on a solid support mostly by chemical means. The complementary half strand from the sample or the probe that is pre-labeled with a radio-isotope or a fluoro-phore is next flown into the same substrate and allowed to hybridize. The non-hybridized material is washed off and the surface is analyzed by picking up the radio or optical signals [11]. By having a prior knowledge about the sequence on the probe we can get information about the sample (Figure 1.2). An advantage of this method is the enhanced processing speed of the samples.

1.1.2 Polymerase Chain Reaction (PCR)

The PCR has established itself as the foremost sample preparation technology for nucleic acids since its first inception in 1985 [12]. The reaction requires four major components, the template DNA, a thermostable DNA polymerase (TAQ), a set of short oligonucleotide primers specific to known sequences on the template strand and

individual dinucleotide triphosphates of nucleotides (dNTPs) (Adenine, Thymine, Cytosine and Guanine) [13]. As indicated in figure 1.3 the reaction proceeds in repeated cycles of three temperatures. The first temperature, from 94-96 deg. C, separates and denatures the two template strands, the second temperature, typically 45-60 deg. C hybridize the primers to the complementary sequences on the parent strand and the third temperature step of 72 deg. C activates the DNA polymerase which forms daughter strands, extending the primer sequences by adding individual di-nucleotides from the solution thus building the whole sequence. This three temperature process is used to double the template strand every cycle and with optimal efficiency may be able to produce 2^n copies in n such thermal cycles. The optimal efficiency is achieved at smaller values of 'n'. However the efficiency of the reaction decreases with the increasing number of cycles. The reaction can be described in terms of concentration of DNA molecules as a function of the number of cycles completed:

$$[DNA]_{final} = [\prod_{i=1}^{n}(1+\varepsilon_i)][DNA]_{initial_i} \qquad (1)$$

At lower values of i the efficiency 'ε' of the reaction is 1; but, at higher values of 'i', it decreases as the participating components like primers and di-nucleotides are consumed towards the end of the reaction [3]. The careful control of temperatures and initial reactant concentrations are necessary to maximize reaction yield and minimize the number of required cycles. The PCR exhibits several notable advantages over competing techniques, including exponential amplification, relatively few reagents, and a simple reaction scheme involving minimal participating reagents. There are several variants of PCR which enhance its utility and broadens the scope of its applications. Some of the

widely used variants include reverse transciptase PCR, multiplexed PCR, real time PCR etc. The reverse transcriptase PCR starts with the generation of the c-DNA (complementary DNA) for the corresponding RNA of interest, thereby running the amplification protocol with the c-DNA templates [14]. The multiplex PCR is a process where the multiple DNA templates may be amplified together in the same reaction using multiple primers. In cases where the melting temperatures of different primers within a multiple reaction prevent successful amplification using a single annealing temperature, step- down PCR is used where a series of successively lower annealing temperatures allow hybridization of the widely varying primer sets to multiple templates [15]. Another widely used protocol is the real time PCR which gives an immediate snap-shot of the reaction [16]. This can be performed in two ways. In the first method , an intercalating fluorescent dye present in the reaction mixture labels the amplified DNA as the reaction proceeds. In the second method, a dual labeled fluorescence detection complementary probe is included in the reaction mixture which hybridizes to the amplified product [16]. The probe has a fluorescent dye at one end and a quencher molecule at the other end. During the extension step the probe is cleaved by the polymerase thus enhancing the fluorescence level.

1.1.3 Electrophoresis

The electrophoresis is a separation technique based essentially on differences in net charge and mass shape and is widely used for the resolution of a mixture of biological molecules such as peptides, proteins and nucleic acids [17]. The addition of a mixture of analytes in a narrow zone at a certain distance from the electrodes greatly improves

separation. The electrophoresis in most biochemical laboratories is carried out using a supporting media such as agarose, polyacrylamide, starch, cellulose acetate, paper etc. These media being porous tend to protect the bands from diffusion and also act as molecular sieves [3]. The electrophoresis has also been carried out in free buffer solution filled capillaries; but, it is not a powerful technique because of band broadening due to heating effects and diffusion of the molecules. The key parameter measured in electrophoresis using gel matrices is the sample mobility μ. This is the velocity per unit electric field . In one dimension,

$$\mu = \frac{v}{E} \qquad (2)$$

where v is the velocity measured in cm/sec and E is the electric field measured in volts/ cm. The double stranded DNA behaves in free solution electrophoresis as a free draining coil. This means that each segment of the chain is able to interact with the solvent in a manner essentially independent from any of the others. The frictional coefficient of the molecule, f, as felt by the coil (sample) as it moves through the fluid is proportional to the length of the coil, L.

$$f = \alpha_1 L \qquad (3)$$

The DNA has a constant charge per unit length. There is one negative charge for each phosphate ; a significant fraction of this charges is effectively screened by bound counter-ions; but, the net result is still a charge Z proportional to length L:

$$Z = \alpha_2 L \qquad (4)$$

The net steady state velocity in electrophoresis is the result of equal, opposite electrostatic forces accelerating the molecule, ZE, and frictional forces, fv retarding the motion. Thus in free solution electrophoresis:

$$ZE = fv\,. \qquad (5)$$

Therefore,

$$v = \frac{\alpha_2}{\alpha_1} E\,. \qquad (6)$$

In other words the velocity of the DNA molecule or its mobility in free solution electrophoresis is size independent. Some other common problems associated with free solution electrophoresis are convective instabilities. The placement of an electric field across a conductive solution leads to significant current flow and heating. This heating produces non-uniformities in temperature, and convective solvent motion will result from the non-uniformities. The presence of bands of dissolved solute molecules leads to regions with local bulk density differences. These dense zones are gravitationally unstable. If electrophoresis is carried out vertically, the dense zone can simply fall through the solution. In horizontal electrophoresis, any local fluctuations of temperature leads to zone collapse. The presence of gel matrices in the electrophoresis of DNA molecules provides band stability by enhancing the mechanical strength and enhances the ability of size based separation. In typical gel electrophoresis the entire sample is continuous gel matrix and all molecules move directly through this matrix. Generally, the gel matrices used have a very wide range of pore sizes. As a result relatively small molecules can move through almost all pores. They experience the gel matrix as an open network, and they can take relatively straight paths under the influence of electric field.

In contrast, large molecules can pass through only a restricted subset of the gel pores and they have to take longer paths in order to find these correct sized pores. This means that the small molecules will move faster than the large molecules thus providing a size based separation of the DNA molecules.

1.1.4 Microsystems and Micro-fluidics

Microsystems, "literally, mean 'very small systems' or 'systems made of very small components.' They do something interesting and useful. The name implies no specific way of building them and no requirement that they contain any particular type of functionality. The name Micro-electromechanical systems (MEMS), on the other hand, takes a position: Micro , establishes a dimensional scale, electro suggests either electricity or electronics (or both), Mechanical suggests moving parts of some kind. Although the name MEMS suggests limited domains of work but still the concept of MEMS has outgrown to encompass many other types of small things, including thermal, magnetic, fluidic, chemical, biological, and optical devices and systems, not necessarily with moving (Mechanical) parts [18]. Thus Microsystems engineering is highly multidisciplinary and involves the manufacturing, testing and packaging of MEMS equipments. Regular Applications of Microsystems in the aerospace, automotive, biotechnology, consumer products, defense, environmental protection and safety, healthcare, pharmaceuticals and telecommunications industry has created a niche for micro-systems in the society and has led to a growing demand for the innovation and integration of MEMS and micro-system technology.

From the last decade the focus in micro-systems research has begun to shift to fluidic systems [19]. The development of micro-flow sensors, micro-pumps, and micro-valves dominated the early stage of micro-fluidics research in the late 1980's. The field started developing rapidly in other areas, since the introduction by Manz et al. at the 5th international conference on solid state sensors and actuators (transducers '89) which indicated that life sciences and chemistry are the main application fields of micro-fluidics [20]. Micro-fluidics has grown since then into a research discipline dealing with the transport phenomena in fluid based devices at the microscopic length scale. The main advantage of this discipline is utilizing the scaling laws for new effects and better performance. The advantages are mainly twin-fold, viz., the microscopic fluid volumes that these devices can handle and the flexibility of having a large or small sized surrounding instrumentation with a miniaturization of the space, which handles the fluids. The field of micro-fluidics is also equally multidisciplinary as compared to Microsystems technology with the engineers exercising their enabling micro-technologies and analytical chemists, biochemists etc. taking advantage of the new effects and better performance of these technologies. They are interested primarily in shrinking down the flow channels of chemicals to microns/ submicron size. Current focus in developing micro-fluidic research can be broadly categorized as

1. Application driven development of devices
2. Development of new, reliable and economical fabrication technology for these devices.

Both these aspects have a chorological phasing of research. The device development aspect began with work on a number of silicon micro-valves, pumps and flow sensors

(1980s thru mid 1990s). This phase had certain limitations. If we consider uniformity of energy density at all scales then, at the micro scale owing to the extremely less volumes, the energy given out by these devices is extremely small. Also, the surface to volume ratio being length (microns) inverse, the surface area automatically becomes huge in comparison to the volume. Large surface area means large viscous forces, which in turn require a large actuation level, which is normally provided by external sources. The second phase (mid 1990s onward) concentrated on non-mechanical actuation schemes such as electro-kinetic flows, surface tension driven flows, electromagnetic forces and acoustic streaming effects. This phase has led into the gradual shift of micro-fluidic applications from conventional field such as flow control, Chemical analysis, biomedical diagnostics, and drug discovery to newer applications such as distributed energy supply, thermal management and chemical production.

The second aspect in micro-fluidic research is developing a suitable fabrication process. Similar to the prior aspect this technology development also had a paradigm shift from development of micro-fluidic devices with integrated sensors and actuators made in silicon using surface and bulk micro machining techniques (up to mid 1990s) to plastic micromachining and use of photolithography, contact printing and replica molding processes on an extremely biocompatible material called Poly (dimethyl) Siloxane (hence forth called PDMS), which is a kind of silicon rubber. A problem faced worldwide in such micro-fabrication process is the absence of a well-defined study of the bonding strength between the various layers used to make these devices. Although, most of the research papers mention the Oxygen Plasma activation of participating surfaces leading to strong chemical (Silanol) bonds between them [21,22], yet these papers only define a

certain set of parameters, which are specific to their plasma generating setup and not valid in general [23,24]. With these newer and easier fabrication techniques being widely used in the laboratory and industry level, an important requirement of all the micro fluidics/ biosensors research and industry is the development of a general regime, which defines a systematic method of gauging the bond strength between the participating surfaces. This enhances the reliability of the devices and also gives a structured approach to its future large-scale manufacturing.

1.1.5 Processing using Photolithography, Contact Printing and Replica Molding

Photolithography invented in 1959 is the most successful technology in micro-fabrication [25]. It can be called the workhorse of MEMS and semiconductor industry. The photolithographic techniques currently used for manufacturing microelectronic structures are based on a projection-printing system (usually called a stepper) in which the image printed on a transparency is projected onto a thin film of photoresist (spin-coated on a wafer) through a high numerical aperture lens system. The resolution R of the stepper is subject to the limitations set by optical diffraction according to the Rayleigh criterion given by

$$R = k1.\lambda/NA \qquad (7)$$

Where λ is the wavelength of the illuminating light, NA the numerical aperture of the lens system, and k1 a constant that depends on the photoresist's ability to distinguish between changes in intensity of exposure. (typically K1 is of the order of .75) [26]. The minimum feature size that can be obtained practically is approximately the wavelength (λ) of the light used. As a result, illuminating sources with shorter wavelengths are

progressively introduced into photolithography to generate structures with smaller feature sizes [27] As structures become increasingly small, the level of complexity and cost involved in producing them goes up. Contact printing is an efficient method for pattern transfer. A conformal contact between the stamp and the surface of the substrate is the key to its success. Printing has the advantage of simplicity and convenience. Once the stamp is available, multiple copies of the pattern can be produced. Printing is an additive process; the waste of material is minimized. Printing also has the potential to be used for patterning large areas.

Replica molding duplicates the information–for example, the shape, the texture, and the structure–present in a master. It accommodates a wider range of materials than does photolithography and allows duplication of three-dimensional structures in a single step. It is used for the mass production of diffraction gratings, compact disks, microtools etc. Replica molding with an appropriate material enables highly complex structures in the master to be faithfully duplicated into multiple copies with nanometer resolution. [28] The weakness of replica molding processes come from Van der waals interactions, wetting, and kinetic factors such as filling of the mold [29, 30]. After the pattern transfer process using the above techniques, the devices are given shape by stacking different layers above each other. By this technique enclosed chambers and fluidic channels can be made between various substrates using a variety of different wafer level bonding techniques.

1.1.6 Wafer Level Bonding Techniques

Wafer bonding is used to join two or more layers of any MEMS device.

There are three main categories of wafer bonding techniques.

- Field assisted bonding
- Bonding with an intermediate layer
- Direct bonding

1.1.6.1 Field Assisted Bonding

This method is used to bond certain types of glasses to conductors using an electric field and high temperature. The mechanism involved in this process is enhancement of ionic mobility of sodium ions in the glass. Pyrex-7740, [31] having a coefficient of thermal expansion nearly same as Silicon is widely used in this type of bonding. A piece of amorphous silicon deposited Boro-float glass is kept over an equally cleaned piece of Pyrex wafer in an apparatus shown by the schematic as in figure 1.4.

The apparatus consists of a hot plate on which the specimens to be bonded are heated to temperatures between 300-500^{o}C and a DC power supply which is connected in such a way that the silicon is positively biased with respect to glass. An ammeter is connected in series to measure the current during bonding and monitor the progression of bonding. A thermocouple attached to the hot chuck reads the temperature and displays it during bonding or anytime when the system is switched on. Usually bonding temperature of 350-400^{o}C and 1-1.2 kV for 3 hr is used for this kind of bonding.

On applying voltage across the stack the positive Na^{+} migrate from the lower glass surface towards cathode creating a net negative charge on its surface and the O^{-2} migrates

from the (less than 20 nm thick) [32] oxide layer on amorphous silicon surface towards the anode thus developing a net positive charge on its surface and also oxidizing the silicon atoms in this process. This creates a depletion region in-between the layers, which results in the formation of a strong field between amorphous silicon layer and the lower glass layer leading to fusion of oxidized silicon into the structure of glass. [33] The fusion results from the ambient temperature and field. The current is measured across the circuit and the drop in the current value to zero marks the completion of the bonding process.

1.1.6.2 Bonding with an Intermediate Layer

This technique is also called adhesive bonding and uses an intermediate layer to glue the surfaces together. Based on what type of material is to be bonded the glue can be glass, epoxies, photoresist or other polymers.

A thin intermediate glass layer is very often used for bonding silicon wafers thermally. This layer of glass can be sprayed, screen-printed or sputtered on substrate. Epoxies such as PDMS and SU-8 (UV curable negative photoresist) can be used as intermediate layers in micro-fluidic devices. The main advantages are the low process temperature and versatility of use of all different kind of substrate.

1.1.6.3 Direct Bonding

This category of bonding involves the bonding of two substrates of same material to one another. A variety of substrates like glass, silicon, polymers, ceramics and metals can be bonded to each other directly. In case of Silicon the first step is the cleaning and hydration of the surfaces to be bonded. They must be smooth and free of contaminants

completely. Contaminant particles create gaps, which cause the bonding failure locally. After thorough cleaning of the surfaces to be bonded they are brought into contact with each other thus causing the Hydrogen bonds to develop in-between them, which provides a modest degree of adhesion. This contacted pair is next placed into a high temperature oven such that the two layers fuse into one another [34].

In case of glass, direct bonding is achieved by post cleaning heating of the two surfaces of soda-lime glass containing SiO_2, Na_2O, CaO, MgO and a small amount of Al_2O_3. The glass wafers are cleaned in an ultrasonic bath using water, hydrogen peroxide (25%) and ammonia (25%)[35]. Heating of the annealed and dehydrated wafers is done by heating the assembly together at 600 degrees centigrade for 6 to 8 hours.

There are many polymers that can be normally bonded at temperatures above their glass transition temperature. Some polymers with low surface energy as PDMS can be bonded to itself and to glass after a surface activation with oxygen plasma. The mechanism of bonding in this involves the oxidation of the surface layer, which increases the concentration of hydroxyl groups, and this leads to the formation of strong intermolecular bonds. As bonds formed by this method is irreversible, it is commonly used in micro-fabrication of fluidic devices. Although PDMS can be bonded to itself or another glass piece by using oxygen plasma, it cannot be integrated with other surfaces particularly metals and ceramics. Such a bonding regime would be particularly useful to micro-scale heat transfer problems and also for other applications like outdoor insulation etc. We have used a novel polymer material spin-on-glass (SOG) for integrating PDMS to these other substrates particularly silicon and silicon dioxide which are widely used for micro-fabrication purposes.

1.2 Objectives

The following are the objectives of our study:

1. Develop a good fabrication methodology for realizing the DNA analyzer on a chip,
2. Develop a working prototype of an on-chip PCR reactor,
3. Develop a low voltage working capillary electrophoresis platform,
4. Develop a clean gel system and integrate the on chip capillary with a set of parallel waveguides/ optical fibers for realizing a micro-total-analytical system capable of picking up trace isolates of DNA.

1.3 PCR Assay for Testing the Device

We used Infectious Bovine Rhinotracheitis (IBR) virus as the test assay for our on-chip studies. We used this test assay for testing on-chip amplification, on-chip capillary electrophoresis and the investigation of the conducting gel composite. Two important reasons for this choice are: a long thermal cycling time which evaluates the reliability of our device and a strong fluorescence response of the viral genome in any standard laboratory gel or capillary setup providing the replicability of detection of amplification [36]. The IBR virus was originally recognized as a respiratory disease of feeder cattle in the western United States during the early 1950s [37]. The IBR virus can persist in a clinically recovered animal for years as it remains inactive and "hidden" following an infection and is thought to be re-activated by stresses applied to the animal. The virus that causes IBR is capable of attacking many different tissues in the body and, therefore, is capable of producing a variety of clinical disease forms depending on the infected tissue.

The clinical diseases caused by the IBR virus can be grouped as (1) respiratory tract infections, (2) eye infections, (3) abortions, (4) genital infections, (5) brain infections, and (6) a generalized infection of newborn calves [38].

1.4 Summary of Accomplishments

1.4.1 Use of SOG for Multi Level Wafer Bonding (Chapter 2)

In this work we have investigated and developed a clean bonding protocol of PDMS with a variety of surfaces with different surface chemistry using Oxygen Plasma and an intermediate Spin on Glass (Methyl silsesquioxane) (MSSQ) layer making PDMS irreversibly sealed to oxidized silicon substrates. The contemporary literature has referred to wafer level bonding using plasma oxidation of silicon, silicon dioxide and PDMS surfaces for realizing several micro-fluidic devices [39]. However, the researchers did not attempt to quantify the bond strengths of such wafer assemblies. We have found out that the bond strengths between PDMS and Silicon surfaces and thermally grown oxide surfaces are lower than those between plasma oxidized SOG and PDMS surfaces. The ATR-FTIR performed on a plasma exposed SOG coated surface and a plain silicon dioxide surface show a marked difference in the number of surface hydroxyl groups which are active sites for irreversible bonding. This proves the significantly higher bond strength between the SOG-PDMS in comparison to the silicon dioxide-PDMS surfaces . Hence, the developed SOG coating provide a universal approach of bonding PDMS to a variety of substrates. We have also performed a quantitative contact angle based bond strength estimation for SOG-PDMS bonds by following the protocol developed by us in

an earlier work [40]. This gives us a set of optimum exposure parameters providing irreversible seals capable of sustaining upto 83 psi air pressure, measured by using standardized blister test [41, 42].

1.4.2.Micro-fabricated PCR Platforms (Chapter 3)

Micro-fabricated assays find a prominent application in nucleic acid amplification by polymerase chain reaction (PCR) in micro-fabricated platforms [43]. PCR is an in-vitro technique for rapidly synthesizing large quantities of a given DNA segment from an initial template DNA. [44]. In this respect, it is worth mentioning that the PCR on chip devices up to this date have witnessed two different design protocols. The type I PCR devices, known as the space domain PCR [45], contain three different heat zones and intra-zonal fluid movement realized by various off chip actuation mechanisms like syringe or peristaltic pumps [46, 47]. The two movement regimes followed in this case are either rotary circulation [48] or linear [49] movement in a single channel serpentinely mounted over the different zones to execute sequential PCR cycles. Although these devices have extremely high speeds of amplification and can amplify small sample volumes at lower powers (380mW) [50], they have several limitations. Some of these use expensive accessories for fluid circulation or maneuvering [46, 47, 48, 49]. These designs also have relatively less flexibility for changing the pattern of PCR cycles. In addition, nanoliter size samples require sophisticated dispensing protocols for sample handling [51]. The type II devices, known as the time domain PCR, involve the use of chambers[52] and capillaries [53] of micron size with different direct contact or non contact means of temperature control. A lot of configurations like conventional

thermocyclers [54], peltier heaters[55], thin film resistive heaters [56], infra-red mediated heating [44] etc. have been used for thermal cycling in these devices. While the conventional thermocyclers provide a low rate of heating/ cooling sometimes resulting in a loss in PCR amplification efficiency [44], the thermoelectric means involve sophisticated temperature control equipment and are not compact [57]. The thin film heaters have extremely high heating/ cooling rates at a relatively high power (around 10-11 watts) [58] and can realize a compact device but posses limitations like thin film degradation while anodic and fusion bonding particularly in glass silicon architectures and bubble formation due to fluid contact with heating element in case of direct contact heating [59]. The thin film heaters patterned underneath etched silicon chambers can be operated at power values as low as 2.5 Watts with faster temperature ramp-up/ ramp-down [60]. However, the fabrication processes for Silicon pose other challenges as discussed earlier. The non contact means of heating involve usage of high power infrared heating lamps [39] and other expensive optical and control accessories. Further, in microfabricated platforms, various surfaces have been subjected to different passivation techniques to prevent the inhibition of PCR reaction [61]. Glass and silicon substrates have been silanized by Mathies et. al. [62], coated with surfasil and polyaniline by Poser et. al. [63] or with bis(trimethylsilyl) trifluoroacetamide by Landers et. al. [64] to make them PCR friendly. Laser machined Polyimide substrates have been coated with Amorphous Teflon [49]. Giordano et. al. [65] have explored many additives to PCR reaction which dynamically coat or adsorb to glass surfaces as an alternative to silanization processes. Many prototypes of both type of devices have been demonstrated using PDMS because of the inert nature of its surface, simplicity and lower expense of

fabrication. For example, Quake et. al [51]. showed a rotary PCR system in PDMS capable of handling 12 nL fluidic volume with no surface modification. Hong et. al. [66] have demonstrated PCR micro chips, 40-50 microliter in volume made with glass and PDMS and externally heated with sophisticated thermoelectric means. They used Bovine Serum Albumin to prevent non-specific adsorption of proteins to the glass substrate and the hydrophilic PDMS right after the oxygen plasma treatment. Backhouse et. al. [67] have demonstrated PCR by holding 5-6 microliter of fluid in a glass PDMS platform in-between two externally actuated valves over a thermoelectric source without any surface modification. The valve actuation is achieved in this case by expensive high precision servomotors as other simpler mechanisms used were reported to have failed the PDMS structure due to rupture or leaking of channels. The PDMS chamber was also reported to get ruptured when the contained fluid was heated to 120 deg. C. Shin et. al. [68] has demonstrated a 2 microliter reaction mixture by confining this small sample volume with air pressure in between two molded PDMS pieces selectively coated with Parylene and bonded together strongly by plasma oxidation techniques. Although the surface oxidation provided very good bond strength and subsequently made the prototype robust, the post exposure hydrophilic nature of the PDMS surface has been reported to absorb proteins which subsequently inhibited the PCR process, thus necessitating an inert Parylene coating. Duffy et. al. [69] has reported the relative ease of filling hydrophillic oxidized PDMS channels of 55 microns thickness in comparison to their hydrophobic counterparts with high surface energy liquids like water. This may be a potential reason of not investigating the PDMS channels and chambers after post exposure hydrophobic recovery. The two major challenges in all time domain configurations of PCR devices in

PDMS are (a) robust design capable of providing minimum sample loss at optimum power and (b) obtaining a biofriendly surface for the PCR protocol.

In this section we have explored an optimization regime of design and fabrication process for developing a robust prototype which forms a closed system with high sealing abilities without use of any sophisticated accessories like externally controlled valves or compressed air. In addition our device has favorable properties as minimal non-specific binding of DNA over hydrophobic surfaces reported by Miyachi et. al. [70] and minimization of non-specific binding of the Taq DNA polymerase by the use of Hot Start TAQ by Wilding et. al. [71]. We have demonstrated PCR amplification of a 527-bp viral DNA of the Infectious Bovine Rhino-tracheitis (IBR) with template concentrations (pico-gram level) far below their clinical values using Hot Start TAQ over PDMS and structurally similar SOG (Spin on glass) surfaces after post-exposure recovery of hydrophobicity. We do not need to use any additional surface coatings for the PCR process. The chamber and channels in PDMS used for this amplification process posses a depth of 200 microns and a moderate 6 micro-liter volume. This ensures smooth microfluidic operation of the PCR mix while loading and unloading, not withstanding the highly hydrophobic nature of the channel and chamber surfaces. The results have been substantiated with fluorescence studies by flowing a labeled RT-PCR (real time polymerase chain reaction) product [72] inside the channel/chamber and washing it out with elution buffer and RNase free water with a syringe pump. We observed a steady decline in fluorescence level with time until the background fluorescence level of the buffer solution is reached. We believe that a chamber surface with non- sticking inner walls has been developed with the plasma oxidation and post exposure hydro-phobicity

recovery processes. We have further optimized a PDMS-silicon (with oxide layer) chip with a numerically simulated unique serpentine heater design capable of rapid thermal cycling at low power (a possible explanation of minimal evaporation). We provide a thorough characterization of the serpentine heaters, which reveals its superiority in working at lower power values in comparison to thin continuous platinum films used in many earlier designs. A simplified labview controlled instrumentation was designed to drive the thermal cycling with a sensing thermocouple at 4.77 watts power, which can be easily provided by a battery (enhancing the field applicability of the prototype). Further, we have successfully explored the reusability of our platform by alternate use of positive and negative control and consecutively running this chip for multiple number of times. Cross contaminations from alternate reactions is a major problem in all on-chip PCR platforms [73] which necessitates their disposability after every reaction. We plan to investigate this aspect for this chip in our future endeavors.

1.4.3 Micro-fabricated Capillary Electrophoresis Systems and Novel Nano-composite Materials for Sieving Matrices (Chapters 4 & 5)

The micro-fabrication technology has been widely used to various fields of biotechnology and biomedical sciences [74-79], especially in analytical fields including capillary electrophoresis [80-89]. Manz et. al. [84] reported that a microstructure fabricated on a glass plate could be used for CE to perform high quality and high speed separations. Micro-fabricated CE chips have been used to separate fluorescent dyes [84], fluorescently labeled amino acids [85], and short nucleotides [86], restriction DNA fragments [85] etc. The potential benefits of such micro-fabricated systems include

reduced size and lower consumption of samples and reagents, shorter analysis times, greater sensitivity, insitu and real time analysis and disposability [83]. In case of glass made CE chips the open channels fabricated on substrates are enclosed with another substrates with high sealing ability. However, the sealing processes used are complicated and time consuming mostly by subjecting to a high electric field as in the case of anodic bonding or heating both substrate to a high temperature as in fusion bonding. [87-90]. Polymers such as PDMS offer an attractive alternative to glass as less expensive and less fragile materials for micro-fabricated CE chips [91,92]. We have chosen a glass-PDMS system to realize a capillary which has been used to resolve a 100-1000 bp gene marker within 50 secs at an operating voltage of 300V. We have also used platinum nano-particles to dope agarose gels to obtain high conductivity gel matrix capable of electrophorescing with high sample mobility at lower electric fields (chapter 4). As the final objective of our assay is to detect intercalated DNA stains with optical fiber, we have also developed a gel material using a tri-co-block-polymer (F127) with low scattering and background fluorescence which is able to resolve trace concentration of the sample (chapter 5). We plan to dope this material with nano-platinum and load it in capillaries to make a field deployable low voltage capillary electrophoresis system. The end goal is a complete integration of a device with PCR chamber, capillary electrophoresis and optical detection all on the same chip for analysis of samples.

1.5 References

1. Nucleic acid hybridization – general aspects, http://www.roche-applied-science.com/PROD_INF/MANUALS/InSitu/pdf/ISH_33-37.pdf.
2. T. Weissensteiner, HG Griffin, AM Griffin, " PCR Technology: Current Innovations, Second Edition." Boca Raton, Florida, CRC press, pp.27-35, 1995.
3. E.T. Lagally, H.T. Soh, "Integrated genetic analysis Microsystems", *Critical reviews in solid state and materials science*, Vol. 30, pp.207-233, 2005.
4. F.S. Collins, E.D. Green, A.E. Guttmacher, M.S. Guyer, "A vision for the future of genomics research", *Nature*, Vol. 422, pp.835-847, 2003.
5. A.T. Woolley, D. Hadley, P. Lander, A.J. Demello, R.A. Mathies, M.A. Northrup, "Functional integration of PCR amplification and capillary electrophoresis in a micro-fabricated DNA-analysis device", *Analytical Chemistry*, Vol.68, pp.4081-4086.
6. R.C. Anderson, X. Su, G.J. Bogdan, J. Fenton, "A miniature integrated device for automated multistep genetic assays", *Nucleic Acids Research*, Vol. 28, pp.E60-70, 2000.
7. L. C. Waters, S. C. Jacobson, N. Kroutchinina, J. Khandurina, R. S. Foote, J. M. Ramsey, "Microchip device for cell lysis, multiplex PCR amplification, and electrophoretic sizing", *Analytical Chemistry,* Vol. 70, pp.158-165, 1998.
8. M. A. Burns, B.N. Johnson, S.N. Brahmasandra, K. Handique, J.R. Webster, M. Krishnan, T.S. Sammarco, P.M. Man, D. Jones, D. Heldsinger, C.H. Mastrangelo, D.T. Burke, "An integrated nanoliter DNA analysis device", *Science,* Vol. 282, pp. 484-486, 1998.

9. C.R. Cantor, C.L. Smith, "Genomics: The science and technology behind the human genome project", *A wiley inter-science publication*, pp.120-125, 1999.
10. Technical note : Manufacturing, quality control and validation studies of gene chip arrays http://www.affymetrix.com/support/technical/technotes/manufacturing
11. K.J. Breslauer, R. Franz, H. Blocker, L.A. Marky, "Predicting DNA duplex stability from the base sequence", *Proceedings of the national academy of sciences USA*, pp.3746-3750, 1986.
12. J.D. Watson, B.M. Kary, F. Francois, R.A.Gibbs, " The polymerase chain reaction", Birkhauser, Boston, pp.75-79, 1994.
13. O. Henegariu, N.A. Heerema, S.R. Dlouhy, G.H. Vance, P.H. Vogt, " Multiplex PCR: Critical parameters and step by step protocols, Biotechniques, Vol. 23, pp. 504-511, 1997.
14. Reverse transcriptase PCR, https://fscimage.fishersci.com/webimages_FSC/ downloads/ reverse transcriptase PCR.pdf.
15. Effect of PCR buffer on multiplex PCR,http://www1.qiagen.com/literature /brochures/pcr/pdf/pcrcha03.pdf
16. Essentials of real time PCR, Applied Biosystems, http://www.icmb.utexas.edu /core/DNA/Information_Sheets/Real-time%20PCR/essentials_of_real_time_ pcr.pdf
17. C. Patrick, "Capillary electrophoresis, Theory and practice", CRC press, London, pp. 200-207, 1993.

18. S.D. Centuria, Microsystem Design, Kluwer Academic Publishers, pp.1-35, Boston / Dordrecht / London, 1993.
19. W.S. Trimmer, Editor, Micromechanics and MEMS: Classical and Seminal Papers to 1990, pp. 40-60, IEEE Press, Piscataway, NJ, 1997.
20. A. Manz, N. Graber, H.M. Widmer, "Miniaturized total chemical analysis system: A novel Concept for chemical sensing," sensors and actuators , Vol.1, pp.244-248, 1990.
21. N.T. Nguyen, S. T. Werely, Fundamentals and applications of Microfluidics, pp. 1-45, Artech House, Boston, 2002.
22. J. Kim, M.K. Chaudhury, M.J. Owen, T. Orbeck , "The mechanisms of hydrophobic recovery of polydimethylsiloxane elastomers exposed to partial electrical discharges", Journal of colloid and interface science, Vol. 244, pp. 200-207, 2001.
23. M.K. Chaudhury, "Self assembled monolayers on Polymer surfaces" , Biosensors & Bioelectronics, Vol. 10, pp.785-788, 1995.
24. X. Ma, S. Cierhart, S.D. Collins, R.L. Smith, "Low temperature bonding for wafer scale packaging and assembly of micromachined sensors paper", Final Report for MICRO Project Industrial Sponsor(s): Kumetrix, Inc., pp. 98-144, 1998-99.
25. X. Younan, G. Whitesides, Soft lithography, *Angew. Chem. Int. Ed.*, Vol. 37, pp. 231-250, 1998.
26. S. Okazaki, "General reviews on photolithography", *J. Vac. Sci.Technol. B*, Vol. 9, pp. 2829-2833, 1991.

27. H.C. Rijsewijk, P.E. J. Legierse, G. E. Thomas, "Cast molding on the micrometer scale", *Philips Tech. Rev.*, Vol. 40, pp.287–297, 1982.

28. B. D. Terris, H. J. Mamin, M. E. Best, J. A. Logan, D. Rugar, "Cast molding on the nanometer scale", *Appl. Phys. Lett.* , Vol. 69, pp. 4262–4264, 1996.

29. M.G. Allen, S.D. Centuria, "Analysis of critical debonding pressures of stressed thin films in the blister test", *Journal of Adhesion*, Vol. 25, pp.303-305, 1988.

30. Personal communication, A. Dutta, Nanotech Center, Texas Tech university.

31. K.B. Albaugh, D.H. Rasmussen, H.M. Mott-Smith, "Mechanisms of Anodic bonding of silicon to Pyrex glass", *Physics Review*, Vol. 28, pp.727-735, 1926.

32. H.K. Yasuda, "Plasma polymerization and plasma treatment of polymers", *Journal of Applied polymer science*, Vol.42, pp.355-357, 1987.

33. L.A. Arzimovich, Elementary Plasma Physics, pp. 18-25, Blaisdell Publishing Company, New York, 1980.

34. F. I. Boley, Plasmas –laboratory and cosmic, pp.230-234, D. Van Nostrand Company, Inc., Priceton, New Jersey, 1991.

35. R.A. Auerbach, D.T. Tuma, D.R. Blenner, Lord Corporation, Carnegie Mellon University, Pittsburgh, 1978.

36. L.R. Spott, S. Wikse, "Infectious Bovine Rhinotracheitis", Texas agriculture extension service, Texas A&M university, *Agricultural communications,* pp. 1-3, 2002.

37. J.W. Hong, T. Fujii, M. Seki, T. Yamamoto, I. Endo, "PDMS-Glass hybrid Microchip for gene amplification", *1st Annual International IEEE-EBMS special*

topic conference on microtechnologies in medicine and biology, Lyon, France, pp. 407-410, 2000.

38. M. Fuchs, P.Hubert, J. Detterer, H.J. Rziha, "Detection of Bovine Herpesvirus Type 1 in Blood from Naturally Infected Cattle by Using a Sensitive PCR That Discriminates between Wild-Type Virus and Virus Lacking Glycoprotein E", *Journal of Clinical Microbiology*, Vol.37, pp. 2498-2507, 1999.
39. S. Bhattacharya, A. Datta, J.M. Berg, S. Gangopadhyay, "Studies on surface wettability of Poly dimethyl siloxane and glass under Oxygen plasma treatment and their correlation to bond strength", *Journal of Microelectromechanical systems*, Vol. 14, pp.590-598, 2005.
40. B.C. Giordano, J. Ferrance, S. Swedberg, A.F.R. Huhmer, J.P. Landers, "Polymerase chain reaction in polymeric microchips: DNA amplification in less than 240 secs.", *Analytical Biochemistry*, Vol. 291, pp.124-132, 2001.
41. M.G. Allen, S.D. Centuria, "Analysis of critical debonding pressure of stressed thin films in Blister test", *Journal of Adhesion*, Vol. 25, pp.303-305, 1988.
42. A. Larsson, H. Derand, " Stability of Polycarbonate and Polystyrene surfaces after Hydrophilization with high intensity oxygen RF plasma", *Journal of Colloid and Interface Science*, Vol.246, pp.214-221, 2002.
43. J.W. Hong, K. Hosokawa, T. Fujii, M. Seki, I. Endo, "Micro-fabricated Polymer Chip for Capillary Gel Electrophoresis", Biotechnology Progress, Vol. 17, pp.958-962, 2001.

44. G. Ocvirk, M. Munroe, T. Tang, R. Oleschuk, K. Westra, J. Harrison, " Electrokinetic control of fluid flow in native polydimethyl siloxane capillary electrophoresis devices", *Electrophoresis*, Vol. 21, pp.107-115, 2000.
45. M.A. Northrup, "DNA Amplification with a microfabricated reaction chamber", The digest of technical papers of the 7th International conf. on the Solid State Sensors & actuators, Transducers 93, Yokohama, Japan, pp.924-926, 1993.
46. M.U. Kopp, A. J. DeMello, A. Manz, "Chemical Amplification: Continuous-Flow PCR on a Chip", *Science*, Vol. 28, pp. 1046-1047, 1998.
47. C.S. Liao, G.B. Lee, H.S. Liu, T. M. Hsieh, C.H. Luo, " Miniature RT-PCR system for diagnosis of RNA based viruses", *Nucleic Acids Research*, Vol. 33, pp. 1-7, 2005.
48. J.Y. Cheng, C.J. Hseih, Y.C. Chuang, J.R. Hsieh, "Performing micro-channel temperature cycling reactions using reciprocating reagent shuttling along a radial temperature gradient", *The Analyst,* Vol. 130, pp.931-940, 2005.
49. P.J. Obeid, T.K. Christipoulos, H.J. Crabtree, C.J. Backhouse, "Micro-fabricated Device for DNA and RNA amplification by continuous-flow polymerase chain reaction and reverse transcription-polymerase chain reaction witgh cycle no. selection", *Analytical Chemistry*, Vol.75, pp.288-295, 2003.
50. J. Lu, M. Enzelberger, S. Quake, "A nano-liter rotary device for polymerase chain reaction", *Electrophoresis*, Vol. 23, pp. 1531-1536, 2002.

51. T.L. Rusch, W. Dickinson, J. Che, K. Feiweger, J. Chudyk, M.J. Doktycz, A. Yu, J.L. Weber, "Updated Instrumentation for continuous array genotyping of short insertion/ deletion polymorphisms", Proceedings of the 25th Annual International Conference of the IEEE EMBS, Cancum, Mexico, pp. 321-326, 2003.
52. P. Wilding, M.A. Shoffner, L.J. Kricka, " PCR in a silicon microstructure", *Clinical Chemistry*, Vol. 40, pp. 1815-1818, 1994.
53. A.F.R. Huhmer, J.P. Landers, " Noncontact Infrared Mediated Thermocycling for effective Polymerase Chain Reaction Amplification of DNA in Nanoliter Volumes", *Analytical Chemistry*, Vol. 72, pp.5507-5512, 2000.
54. M. Kokayashi, M. Oomura, T. Kusakawa, Y. Morita, Y. Murakami, K. Yokoyama, E. Tamiya, "Electrochemical Gene Detection with PCR chip", Transducers'01, Eurosensors XV, The 11th International Conference on Soild State Sensors and Actuators, Munich, Germany, 2001.
55. J. Khandurina, T. McKnight, S. Jacobson, L. Waters, R. Foote, J. Ramsey, " Integrated system for rapid PCR-based DNA analysis in microfluidic devices", *Analytical Chemistry,* Vol. 72, pp. 2995-3000, 2000.
56. S. Stern, C. Brooks, M. Strachan, A.K. Sill, J.W. Parce, "Micro-fluidic Thermocyclers For Genetic Analysis", Inter Society Conference on Thermal Phenomena, San Diego, pp. 1010-1014, 2002.
57. J.K. Hong, T.Fujii, M. Seki, T. Yamamoto, I. Endo, " PDMS-Glass Hybrid Microchip for gene amplification", 1st Annual, International IEEE-EMBS Special Topic Conference on Micro-technologies in Medicine and Biology, Lyon, France, pp. 1524-1527, 2000.

58. A.Fuchs, H. Jeanson, P. Claustre, J.A. Gruss, F. R. Cavalier, P. Caillat, U. Mastromatteo, M. Scurati, F. Villa, G. Barlocchi, P. Corona, B. Greico, " A silicon lab-on-chip for integrated sample preparation by PCR and DNA analysis by hybridization", 2nd Annual International IEEE-EMBS Special topic conference on Micro-technologies in Medicine and Biology, Madison, Wisconsin, pp. 727-739, 2002.

59. R.A. Mathies, P.C. Simpson, S.J. Williams, "*Process for micro-fabrication of an integrated PCR-CE device and products produced by the same*", US Patent No. 6261431 B1, 2001.

60. J.H. Daniel, S. Iqbal, R.B. Millington, D.F. Moore, C.R. Lowe, D.L. Leslie, M.A. Lee, M.J. Pearce, "Silicon Micro-chambers for DNA amplification", Sensors and Actuators A, Vol.71, pp. 81-88, 1998.

61. M.A. Shoffner, J. Cheng, G.E. Hvichia, L.J. Kricka, P. Wilding, "Chip PCR I, Surface passivation of microfabricated silicon glass chips for PCR", *Nucleic Acids Research*, Vol. 24, pp. 375-396, 1996.

62. S. Poser, T. Schulz, U. Dillner, V. Baier, J.M. Kohler, "Chip Elements for fast Thermocycling", Eurosensors X, Leuven, Belgium, 1996.

63. B.C. Giordano, E.R. Copeland, J.P. Landers, "Towards dynamic coating of glass microchip chambers for amplifying DNA via the polymerase chain reaction", *Electrophoresis*, Vol. 22, pp. 334-340, 2001.

64. J.W. Hong, T. Fujii, M. Seki, T. Yamamoto, I. Endo, "Integration of gene amplification and capillary gel electrophoresis on a polydimethylsiloxane-glass hybrid microchip", *Electrophoresis*, Vol. 22, pp. 328-333, 2001.

65. P.M. Pilarski, S. Adamia, C.J. Backhouse, "An adaptable microvalving system for on-chip polymerase chain reaction", *Journal of Immunological methods*, Vol. 305, pp. 48-58, 2005.

66. Y.S. Shin, K. Cho, S.H. Lim, S. Chung, S.J. Park, C. Chung, D.C. Han, J.K. Chang, "PDMS-based micro PCR chip with Parylene coating", *Journal of Micromechanics and Microengineering,* Vol.13, pp. 768-774, 2003.

67. H. Miyachi, A. Hiratsuka, K. Ikebukuro, K. Yano, H. Muguruma and Isao Karube, "Application of Polymer-Embedded Proteins to Fabrication of DNA array", *Biotechnology and Bioengineering,* Vol. 69, pp. 323-328, 2000.

68. J. Cheng, M.A. Shoffner, G.E. Hvichia, L.J. Kricka, P. Wilding, "Chip PCR II, Investigation of different PCR amplification systems in micro-fabricated silicon-glass chips", *Nucleic Acids Research*, Vol. 24, pp. 380-385, 1996.

69. J.E. Rice, J.A. Sanchez, K.E. Pierce, L.J. Waugh, "Real time PCR with molecular beacons provides a highly accurate assay for detection of Tay-Sachs alleles in single cells", *Prenatal Diagnosis*, Vol. 22, pp. 1130-1134, 2002.

70. D.C. Duffy, J.C. McDonald, O.J.A. Schueller, G.M. Whitesides, "Rapid Prototyping of Microfluidic Systems in Poly(dimethylsiloxane)", *Analytical Chemistry*, Vol. 70, pp. 4974-4984, 1998.

71. J.C. Mcdonald, D.C. Duffy, J.R. Anderson, D.T. Chiu, H.Wu, O.J.A. Schueller, G.M. Whitesides, " Fabrication of microfluidic systems in Polydimethyl siloxane", *Electrophoresis*, Vol. 21, pp. 27-40, 2000.

72. R. Oda, M. Strausbauch, N. Borson, A. Huhmer, S. Jurrens, J. Craighead, P. Wettstein, B. Ekcloff, B. Kline, J. Landers, "Infra-red mediated thermocycling for ultrafast polymerase chain reaction amplification of DNA", *Analytical Chemistry*, Vol. 70, pp.4361-4368, 1998.

73. M. Ibrahim, R. Lofts, P. Jahrling, E. Henchal, V. Weedn, M. Northrup, P. Belgrader, "Real time microchip PCR for detecting signle base differences in viral and human DNA, *Analytical Chemistry*, Vol. 70, pp. 2013-2017, 1998.

74. T. A. Desai, W. H. Chu, J. K. Tu, G. M. Beattle, A. Hayek, M. Ferrari, "Micro-fabricated immuno-isolation of bio-capsules" *Biotechnol. Bioeng*., Vol. 57, pp. 118-120, 1998.

75. J. T. Santini, M. J. Cima, R. Langer, "A controlled release microchip". *Science* Vol. 397, pp. 335-337, 1999.

76. A. H. Nashat, M. Moronne, , M. Ferrari, "Detection of functional groups and antibodies on micro-fabricated surfaces by confocal microscopy" *Biotechnol. Bioeng.,* Vol. 60, pp.137- 146, 1998.

77. H. C. Tai, H.M. Buettner, "Neurite outgrowth and growth cone morphology on micropatterned surfaces" *Biotechnol. Prog. ,*Vol. 14, pp.364-370, 1998.

78. R. Vaidya, L. M. Tender, G. Bradley, M. J. O'Brien, M. Cone, G. Lopez, "Computer-controlled laser ablation: A convenient and versatile tool for micro-patterning bio-functional synthetic surfaces for applications in bio-sensing and tissue engineering" *Biotechnol. Prog.,* Vol.14, pp.371-377, 1998.

79. S.N. Bhatia, U.J. Balis, M.L. Yarmush, M. Toner, "Micro-fabrication of hepatocyte/fibroblast co-cultures: Role of homotypic cell interactions" *Biotechnol. Prog.* , Vol.14, pp.378- 387, 1998.

80. D.J. Harrison, K. Fluri, K. Seiler, Z. Fan, C.S. Effenhauser, A. Manz, "Micromachining a miniaturized capillary electrophoresis-based chemical analysis system on a chip", *Science*, Vol.261, pp.895-897, 1993.

81. C.H. Mastrangelo, M.A. Burns, D.T. Burke, "Micro-fabricated devices for genetic diagnostics." *Proc. IEEE* , Vol.86, pp.1769-1787, 1998.

82. J.M. Ramsey, S.C. Jacobson, M.R. Knapp, "Micro-fabricated chemical measurement systems.", *Nature Med.* , Vol.1, pp.1093-1096, 1995.

83. A. Manz, D.J. Harrison, E.M.J. Verpoorte, J. C. Fettinger, A. Paulus, H. Luedi, M. Widmer, "Planar chips technology for miniaturization and integration of separation techniques into monitoring systems: capillary electrophoresis on a chip" *J. Chromatogr.,* Vol.593, pp.253-258, 1992.

84. C. S. Effenhauser, A. Manz, H. M. Widmer, "Glass chips for high-speed capillary electrophoresis separations with sub-micrometer plate heights", *Anal. Chem.* , Vol. 65, pp.2637-2642, 1993.

85. S. C. Jacobson, R. Hergenroeder, L. B. Koutny, R. J. Warmack, M. Ramsey, "Effects of injection schemes and column geometry on the performance of microchip electrophoresis devices" *Anal. Chem.* , Vol.6, pp.1107-1113, 1994.

86. A.T. Wooley, R. Mathies, "Ultrahigh-speed DNA fragment separations using micro-fabricated capillary array electrophoresis chips." *Proc. Natl. Acad. Sci. U.S.A.* , Vol. 91, pp.11348- 11352, 1994.

87. C.S. Effenhauser, A. Paulus, A. Manz, M. Widmer, High speed separation of antisense oligonucleotides on a micromachined capillary electrophoresis devices. *Anal. Chem*., Vol.66, pp.2949-2953, 1994.

88. S.C. Jacobson, W.A. Moore, J.M. Ramsey, "Fused quartz substrates for microchip electrophoresis" *Anal. Chem.* , Vol.67, pp.2059-2063, 1995.

89. P.C. Simpson, A.T. Wooley, R.A. Mathies, "Micro-fabrication technology for the production of capillary array electrophoresis chips" *J. Biomed. Microdevices,* Vol.1, pp.7-26, 1999.

90. J. Khandurina, S.C. Jacobson, L.C. Waters, R.S. Foote, J.M. Ramsey, "Micro-fabricated porous membrane structure for sample concentration and electrophoretic analysis" *Anal. Chem.*, Vol.71, pp.1815-1819, 1999.

91. R. M. McComick, R.J. Nelson, M.G. Alonso-Amigo, D.J. Benvegnu, H.H. Hooper, "Microchannel electrophoretic separations of DNA in injection-molding platsic substrates", *Anal. Chem.*, Vol. 69, pp.2626-2630, 1997.

92. J.R. Webster, M.A. Burns, D.T. Burke, C.H. Mastrangelo, "An Inexpensive plastic technology for microfabricated capillary electrophoresis chips" *Proc. Micro Total Anal. Sys.,* Vol. 12, pp.249-252, 1998.

1.6 Figures

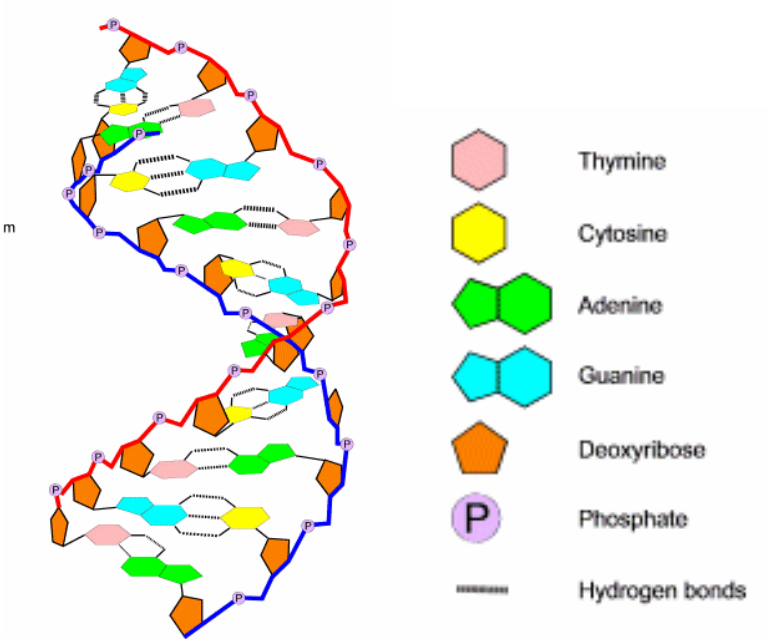

Figure 1.1: Basic DNA structure

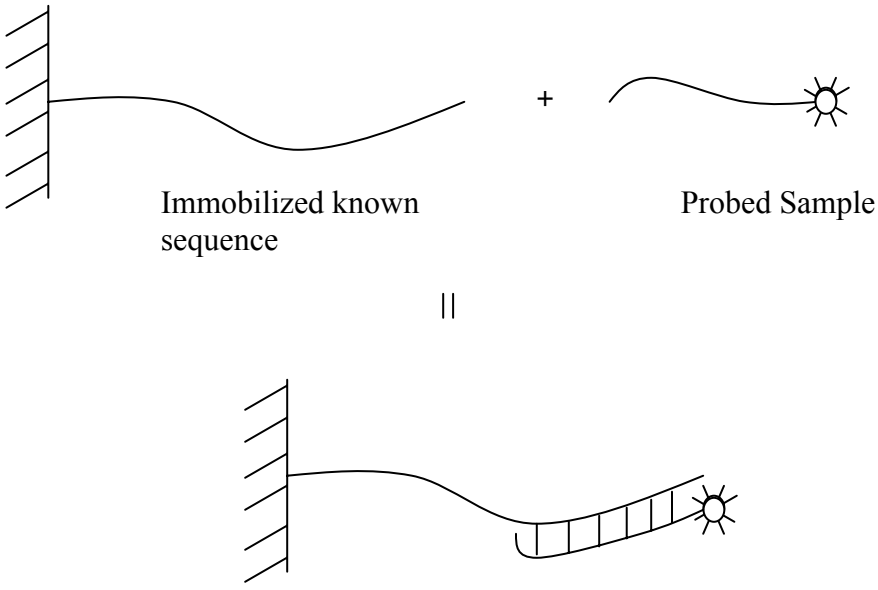

Figure 1.2: Hybridization assay. From prior knowledge of the immobilized segment the sequence of the sample can be deciphered.

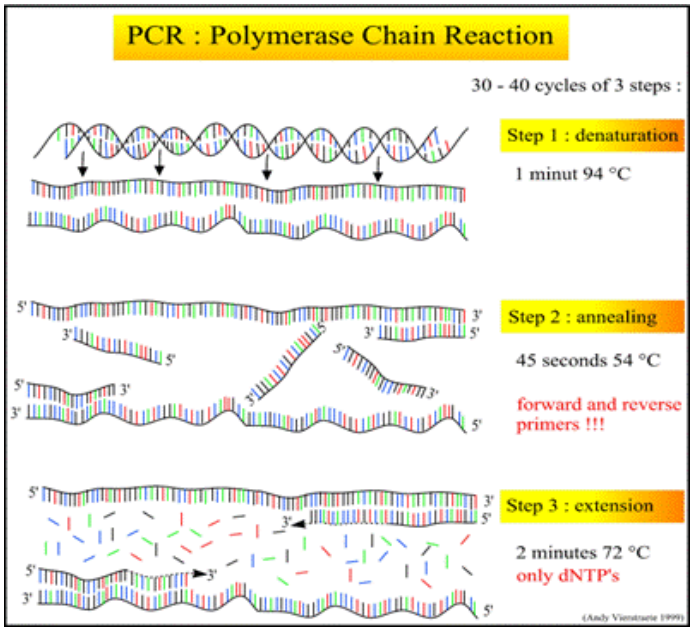

Figure 1.3: Three step Polymerase Chain Reaction process.

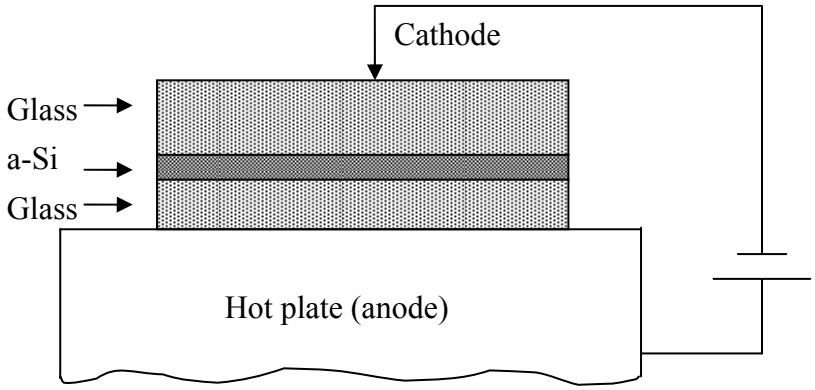

Figure 1.4: Apparatus for anodic bonding of silicon to glass [40]

Chapter 2

MECHANICS OF PLASMA EXPOSED SOG (SPIN-ON-GLASS) AND PDMS (POLY DIMETHYL SILOXANE) SURFACES AND THEIR IMPACT ON BOND STRENGTH

2.1 Abstract

Silicone polymer (PDMS), widely used for micro-fluidic and biosensor applications, possesses an extremely dynamic surface after it is subjected to an Oxygen Plasma treatment process. The surface becomes extremely hydrophilic immediately after oxygen plasma exposure by developing silanol bond (Si-OH), which promotes its adhesion to some other surfaces like, silicon, silicon dioxide, glass etc. Such a surface, if left in ambient dry air, shows a gradual recovery of hydrophobicity. We have found an identical behavior to occur to surfaces coated with a thin continuous film of SOG (Methyl silsesquioxane). The chemistry induced by oxygen plasma treatment of a SOG coated surface provides a much higher density of surface silanol groups in comparison to precleaned glass, silicon or silicon dioxide substrates thus providing a higher bond strength with PDMS. The bonding protocol developed by using the spin coated and cured SOG intermediate layer provides an universal regime of multi level wafer bonding of PDMS to a variety of substrates. The paper describes a contact angle based estimation of bond strength for SOG and PDMS surfaces exposed to various combinations of plasma parameters. We have found that the highest bond strength condition is achieved if the contact angle on the SOG surface is less than 10 degrees.

2.2 Introduction

An important need of the biosensor and micro-fluidic industry is its successful integration to microelectronics. Some of the widely used materials amenable to micro-fabrication processes are glass, silicon, polymethyl methacrylate (PMMA), polydimethyl siloxane (PDMS) etc.[1]. Silicon, being the most widely used material for microelectronic applications, may be thought of as a natural choice for such an integration. However, for defining flow paths fabrication of micron scale features in silicon, expensive deep reactive ion etching (DRIE) processes or extensive use of wet chemical processes is needed. This generates large amounts of environmentally unfriendly waste [2,3]. Replica molded silicone rubber , PDMS, has often been suggested as an alternate route and has been successfully used in diverse applications ranging from micro-fluidics [4], genomics [5] , proteomics [6], metabolomics [7] etc., though its integration with different substrates can be a challenge. A variety of processes are currently used to promote adhesion between PDMS and substrates like glass, silicon, silicon dioxide etc. This includes spun on liquid PDMS acting as adhesion intermediate layer [8] , surface activation by using high pressure, low power gas plasmas [9] , chemical treatment of surfaces [10] thus developing weak Vanderwaals forces of attraction between the various layers etc. Among all these techniques, the use of oxygen plasma produces the strongest SOG-PDMS bonds which are irreversible in nature [9]. The changes in surface texture and chemistry happening in post exposed PDMS surface have been widely studied by many researchers using a variety of techniques like Attenuated Total Reflection Fourier Transform Infra-red spectroscopy (ATR-FTIR) [11], X-ray Photon Spectroscopy (XPS), and Atomic Force Microscopy (AFM), etc. [12-14]. The PDMS material generally

comprises of repeating units of $–O\text{-}Si(CH_3)_2$, which on exposure to oxygen plasma develops silanol groups (Si-OH) at the expense of methyl groups [15]. Several other substrates like glass, silicon or silicon dioxide mainly bond due to the formation of Si-OH bonds on these substrates by oxygen plasma [15] or chemical means [9]. When such a substrate is held in conformal contact with another exposed PDMS piece, the Si-OH groups on both these surfaces condense with each other developing strong intermolecular Siloxane (Si-O-Si) bonds. The PDMS cannot be, however, integrated to other metallic or ceramic substrates where formation of surface hydroxyl groups may not be realized by any means. Such an integration, if developed, may tremendously help micron-scale heat transfer processes [16] or outdoor electrical power applications [17]. In this paper, we report a novel polymer SOG, which can form a hard intermediate surface possessing the same post exposure characteristics as PDMS itself and form an ideal material bonding irreversibly with PDMS. We have further observed a gradual surface relaxation of post exposed SOG coated surfaces by contact angle studies and ATR-FTIR measurements, an effect similar to PDMS surfaces as reported earlier [11]. This provides a direct correlation between the density of surface silanol groups, the contact angle and the bond strength between various participating surfaces. We have further shown a contact angle based estimation of bond strength between PDMS and SOG coated silicon surfaces and have tuned the plasma exposure parameters to achieve a maximum bond strength condition. An universal curve has been plotted using contact angle and bond strength values demonstrating the occurrence of this maximum bond strength condition corresponding to a contact angle of ten degree or less for SOG-PDMS surfaces.

2.3 Experimental

2.3.1 Fabrication of Blisters in PDMS for Bond Strength Between Irreversibly Sealed SOG Coated Wafers and PDMS Surfaces

The bond strength was measured using the blister test [18] wherein a 3mm diameter blister was fabricated in PDMS using photolithography and replica molding processes using SU8 2075 (M/s. Microchem) and RTV 615 (M/s GE Silicones).The masks for selective patterning were designed by Adobe Illustrator and printed by using a high resolution printer [See Fig. 2.1 (a)&(b)]. A 3mm square silicon slide with a 900nm thick thermally grown silicon dioxide was spin coated with SOG, 140nm thick, and thermally cured as per the manufacturer's specification [19] using a hot plate in an inert nitrogen environment. The SOG coated silicon surface and the PDMS were both exposed to an oxygen plasma in a plasma enhanced chemical vapor deposition (PECVD) system and held in conformal contact to each other. After fabricating the blister, an input port was attached to it using a steel pipe and a poly eukaryotic ether ketone (PEEK) (Mc-Master Carr) tubing, which was epoxied to one of the edges [9]. A compressed air bottle with a pressure gauge was used to flow air through this blister and the pressure at which the blister starts to fail was noted down.

2.3.2 Description of the Plasma Tool

We used a capacitatively coupled PECVD tool to expose the PDMS and SOG surfaces. In this system, a 13.56 MHz RF power supply with a maximum power of 300W is used to support the plasma. The flow rate of each gas is regulated using a mass flow controller

before being admitted to the gas manifold. The pressure in the chamber is controlled using a butterfly valve [13] and samples are place on the cathode.

2.3.3 Contact Angle Measurement

The Contact angle measurement is the ideal way to characterize surface hydrophilicity and tracing the dynamic behavior of polymer surfaces like SOG and PDMS after exposure to the oxygen plasma [11]. As the phenomena of surface recovery is very fast, the contact angle tool, comprising of a CCD camera and an image acquisition system, was positioned very close to the plasma exposure tool. This enabled us to capture the image of a droplet of DI water dropped on the polymer surface immediately after the plasma exposure process. Two silicon wafers with SOG coated surfaces and a PDMS blister were simultaneously exposed to Oxygen Plasma and one was used for measurement of the contact angle. The other wafer was used for bonding with a replica molded blister. The bonded assembly was used to investigate the bond strength.

2.3.4 ATR- FTIR Characterization of Post Exposed SOG Surface

The attenuated total reflection fourier transform infrared spectroscopy (ATR-FTIR) is a commonly used method to characterize the chemical structure of the surface [11]. The ATR technique enables the identification of specific molecules and groups located within 100 nm from the surface layer. We used a Nicolet-4700 FTIR spectrometer for measurement of the plasma exposed sample surface. The ATR accessory contained a germanium crystal acting as a waveguide with specimen film placed upside down on one

of its faces. The IR beam grazed past the face of the crystal and the evanescent field extending into facing polymer film provided its surface characteristics.

2.4 Results and Discussion

2.4.1 Change of Contact Angle of SOG Surface with Time

The post exposed SOG surface showed an increase in the advancing contact angle with time. The contact angle of SOG surface before exposure was 83 deg. This changed to almost 7 deg. after exposure. Measurements were taken after 5 mins., 1 hour, 3 hours, 5 hours and 2 days. The contact angle rose from 7 deg. immediately after exposure to around 63 deg. after 5 hours. No change in the contact angle was observed after 2 days indicating full recovery of the surface and saturation in surface recovery rate after 5 hours [Figure 2.2]. A similar surface recovery was found to occur in PDMS where there is a tendency of the methyl groups to appear on the surface from the bulk of the material due to extensive rearrangement of surface bonds due to surface chain scission reactions [17]. The SOG surface being structurally identical to PDMS should have a similar mechanism of chain scission reactions. In order to confirm this hypothesis, we performed an ATR-FTIR spectra on the SOG surface. A similar study indicating a gradual hydrophobicity recovery of PDMS surfaces exposed to corona discharge has been reported earlier [17]. The spectra were taken at $32cm^{-1}$ resolution within 3700 – $2900cm^{-1}$ spectral range covering the –CH and –OH band. The figure 2.3(a) shows the Gaussian fit ATR-FTIR absorption spectra of –CH absorption in the region of 2900-3000 cm^{-1}. A peak was found at 2970 cm^{-1} was assigned to $–CH_3$ (asymmetric) bond stretching vibration [20]. The

figure 2.3(b) shows OH stretching broad band spectra in the 3000-3600 cm^{-1} region for untreated SOG and after exposure to plasma over time [21]. The strong broad absorption band that appears to be approximately at 3500 cm-1 [Fig. 2.3(b)] is attributed to hydroxyl groups, physically adsorbed upon the film surface [20, 22]. We found the surface methyl groups to fall to a very low level immediately after exposure. This was followed by a slow recovery of the surface methyl content after 5 hours. Correspondingly, the surface hydroxyl groups peaked immediately after exposure and gradually reduced with time. We calculated the total area under the Gaussian fitting curve of each –CH and –OH region for untreated sample, immediately after treatment, 1 hour and 5 hour after exposure to plasma [Figure 2.4]. The area under the CH peak changes from 4000 arbitrary units (au) to 2000 (au). Simultaneously, the hydroxyl peak changes from 0 au to 1400 au. This corresponds to a contact angle of 7 deg. The area under the methyl peak rises to 3000 au and the hydroxyl goes down to 600 au after 1 hour of relaxation . The contact angle at this point of time has been found to be 31 deg. The area under the methyl peak after this does not change much and at the end of 5 hours, stabilizes at 3000 au. The area under OH goes down from 1hour of relaxation to 5 hours of relaxation from 600 au to 250au. The contact angle after 5 hours of relaxation is 62 deg., different from the angle of untreated surface (83 deg.). This behavior can be well explained from the area trend. The methyl does not get back to its initial 4000 au level which accounts for a lesser contact angle (62 deg.) after 5 hours of exposure. The sudden jump of angle from 1 hour (31 deg.) to 5 hours (62 deg.) can be explained by the reduction of area under the OH peak from 1 to 5 hours. This indicates a direct correlation between the contact angle and the surface hydroxyl groups.

2.4.2 Correlation Between Bond Strength and Surface Hydroxyl Groups

A strong correlation was found between the surface hydroxyl groups formed due to oxygen plasma exposure on SOG and silicon dioxide and the bond strength. This was investigated by comparing the respective bond strengths of PDMS with thermally grown silicon dioxide and with a SOG coated silicon dioxide surface, both exposed to oxygen plasma. We found that the blister started separating in case of silicon dioxide PDMS bondage at 10 psi. The maximum bond strength obtained by an intermediate SOG layer is enhanced to 75-85 psi, which is by and large the highest bond strength value. We performed an ATR-FTIR on the plasma exposed silicon dioxide surface and a SOG-coated surface. Figure 2.5 shows OH stretching broad band spectra as indicated earlier.[22] The plasma treated SOG layer exhibits a much higher presence of hydroxyl groups than the plasma treated silicon dioxide. The area under the OH peak for the treated SOG sample is calculated to be 22,754 AU (Arbitrary Units) and for the treated silicon dioxide sample, it is calculated to be 2045 AU. There is approximately an order of magnitude increase in the surface OH groups on the treated SOG surface. Correspondingly, the bond strength of SOG-PDMS (83 psi) is approximately an order of magnitude more than the SiO2-PDMS (10psi). We also investigated the effects on contact angle and bond strength of various exposure parameters as discussed in the next section.

2.4.3 Surface Modification Studies of SOG

In this study, we found out the existence of a common scale, to be used for estimation of the bond strengths between various surfaces. We used advancing contact angle

measurements by sessile drop method to determine the correct plasma exposure parameters corresponding to the highest bond strength between participating surfaces. The PDMS and SOG have a high degree of similarity in their surface structures. The main difference in the surface composition of both the polymers is the presence of an additional methyl group on the PDMS surface. The events that occur at an exposed PDMS surface have been detailed by many researchers. These studies indicate an increase in hydroxyl groups and a removal of methyl groups upon exposure to oxygen plasma. As the hydroxyl groups are polar in nature, the surface becomes highly hydrophilic, which is expressed in terms of a change in advancing contact angle of deionized water. We applied the same scale of reference in this work to obtain the highest bond strength between SOG and PDMS surfaces. We varied plasma exposure dosages by varying various parameters like time of exposure, chamber pressure, reactive ion etching power etc. in a PECVD (plasma enhanced chemical vapor deposition) system. The bond strength and contact angle follow similar behavior as in the case of PDMS-Glass and PDMS-PDMS bondage as determined by our group in an earlier work [9]. These are tabulated in Table 2.1. The high contact angle of the SOG surface is owing to the presence of methyl groups in its surface.

2.4.4 Universal Curve for Bond Strength and Contact Angle

We have explored the possibility of a universal trend of all the contact angle bond strength data. We find that there exists a linear trend between the bond strength and contact angle for the SOG-PDMS bond. Figure 2.6 shows the universal curve plotted with data points obtained from experiments with variation in chamber pressure

(represented by blue open triangle), variation in power (represented by green diamond), and variation in time of exposure (indicated by red squares). A linear fit of all these data points are performed to obtain the best fit equation as Y= 77.48 – 1.09X, where "Y" is the bond strength in psi and "X" is the contact angle in deg. If the contact angle is zero, i.e., if the "drop" completely wets the SOG surface, the calculated bond strength from this equation is 77.5 psi, close to the maximum bond strength of 83 psi as observed experimentally. Correspondingly, for a zero bond strength, the contact angle becomes 72 deg., fairly close to the contact angle of the untreated SOG surface (83 deg). The universal curve can be used to predict bond strengths for a known contact angle and vice versa and is an useful plot for researchers working in the micro-fabrication field. We also investigated the bond strengths of PDMS-silicon with native oxide and PDMS to thermally grown Silicon dioxide by using blister test. We found that the blister was separated from these substrates at 60 psi and 10 psi respectively. The maximum bond strength obtained by an intermediate SOG layer is in the range of 75-85 psi which is by and large the highest bond strength value among all these. Thus the SOG layer provides a strong basis for integration of PDMS with silicon, thermally grown silicon dioxide or any other substrate. This provides a good regime for integration of PDMS based micro-fluidic devices to microelectronic structures.

2.5 Conclusion

A thorough surface characterization of the post plasma exposed SOG film using an ATR-FTIR shows a gradual hydrophobic recovery of this surface due to increase in the surface methyl groups and a subsequent dehydroxylation. An advancing contact angle study,

using a sessile drop method, performed on these substrates reveal a gradual increase in surface hydrophobicity with time. We have also found a strong direct correlation between an exposed SOG surface and silicon dioxide surface bonded and the bond strength. We used contact angle and bond strength between SOG and PDMS surfaces to predict the right plasma parameters for a maximum bond strength condition. An universal curve plotted between the contact angle and the bond strength for various plasma parameters show an inverse correlation. The contact angle value predicted from the linear fit closely matches with the no exposure contact angle. We have found that SOG-PDMS bonds are much stronger than the glass-PDMS, PDMS-PDMS or silicon dioxide-PDMS bonds and this gives a general method of bonding replica molded PDMS to different substrates.

2.6 Acknowledgements

The authors gratefully acknowledge the financial support from the National Pork Board and National Institute of Health to carry out this research.

2.7 References

1. B.C. Giordano, J. Ferrance, S. Swedberg, A.F.R. Huhmer, J.P. Landers, "Polymerase chain reaction in polymeric microchips: DNA amplification in less than 240 secs.", *Analytical Biochemistry*, Vol. 291, pp. no. 124-132, 2001.
2. D.L. Flamm, " Mechanisms of silicon etching in Flourine and Chlorine containing plasmas", *Pure and applied chemistry*, Vol. 62, No.9, pp. 1709-1720, 1990.
3. H. Seidel, L. Csepregi, A. Heuberger, H. Baumgarel, "Ansiotropic etching of crystalline solutions in alkaline solutions", *Journal of electrochemical society*, Vol. 137, pp. 3612-3626, 1990.
4. D.J. Beebe, J.S. Moore, Q. Yu, R.H. Liu, M.L. Kraft, B.H. Joe, C. Devadoos, "Microfluid tectonics: A comprehensive construction platforms for microfluidic systems", *Proceedings of natural academy of science*, Vol. 97, pp. 13488-13493, 2000.
5. M.U. Kopp, A. J. DeMello, A. Manz, "Chemical amplification: continuous-flow PCR on a chip", *Science*, Vol. 28, pp. 1046-1047, 1998.
6. S. Mouradian, "Lab-on-a-chip: applications in proteomics", *Current opinion in chemical biology*, Vol. 6, pp. 51-56, 2001.
7. T. Yasukawa, A. Glidle, J.M. Cooper, T. Matsue, "Electro-analysis of metabolic flux from single cells in simple pico-liter-volume microsystems" *Analytical Chemistry*, Vol. 74, pp. 5001-5008, 2002.
8. J. Liu, M. Enzelberger, S. Quake, " A nano-liter rotary device for polymerase chain reaction," *Electrophoresis*, vol. 23, no.10, pp.1531-1536, 2002.

9. S. Bhattacharya, A. Datta, J.M. Berg, S. Gangopadhyay, "Studies on surface wettability of Poly dimethyl siloxane and glass under Oxygen plasma treatment and their correlation to bond strength", *Journal of Microelectromechanical systems*, Vol. 14, No.3, 2005.
10. J.W. Hong, T. Fujii, M. Seki, T. Yamamoto, I. Endo, "Integration of gene amplification and capillary gel electrophoresis on a polydimethylsiloxane-glass hybrid microchip", *Electrophoresis*, Vol. 22, pp. 328-333, 2001.
11. H. Hillborg, U.W. Gedde, " Hydrophobicity changes in silicone rubbers", *IEEE transactions on dielectrics and electrical insulation*, Vol. 6, No.5 , 1999.
12. K. Suzuki, H. Sugai, K. Nakamura, T.H. Ann, M. Nagatsu, " Control of high density plasma sources for CVD and etching", *Vacuum*, Vol. 48, no.7, pp.659-667, 1997.
13. J. Lubguban, T. Rajagopalan, N. Mehta, B. Lalouh, S.L. Simon, S. Gangopadhyay, "Low-K organosilicate films prepared by tetravinyltetramethyl-cyclotetrasiloxane", *Journal of Applied Physics*, Vol. 92, no.2, pp.1033-1038, 2003.
14. M.K. Chaudhury, G.M. Whitesides, " Correlation between surface free energy and surface constitution", *Science*, Vol. 25, pp.1230-1232, 1992.
15. F. Garbassi, M. Morra, L. Barino, E. Occhiello, *Polymer Surfaces. From Physics to Technology*, pp. 345-397, New York: Wiley, 1994.

16. E.G. Colgan, B. Farman, M. Gayes, W. Graham, N. LaBianca, J.H. Magerlein, R.J. Polastre, M.B. Rothwell, R.J. Bezama, R. Choudhury, K. Martsan, H.Toy, J. Wakil, J. Zitz , R. Schmidt , " A practical implementation of Silicon microchannel coolers for high power chips", *21st IEEE SEMI-Therm symposium*, pp. 15-17, 2005.
17. H. Hillborg, U.W. Gedde, "Hydrophobicity recovery of polydimethyl siloxane after exposure to corona discharges", *Polymer*, Vol. 39, No. 10, pp. 1991-1998, 1998.
18. P. Silberzan, S. Perutz, E.J. Kramer, M.K. Chaudhury, " Study of the self-adhesion hysteresis of a siloxane elastomer using the JKR method", *Langmuir*, Vol. 10, pp.2466-2470, 1994.
19. Product catalogue, " *Spin on Glasses and Spin on dielectric materials*", www.flimtronics.com.
20. Benesi H.A., Jones A.C., "An infrared study of the water-silica gel system," *Infrared Study of the Water-Silica Gel System,* Vol. 63, p179-182, 1959.
21. M.L. Hair, *Infrared Spectroscopy in Surface Chemistry*, pp. 240-290, Marcel Dekker, Inc. New York (1967)
22. B. Lahlouh, J.A. Lubguban, G. Sivaraman, R. Gale, S. Gangopadhyay, "Silylation Using a Supercritical Carbon Dioxide Medium to Repair Plasma-Damaged Porous Organosilicate Films," *Electrochemical and Solid- State Letters*, Vol. 7, No. 12, G338-341, 2004.

2.8 Figures

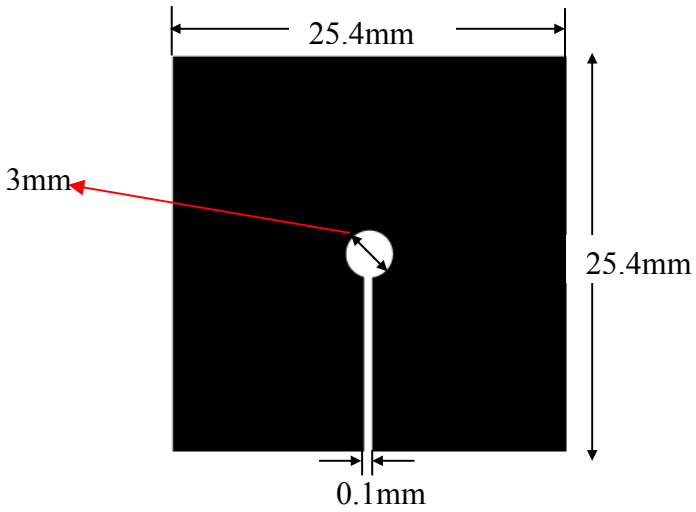

Fig. 2.1(a): Blown-up view of adobe illustrator mask for Blister.

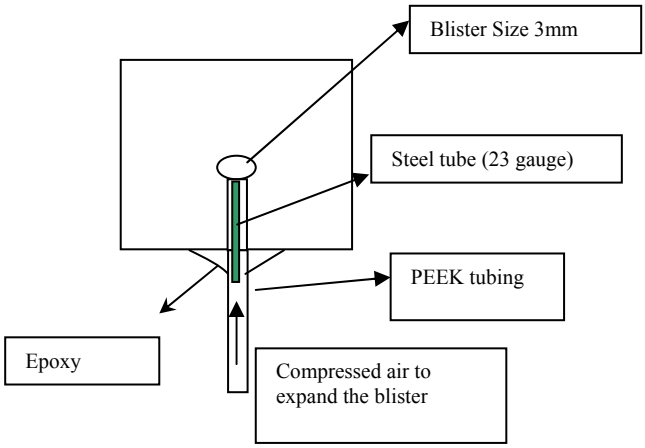

Fig. 2.1(b): Schematic of a blister assembly

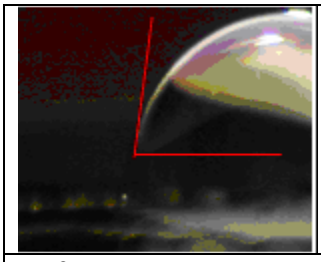	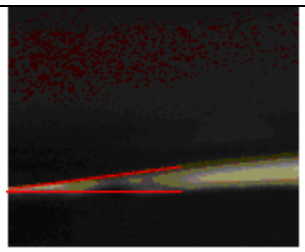	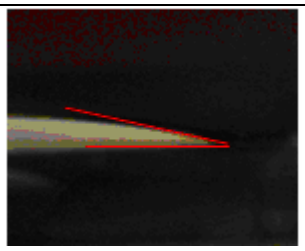
Before exposure	Immediately after exposure	After 5 mins
Contact angle = 83.01	Contact angle = 7.049	Contact angle = 12.75
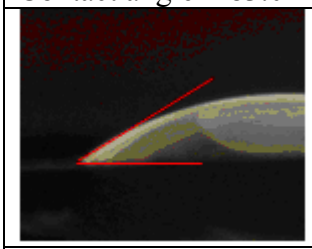	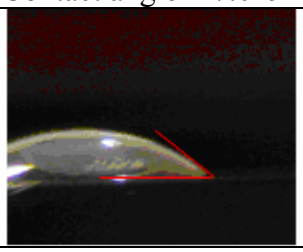	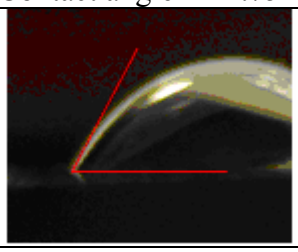
After 1 hour	After 3 hours	After 5 hours
Contact angle = 31.58	Contact angle = 38.68	Contact angle = 62.41
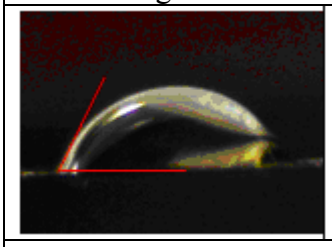		
After 2 days		
Contact angle = 63.94		

Fig. 2.2: Contact angle photographs of post exposed SOG surface with relaxation time

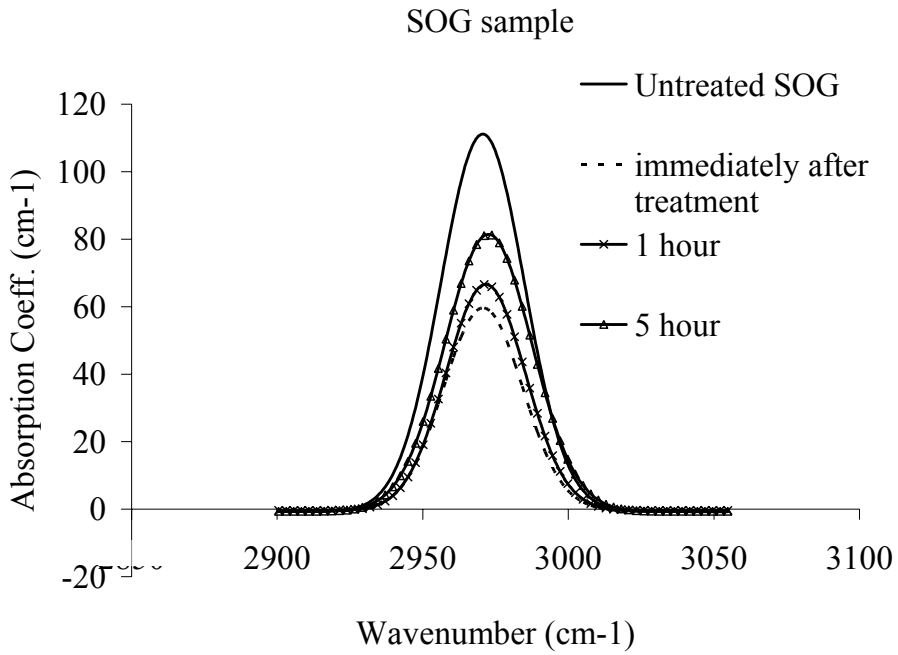

Fig.2.3(a): Gaussian fit ATR-FTIR spectra of methyl group for untreated SOG, after plasma treatment (immediately after exposure, 1hour and 5 hour).

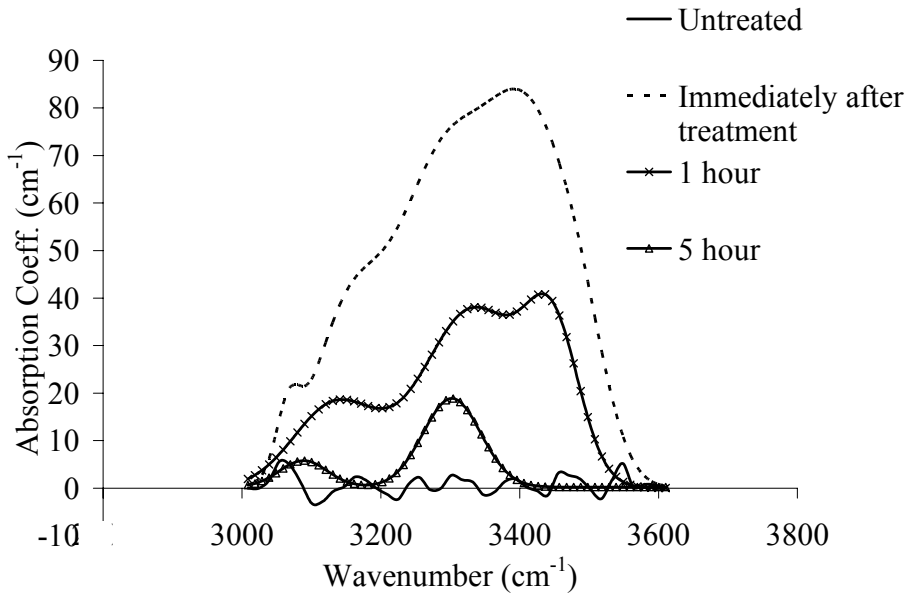

Fig. 2.3(b): Gaussian fit ATR-FTIR spectra of OH absorption band for untreated SOG, after plasma treatment (immediately after exposure, 1 hour and 5 hour).

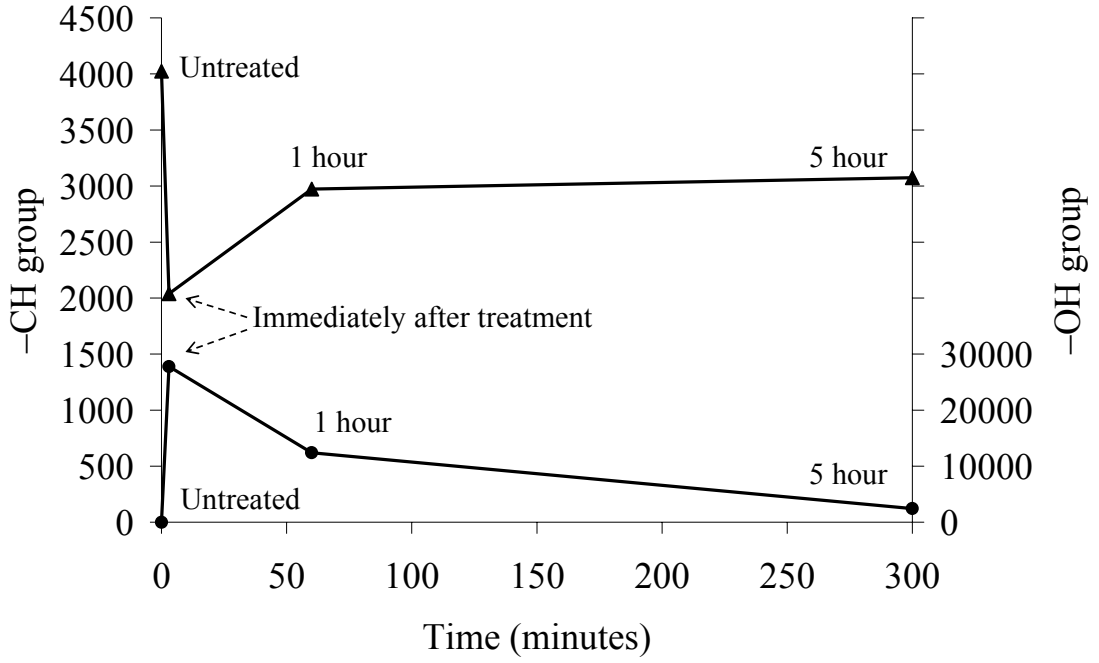

Fig. 2.4: Total area under Gaussian curve in arbitrary units of CH and OH region for untreated, immediately after treatment, 1 hour and 5 hours. ▲ is for –CH region and ● is for –OH region.

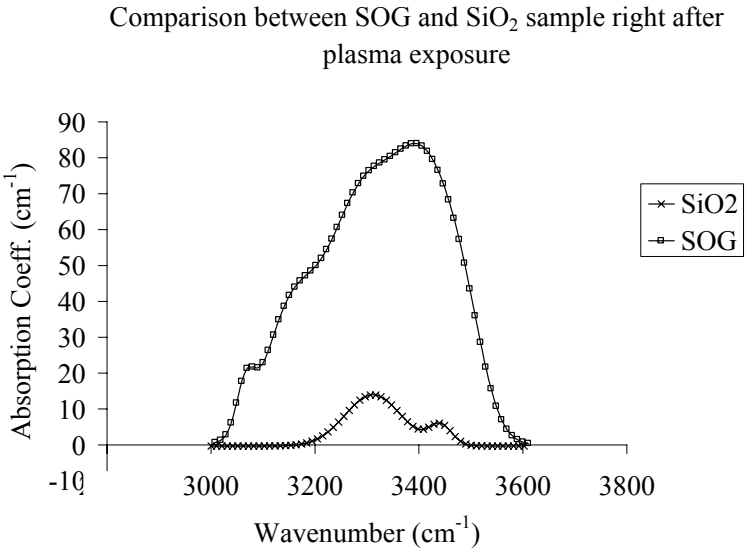

Fig. 2.5: Comparison between SOG and SiO2 surfaces immediately after plasma exposure. (Area under the OH peak for SOG= 27,745 (Au), Area under the OH peak for SiO2 = 2045(Au))

Table 2.1: Contact angle and bond strength data for various chamber pressures, RIE powers and Time of exposure values.

S.N.	Chamber Pressure (mTorr)	RIE Power (W)	Time of Exposure (secs)	Surface Hydrophilicity measured by contact angle		Bond Strength Measured by separation pressure	
				Surface Type	Contact Angle, Error $\pm 2.5^{o}$	Bond Type	Pressure, Error $\pm$ 2psi
1	100	20	35	SOG	34.8	SOG-PDMS	30
2	400				25.5		40
3	900				4.6		78
4	1200				17.9		45
5	1400				74.6		5
6	900	5	35	SOG	30.7	SOG-PDMS	40
7		10			4.6		80
8		20			3.9		85
9		30			32.2		52
10	900	20	20	SOG	10.5	SOG-PDMS	60
11			30		4.1		76
12			35		4.5		80
13			40		9.5		65
14			45		8.3		58

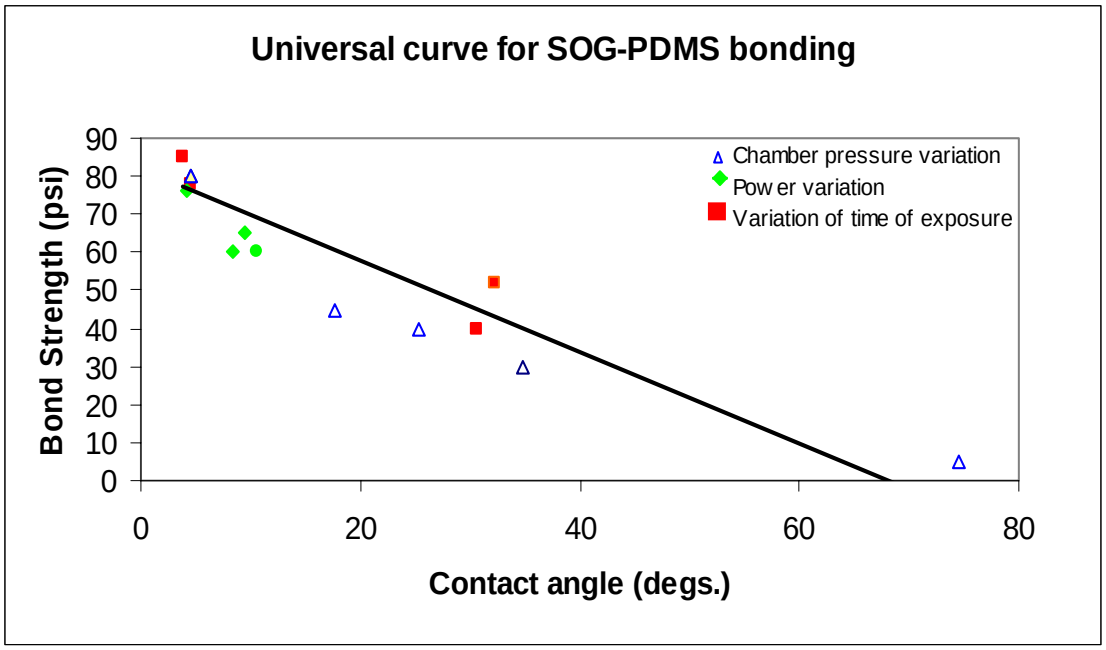

Fig. 2.6: Universal curve for SOG-PDMS bonding.

Chapter 3

OPTIMIZATION OF DESIGN AND FABRICATION PROCESS FOR REALIZATION OF A PDMS-SOGSILICON DNA AMPLIFICATION CHIP

3.1 Abstract

A novel on-chip inexpensive platform to perform DNA amplification has been fabricated by optimizing the design and microfabrication processes using PDMS (Poly Dimethyl Siloxane) and silicon. The silicon base contains a set of microfabricated platinum heater structures on the bottom with a 140 nm thick SOG (Spin On Glass) layer on the top and a 3 µl replica molded PDMS chamber with feed channels and inlet-outlet ports bonded to this film. The plasma exposed SOG surface is found to undergo recovery of hydrophobicity with time as indicated by an increase in advancing contact angle. This hydrophobic recovery of the micro-chamber and channels eliminate the need for various surface passivation techniques for PCR (Polymerase Chain Reaction) chips. A thermal cycler with flexible PCR cycle control is designed and implemented by using a sensing thermocouple. The ramp-up and -down times are almost $1/10^{th}$ of any conventional system obtained by using 4.77 W power value. A comparison made between contemporary continuous platinum film based on chip heater designs and our serpentine design shows a reduction of ramp up and down time by almost five times. The amplification has been tested using picogram level template DNA concentration on this platform. We have further been able to show negligible non-specific binding of the template DNA to the hydrophobic interiors of our device by fluorescence measurements using FAM labeled RT-PCR products. We have been able to successfully demonstrate multiple usage of this chip without cross contamination from the previous run by introducing a wash step in between with elution buffer and RNase free water

which gives us a future direction of investigating the reusability of this platform for multiple PCR runs.

3.2 Introduction

Replica molded PDMS has been widely used as an amenable micro-fabrication material due to its inexpensive fabrication process, simple bonding technique and relatively low waste generation, which occurs only during the fabrication of a glass or silicon master [1,2]. Of significant importance is the area of nucleic acid amplification by polymerase chain reaction (PCR) using PDMS based micro-fabricated platforms [3]. The PCR is an in-vitro technique for rapidly synthesizing large quantities of a given DNA segment from an initial template DNA. [4]. PCR on-chip devices up to this date have witnessed two different design protocols, namely the space domain and time domain devices. Conceptually, all space domain PCR devices [5], contain three different heat zones and intra-zonal fluid movement realized by various off-chip actuation mechanisms like syringe or peristaltic pumps [4,6,7,8]. The time domain PCR chambers, on the other hand, involve the use of chambers [9] and capillaries [10] of micron size with different direct contact or non-contact means of temperature control [11-14, 3]. There are several advantages and limitations in both design.The space domain PCR devices can amplify minimal sample volumes at low powers [15]; but, involve sophisticated fluid maneuvering and dispensing protocols [5] and less cycle flexibility. The time domain designs are more flexible to adapting different PCR protocols; but, have limitations like use of higher (10-11 Watts) power, thin film degradation in contact heating and use of expensive accessories in non-contact mediated heating. Also, in microfabricated platforms, various surfaces have been subjected to different passivation techniques to prevent the inhibition of PCR reaction [16-18, 10, 7]. Many prototypes of both type of devices have been demonstrated using PDMS because of the inert nature of its surface, simplicity and lower expense of fabrication [19-21]. Researchers have used inert coatings like

Bovine Serum Albumin [19] and Parylene [21] over oxygen plasma treated hydrophilic PDMS surfaces to prevent non-specific adsorption of proteins. They have, however, not investigated the behavior of these surfaces after the post exposure hydrophobic recovery. One reason for this could be the ease of filling PDMS channels of thickness 50 microns or below before their hydrophobic recovery [22].

In this paper, we have explored an optimization regime of design and fabrication process for developing a robust prototype, which forms a closed system with high sealing abilities. In addition, our device has favorable properties like no non-specific binding of DNA and Hot Start TAQ [23,24] over the hydrophobically recovered surfaces without the use of any separate surface passivation techniques. We have demonstrated PCR amplification of a 527-bp viral DNA of the Infectious Bovine Rhinetracheitis (IBR) with template concentrations (pico-gram level) far below their clinical values. The chamber and channels in PDMS used for this amplification process posses a depth of 200 microns and a moderate 6 microliter volume ensuring smooth microfluidic operation of the PCR mix while loading and unloading, not withstanding their highly hydrophobic nature. We have analyzed the unique hydrophobicity recovery of the SOG and PDMS surfaces using advancing contact angle of deionized water at various times after an oxygen plasma exposure. We have further substantiated our results with fluorescence studies by flowing a labeled RT-PCR (real time polymerase chain reaction) product [25] inside the channel/chamber and have developed a workable wash cycle for the labeled DNA by using elution buffer and RNase free water. We have further optimized a PDMS-silicon (with oxide layer) chip with a numerically simulated unique serpentine heater design capable of rapid thermal cycling at low power (a possible explanation of minimal evaporation). We have developed a clean bonding protocol using an intermediate Spin on Glass (Methyl silsesquioxane) (SOG) layer making PDMS irreversibly sealed to oxidized silicon substrates with an almost one order of magnitude higher bond strength than thermally grown silicon dioxide. Attenuated total reflection

fourier transform infrared spectra (ATR-FTIR) performed on a plasma exposed SOG coated surface and a plain silicon dioxide surface show a marked difference in the number of surface hydroxyl groups, which are active sites for surface bonds. Further, we have successfully explored the reusability of our platform by alternate use of positive and negative control and consecutively running this chip for multiple number of times.

3.3 Design and Optimization

3.3.1 Design of the PCR Chamber

Figure 3.1(a & b) shows the schematic of the device, a picture of the setup and heaters. The device comprises of a replica molded piece of PDMS with a chamber (diameter= 3mm, depth = 450 microns) and channels (depth = 450 microns, width = 1mm, length =12mm) leading to the inlet/outlet reservoirs (diameter = 1.5mm, depth = 450 microns) bonded to a 25.4mm X 25.4mm SOG coated silicon wafer. The silicon has a 1 micron thick oxide layer on both sides to insulate the heater fins from shorting. Ports were mounted over the inlet/outlet reservoirs for guiding PCR mix into the chamber. A thermocouple snuggly fitted inside a glass pipe with its sensing end projected outside the pipe and coated with a thin layer of epoxy was inserted into a pre-drilled hole on the top of the PDMS chamber [See figure 3.1]. The thin layer of epoxy at the tip of the thermocouple protects the TAQ polymerase from direct contact with the tip. The inhibition in the activity levels of the TAQ polymerase enzyme as it comes in contact with thermocouple tip was reported in an earlier work [27].

3.3.2 Design of Heaters

We developed a serpentine heater design by solving a simple two dimensional steady state heat conduction problem ($\nabla^2 T = 0$), $\nabla^2 = \frac{\partial^2}{\partial x^2} + \frac{\partial^2}{\partial y^2}$ [Figure 3.2]. The shape defined by one element of the serpentine design is an enclosed area with the hatched lines whose steady state thermal behavior is investigated by assuming the temperature boundary conditions to be 95^0C on three sides corresponding to the thin platinum heater lines and 24_0C (room temperature) on one side corresponding to the open side. The transient part of the heating problem is eliminated as the requirement of a PCR process is holding the fluid volume at different fixed temperatures for a certain amount of time independent of the ramp up or cooling rate [28]. The ramping up or cooling rate is important in only providing a time advantage for on-chip devices. We used a 3mmX3mm square area on the silicon surface to fabricate the heaters. The serpentine heater design was investigated with an intention of maintaining the temperature within $+1_0$C as desirable for any standard PCR process. Figure 3.2 (a) shows a schematic of the Platinum heaters. The solutions were evaluated by assuming a heater y spacing as 3mm [See Figure 3.2(b)] and by varying the x dimension from 50 microns to 75 microns to evaluate the optimum x spacing between the heater fins. We assumed 50 microns to be the minimum inter fin distance and the width of the platinum lines 150 microns in order to obtain a low overall resistance. Figure displays plots showing the different temperature distributions for different heater spacing. We solved the equation numerically with y distance of 100 microns from the edge of the heaters and found the temperature to vary between $+1_0$ C upto a heater 'x' spacing of 70 microns [Fig. 3.3], which we selected as our designed spacing. A 400nm thick platinum layer used for realizing this heater design posses a resistance value of 380~400 ohms necessitating the use of higher voltage. For operating the chip on a much lower power (~ 5 W), we reduced the resistance into a parallel combination. The overall resistance reduced to around 100~120 ohms and the "y" spacing

reduced to 0.9mm. We evaluated the solution again using a 70 microns “x” spacing for this new “y” spacing value and found that the temperature distribution was unchanged. We have also compared the performance of this serpentine heater design over continuous thin films of a similar area, as will be discussed in the results and discussion section, to find remarkably higher heating/ cooling rates.

3.4 Experimental

3.4.1 Fabrication of the Device

The heaters were fabricated on a silicon wafer with a thermally grown oxide layer of 1 micron thickness using standardized sputtering and lift off processes to realize a 20nm ‘Ti’ and a 400nm ‘Pt’ layer. [see fabrication flow chart, Fig. 3.4].The surface of the silicon wafer opposite to heater structures was spin-coated with a 140nm thick Spin on Glass [M/s Filmtronics] and thermally cycled as per the manufacturer’s specifications. The PDMS channels were fabricated using standaridized SU8 lithography (2075, M/s Microchem) and RTV 615 (M/s. GE Silicones). Ports were mounted on the inlet/ outlet reservoirs before casting the liquid PDMS and the cast was irreversibly sealed to the SOG coated substrate in a plasma etcher using 20W RIE power, 900 mTorr chamber pressure, 182 sccm oxygen flow rate and 35 secs time of exposure. These optimized parameters were suited to a maximum bond strength condition by using a methodology reported earlier by our group [29]. We used a K type, 5SRTC series, thermocouple for sensing the temperature .

3.4.2 Thermal Cycling System

We have established an automated thermal cycling system control using National Instrument’s Labview software. The control is executed by a current controller with a power MOSFET serving

as a PWM (Pulse Width Modulation) device by varying the duty cycle of the gate voltage as a switch. Figures 3.5(a) and (b) show the circuitry and the real time plot of one complete PCR cycle. The temperature control is realized by a PID controller programmed in Labview, the output of which is a continuous 100 Hz pulse train with varying duty cycle depending on the difference between the temperature set point and the measured value. The number of cycles and temperature set point of different cycles can be flexibly changed by a 2-D array. A thermal cycle is executed by reading this control array. The full IBR cycle normally takes 270 mins. in a conventional setup [30], in which the hold times at fixed temperature points is 115 mins. The remaining 155 mins. is the ramp up and cooling down time of the huge metal block sample vial holder. As indicated in Figure 3.5(b), the total IBR cycle takes around 129 mins. in the on-chip setup, of which 115 mins. are the required hold times. The ramp-up and -down times add up to around 14 mins., which is reduced by a factor of 10 from that of the conventional system. This result is achieved at a much lower input power compared to other on-chip PCR devices [13] reported with similar architecture.

3.4.3 PCR Reaction

The on-chip PCR reaction was carried out using a PCR amplification kit (M/S Qiagen). Twenty microliter of PCR mix was prepared by mixing 2 µl of 10X buffer, 0.4 µl of dNTP, 0.1 µl of TAQ, 15.5 µl RNase water, 1 µl of primer and 1 µl of sample in a Fisher Vortex Genie 2 mixer, followed by centrifugation. Five microliter of sample was amplified in a standard Perkin Elmer PCR machine and 6 µl was put through the inlet port into the channels and chamber of the onchip PCR device. Mineral oil was used to lower sample evaporation, and the ports were epoxied before executing the thermal cycle. We started with a 7 ng/ µl concentration of the template DNA and diluted this 100,000:1 times to obtain a template solution with .07 picogram/ µl . We could successfully amplify both these samples in our PCR chip. The literature reports initial concentrations of the DNA template in the range of .01 ng/ µl [9] to 30 ng/ µl. [21], amplified in

chip based PCR devices. We have been able to amplify template concentrations at least three orders lower than the existing devices using the hydrophobically recovered surfaces. To investigate the non-specific binding effects we performed contact angle studies and fluorescence characterization of the hydrophobic interiors of our chip as discussed in the results section. A suitable wash cycle comprising of a 20mins. wash with elution buffer followed by flowing RNase free water for 10mins using 87 µl/ min. flow rate was developed. One test chip after one successful PCR cycle was reused to amplify another PCR mix without any template DNA after thorough washing. As this sample was run through gel we did not see any stain, which gives us a future direction of making this chip into a reusable amplification platform.

3.5 Results and Discussions

3.5.1 Efficiency of Serpentine Heater Design

The serpentine heater design was compared to a similar sized thin continuous film heater. Figure 3.6(a) shows a photograph of both designs placed side by side in an inhouse designed microelectronic packaging board. The heater ends were wire-bonded to the copper connectors over the packaging board. The resistance was measured to be 133 ohms and 33 ohms for the serpentine and the continuous designs respectively. A current source supplying current of 380 mA was connected to the continuous film heater. The heater was thermally cycled between 95 and 58^{0}C at this fixed power value (4.77 W) for 12 cycles [Fig. 3.6 (b)]. The selected two temperature limits are typically applicable for any PCR process. The total time required to ramp the temperature up and down 12 times was found to be 2180 secs for this power value. The same power value was applied to the serpentine heater design. This corresponded to a 189 mA current and 133 ohm resistance.

The total time for ramping the temperature up and down for the same 12 cycles for this design was 561 secs. We believe that this increase in heating rate for the same input power is mainly due to lower thermal mass of the serpentine design compared to the continuous thin film design. Also, the cooling rate is high due to an increased contact area of the serpentine design with air enhancing heat convection.

3.5.2 Surface Wettablility Studies of SOG

In our earlier work [29], we performed an in-depth study on the behavior of glass and PDMS surfaces after oxygen plasma exposure. Using the sessile drop method, we were able to correlate the advancing contact angle for different plasma exposure parameters and tune that to the highest bond strength between the participating surfaces. The unexposed PDMS or SOG surface normally contains O-Si(CH_3)$_2$, which on exposure to oxygen plasma develops polar silanol groups at the expense of methyl groups [31]. This renders the surfaces highly hydrophilic which is expressed in terms of a change in advancing contact angle. We obtained the best plasma exposure parameters by this method as 20W RIE power, 900 mTorr chamber pressure, 182 sccm oxygen flow rate and 35 secs time of exposure. We plan to report this analysis as a separate study. The maximum bond strength between the SOG and PDMS surfaces was found out by doing blister tests [29] as 83 psi The unexposed contact angle of SOG surface is around 83 deg which reduced to 7 deg. after exposure We found out the bond strengths of PDMS to thermally grown silicon dioxide to be 10 psi with the same method. We performed an ATR-FTIR on the plasma exposed silicon dioxide surface and the SOG coated surface using a Nicolet 4700 spectrometer. Figure 2.5, Chapter 2 shows OH stretching broad

band spectra in the 3000-3600 cm^{-1} region for plasma treated silicon dioxide and the SOG surfaces [32].The strong broad absorption band that appears to be approximately at 3450 cm-1 [Fig. 2.5, Chapter 2] is attributed to hydroxyl groups [33, 34]. The plasma treated SOG layer exhibits a much higher presence of hydroxyl groups than the plasma treated silicon dioxide. The area under the OH peak for the treated SOG sample is calculated to be 22,754 AU (Arbitrary Units) and for the treated silicon dioxide sample it is calculated to be 2045 AU. There is approximately an order of magnitude increase in the surface OH groups on the treated SOG surface. Correspondingly, the bond strength of SOG-PDMS is approximately an order of magnitude more than that of the SiO2-PDMS). The SOG thus provides a strong basis for integration of PDMS with silicon, thermally grown silicon dioxide or any other substrate.

3.5.3 Change of Contact Angle of SOG Surface with Time

The post-exposed SOG surface showed an increase in the advancing contact angle with time. Measurements were taken after 5 mins., 1 hour, 5 hours and 2 days. The contact angle rose from 7 deg. immediately after exposure to around 63 deg. after 5 hours. No change in the contact angle was observed after 2 days indicating a full recovery of the surface and saturation in surface recovery rate after 5 hours [Figure 2.2, Chapter 2]. A similar surface recovery was found to occur in PDMS, where there is a tendency of the methyl groups to appear on the surface from the bulk of the material due to extensive rearrangement of surface bonds because of surface chain scission reactions. The SOG surface being structurally identical to PDMS should have a similar mechanism of chain scission reactions [35]. In order to confirm this hypothesis, we have performed an ATR-

FTIR spectra on the SOG surface and have found a gradual methylation and dehydroxylation with post exposure relaxation time, the details of which has been reported in Chapter 2. A similar study indicating a gradual hydrophobicity recovery of PDMS surfaces exposed to corona discharge has been reported earlier [35].

3.5.4 Non-specific Binding of DNA to Channel and Chamber Walls (Fluorescence Studies with Labeled DNA)

We have studied the effect of non-specific binding on the hydrophobic interiors of the chamber by flowing FAM labeled RT-PCR products [25] with an excitation maximum at 494nm and an emission maximum at 520nm. We fabricated two PCR devices in a manner as detailed earlier using a 170 micron thick glass slide [M/S Gold Seal] as the base instead of the heater patterned silicon wafer. The glass was used instead of silicon to accommodate the imaging modalities associated with the characterization instrument. We spin-coated SOG on this substrate and bonded a replica molded PDMS layer containing the channels and chambers thus providing an architecture identical to our device. We used a 1X50 Olympus inverted fluorescence microscope with an emission and excitation monochormator for characterization of the fluorescence intensity in the channels and the chamber. Ten microliters of FAM labeled RT-PCR (real time polymerase chain reaction) products was flown into the microchamber in one of the devices at a rate of 87 micro-liters/ min. using a syringe pump. The fluorescence level was measured using a photodiode connected to the objective through a monochromator. The data of this photodiode is digitally acquired by a computer and a temporal plot is generated. Following this, an elution buffer solution [36] (M/S Qiagen Inc.) was used to wash off

the labeled DNA from the chip in a similar manner as described earlier for 20 mins. The corresponding real time change in fluorescence intensity was plotted with time. Figure 3.7 (a) shows plots of the fluorescence intensity change observed in the device during the wash cycle. The intensity changed from 2 V to a constant 0.06 V value after 400 sec. At the end of 1200 secs a forced injection of RNase free water was provided by utilizing an on-chip plumbing arrangement and then the buffer flow was continued. The residual fluorescence dropped to 0.02 V after the RNase water flow and changed no further. The second device in which the labeled DNA had not been flown was injected with elution buffer in a similar manner for background measurement purposes. Figure 3.7 (b) shows a magnified view of the background fluorescence of the buffer from the second device with the residual fluorescence left over after the wash cycle from the first device. Both these parameters are plotted on the same time scale for an easy comparison. Both values superpose on each other showing that there is no non-specific binding of the labeled DNA inside the chamber or channel. We have further investigated amplification on the same chip after 20 mins. of washing with elution buffer and 10 mins. with RNase free water. The chip was injected with a PCR mix without the template and the thermal cycle was run. We could not see any fluorescent stain after running the post PCR mix through agrose gel as detailed in the next section.

3.5.5 Polymerase Chain Reaction Using the Chip

We used Infectious Bovine Rhinotracheitis (IBR) virus as the test assay for our on-chip studies. We used this test assay for testing on-chip amplification due to two main reasons. These are a long thermal cycling time which evaluates the reliability of our device and a

strong fluorescence response of the viral genome in any standard laboratory gel setup [37]. We performed two trials with 7ng of template DNA using our on-chip device and got conformity of amplification when the PCR product was electrophoresced with a standardized gel slab made out of a 2% agarose solution [Promega, Inc., Madison, WI]. Each time, a portion of the sample was amplified in the standard PCR machine for conformity of amplification. Figures 3.8 (a) and (b) show two such on-chip trials. In the first trial a 5 µl sample volume was amplified in the on-chip chamber. The amplified sample was removed from the micro-chamber and the inlet and outlet port side by using a hypodermic syringe. The extracted sample was run in four side- by-side wells of the gel [Fig. 3.8(a)] with the wells marked 1 used for the standard DNA ladder [M/S Qiagen Inc.], 2 for the sample amplified in the conventional setup [conformity sample], 3 for the sample from our micro-chamber [test sample] and 4 and 5 for the fluid extracted (mineral oil) from the inlet/ outlet ports. A 180 V DC potential was applied across the gel slab for 30 mins for electrophoresis. The post electrophoresis gel image indicates bands at the 527 bp region showing amplification in wells 2 and 3. Wells 4 and 5 do not show any bands because the extracted fluid was viscous and comprised mainly of mineral oil due to sample evaporation. The well 1 shows the electrophoresced DNA ladder with a bright band indicating the position of the 527 bp target stain. The other bands obtained on the gel along tracks 2 and 3 show conformity of amplification In the second trial, a new test chip with a better sealing design obtained by capping the inlet and outlet ports using epoxy, was used for amplification of the same viral DNA. Figure 3.8 (b) shows the gel image of the results. The sample was loaded in the gel pockets following the same scheme as mentioned earlier. The post electrophoresis gel image shows bands in front of

all the wells. The bands on the track 4 and 5 show amplification for the fluid extracted from the inlet and outlet ports. This may be attributed primarily to minimal sample loss by evaporation because of a better sealing design and also to temperature uniformity of the whole surface within $\pm$ 1^0C (PCR limit) due to better thermal conductivity of silicon. The repeated amplification of the PCR mix in our micro-chamber shows that the hydro-phopically recovered SOG and PDMS surfaces are not PCR inhibitors as silicon or glass substrates. The post-plasma exposed PDMS surface has been used to perform successful amplification by Xiang et. al. earlier [20]. We demonstrate a similar behavior of the SOG surface. One prominent cause of contact inhibition of PCR reaction as indicated in reference 16 is the ability of the DNA to preferentially bind to some substrates. This is attributed to the fact that the DNA, being negatively charged, binds to polar groups on any surface. As both PDMS and SOG have shown post exposure surface relaxation making the surfaces more and more non polar, the negatively charged DNA does not bind to it.

We have also tested the sensitivity of our chamber by diluting the template DNA with RNase-free water. Results have been obtained with both a conventional thermal cycler and the on-chip amplifier. We started with a standard DNA sample (7 ng/µl) as used in the conventional setup and diluted this with RNase water in the ratios 10:1, 100:1, 1000:1, 10000:1 and 100000 :1. We took 5 microliter volumes of each of these dilutions and amplified it in the conventional thermo-cycler successfully. We tried the highest dilution (corresponding to .07picogram/ µl) of the initial template in the on-chip device. On running through a slab gel, we got positive results for this dilution level. Figure 3.9 (a) shows a post electrophoresis gel image of this trial demonstrating successful

amplification. This experiment has further established the efficiency comparison of our test chip with any conventional thermo-cycler. No non-specific binding to the channels and chambers of our devices occurred as evident from the fluorescence studies. The space domain PCR devices by virtue of their ability to handle smaller fluidic volumes may be able to amplify template concentrations in the similar range as our device; but, have other limitations as discussed before. We hypothesize that the extremely hydrophobic nature of the chamber and channels in our time domain PCR device provides ideal surfaces for amplification with miniscule quantities of starting templates without requirement of other sophisticated accessories for precision fluid maneuvering. We further ran an amplification cycle in an used chip after thorough washing with Elution buffer for 20 mins. followed by RNase free water for 10 mins. However, this time, we put PCR mix without the template DNA. Figure 3.9 (b) shows the post electrophoresis gel image of the PCR products. As can be seen, there are no stains observed in the wells 2 and 3 implying that there were no DNA residues from the previous amplification run.

3.6 Conclusions and Future Work

We have optimized the micro-fabrication and design process of a PDMS-SOG-Silicon on-chip DNA amplifier for amplification of a 527 fragment of the IBR viral genome using a 51 cycle PCR process and have successfully amplified 0.07 picograms/ µl of template using this device. Fluorescence studies performed on the chip with labeled DNA indicates no non-specific binding of the DNA to the hydrophobic walls of the chamber. The chip is extremely durable and can be thermally cycled for a significant amount of time without any damaging thermal stresses, which is a main reason for failure of Glass

PDMS micro-chambers [20]. We have further developed an unique serpentine heater design through numerical simulation. We have realized a 10 fold faster ramp up and down rates with this serpentine design over its continuous counterpart [20]. In comparison to identical architectures, we have been able to achieve similar ramp up and down rates (3 deg. C/ sec) at a lower input power value (4.77 W). We have optimized the SOG-PDMS bond strength a maximum of 83 psi. This is much higher in comparison to PDMS- silicon dioxide. We characterized the silicon dioxide surface immediately after plasma exposure with an ATR-FTIR indicating very less presence of Si-OH in comparison to another exposed SOG surface. We have also traced a recovery of SOG surface with an increase in post exposure relaxation time. This provides a non sticking hydrophobic surface of the chamber walls. We have also tested our chip with sequential positive and negative control and observed no bound DNA left over from previous amplification runs after the wash step. Our final goal will be to realize a completely integrated platform on a single chip with capabilities of PCR amplification, microfluidic transport, gel electrophoresis and optical detection with on-chip waveguides.

3.7 Acknowledgements

The authors gratefully acknowledge the financial support from the National Pork Board and National Institute of Health to carry out this research. The authors also gratefully acknowledge the help of Xiaohui Chen, a doctoral student and Dr. Kevin Gillis, Associate Professor, Biological Engineering Department, University of Missouri, Columbia for Fluorescence characterization studies on the PCR chamber.

3.8 References

1. J.W. Hong, K. Hosokawa, T. Fujii, M. Seki, I. Endo, "Micro-fabricated Polymer Chip for Capillary Gel Electrophoresis", *Biotechnology Progress*, Vol. 17, pp.958-962, 2001.
2. G. Ocvirk, M. Munroe, T. Tang, R. Oleschuk, K. Westra, J. Harrison, " Electrokinetic control of fluid flow in native polydimethyl siloxane capillary electrophoresis devices", *Electrophoresis*, Vol. 21, pp.107-115, 2000.
3. B.C. Giordano, J. Ferrance, S. Swedberg, A.F.R. Huhmer, J.P. Landers, "Polymerase chain reaction in polymeric microchips: DNA amplification in less than 240 secs.", *Analytical Biochemistry*, Vol. 291, pp. no. 124-132, 2001.
4. M.A. Northrup, "DNA Amplification with a micro-fabricated reaction chamber", in the digest of technical papers of the 7th International conf. on the Solid State Sensors & actuators, Transducers 93, Yokohama, Japan, pp.924-926, 1993.
5. M.U. Kopp, A. J. DeMello, A. Manz, "Chemical Amplification: Continuous-Flow PCR on a Chip", *Science*, Vol. 28, pp. 1046-1047, 1998.
6. C.S. Liao, G.B. Lee, H.S. Liu, T. M. Hsieh, C.H. Luo, " Miniature RT-PCR system for diagnosis of RNA based viruses", *Nucleic Acids Research*, Vol. 33, pp. 1-7, 2005.
7. J.Y. Cheng, C.J. Hseih, Y.C. Chuang, J.R. Hsieh, "Performing micro-channel temperature cycling reactions using reciprocating reagent shuttling along a radial temperature gradient", *The Analyst*, Vol. 130, pp.931-940, 2005.
8. P.J. Obeid, T.K. Christipoulos, H.J. Crabtree, C.J. Backhouse, "Micro-fabricated Device for DNA and RNA amplification by continuous-flow polymerase chain

reaction and reverse transcription-polymerase chain reaction with cycle no. selection", *Analytical Chemistry*, Vol.75, pp.288-295, 2003.

9. P. Wilding, M.A. Shoffner, L.J. Kricka, " PCR in a silicon microstructure", *Clinical Chemistry*, Vol. 40, pp. 1815-1818, 1994.
10. A.F.R. Huhmer, J.P. Landers, " Non-contact Infrared Mediated Thermo-cycling for effective Polymerase Chain Reaction Amplification of DNA in Nano-liter Volumes", *Analytical Chemistry*, Vol. 72, pp.5507-5512, 2000.
11. M. Kokayashi, M. Oomura, T. Kusakawa, Y. Morita, Y. Murakami, K. Yokoyama, E. Tamiya, "Electrochemical Gene Detection with PCR chip", Transducers'01, Eurosensors XV, The 11th International Conference on Soild State Sensors and Actuators, Munich, Germany, 2001.
12. J. Khandurina, T. McKnight, S. Jacobson, L. Waters, R. Foote, J. Ramsey, " Integrated system for rapid PCR-based DNA analysis in micro-fluidic devices", *Analytical Chemistry,* Vol. 72, pp. 2995-3000, 2000.
13. S. Stern, C. Brooks, M. Strachan, A.K. Sill, J.W. Parce, "Micro-fluidic Thermocyclers For Genetic Analysis", Inter Society Conference on Thermal Phenomena, San Diego, 2002.
14. J.K. Hong, T.Fujii, M. Seki, T. Yamamoto, I. Endo, " PDMS-Glass Hybrid Microchip for gene amplification", 1st Annual, International IEEE-EMBS Special Topic Conference on Micro-technologies in Medicine and Biology, Lyon, France, 2000.
15. J. Lu, M. Enzelberger, S. Quake, "A nano-liter rotary device for polymerase chain reaction", *Electrophoresis*, Vol. 23, pp. 1531-1536, 2002.

16. M.A. Shoffner, J. Cheng, G.E. Hvichia, L.J. Kricka, P. Wilding, "Chip PCR I, Surface passivation of microfabricated silicon glass chips for PCR", *Nucleic Acids Research*, Vol. 24, pp. 375-396, 1996.

17. R.A. Mathies, P.C. Simpson, S.J. Williams, "*Process for micro-fabrication of an integrated PCR-CE device and products produced by the same*", US Patent No. 6261431 B1, 2001.

18. B.C. Giordano, E.R. Copeland, J.P. Landers, "Towards dynamic coating of glass microchip chambers for amplifying DNA via the polymerase chain reaction", *Electrophoresis*, Vol. 22, pp. 334-340, 2001.

19. J.W. Hong, T. Fujii, M. Seki, T. Yamamoto, I. Endo, "Integration of gene amplification and capillary gel electrophoresis on a polydimethylsiloxane-glass hybrid microchip", *Electrophoresis*, Vol. 22, pp. 328-333, 2001.

20. Q. Xiang, B. Xu, R. Fu, D. Li, " Real time PCR on disposable PDMS chips with a miniaturized thermal cycler", *Biomedical microdevices*, Vol.7, pp. 273-279, 2005.

21. Y.S. Shin, K. Cho, S.H. Lim, S. Chung, S.J. Park, C. Chung, D.C. Han, J.K. Chang, "PDMS-based micro PCR chip with Parylene coating", *Journal of Micromechanics and Micro-engineering*, Vol.13, pp. 768-774, 2003.

22. D.C. Duffy, J.C. McDonald, O.J.A. Schueller, G.M. Whitesides, "Rapid Prototyping of Micro-fluidic Systems in Poly(dimethylsiloxane)", *Analytical Chemistry*, Vol. 70, pp. 4974-4984, 1998.

23. H. Miyachi, A. Hiratsuka, K. Ikebukuro, K. Yano, H. Muguruma, I. Karube, "Application of Polymer-Embedded Proteins to Fabrication of DNA array", *Biotechnology and Bioengineering*, Vol. 69, pp. 323-328, 2000.

24. J. Cheng, M.A. Shoffner, G.E. Hvichia, L.J. Kricka, P. Wilding, "Chip PCR II, Investigation of different PCR amplification systems in micro-fabricated siliconglass chips", *Nucleic Acids Research*, Vol. 24, pp. 380-385, 1996.

25. J.E. Rice, J.A. Sanchez, K.E. Pierce, L.J. Waugh, "Real time PCR with molecular beacons provides a highly accurate assay for detection of Tay-Sachs alleles in single cells", *Prenatal Diagnosis*, Vol. 22, pp. 1130-1134, 2002.

26. A. Larsson, H. Derand, " Stability of Polycarbonate and Polystyrene surfaces after hydrophilization with high intensity oxygen RF plasma", *Journal of Colloid and Interface Science*, Vol.246, pp.214-221, 2002.

27. R. Oda, M. Strausbauch, N. Borson, A. Huhmer, S. Jurrens, J. Craighead, P. Wettstein, B. Ekcloff, B. Kline, J. Landers, "Infra-red mediated thermo-cycling for ultrafast polymerase chain reaction amplification of DNA", *Analytical Chemistry*, Vol. 70, pp.4361-4368, 1998.

28. M. Ibrahim, R. Lofts, P. Jahrling, E. Henchal, V. Weedn, M. Northrup, P. Belgrader, "Real time microchip PCR for detecting single base differences in viral and human DNA", *Analytical Chemistry*, Vol. 70, pp. 2013-2017, 1998.

29. S. Bhattacharya, A. Datta, J.M. Berg, S. Gangopadhyay, "Studies on surface wettability of Poly dimethyl siloxane and glass under Oxygen plasma treatment and their correlation to bond strength", *Journal of Microelectromechanical systems*, Vol. 14, No.3, 2005.

30. M. Fuchs, P. Hubert, J. Detterer, H.J. Rziha, "Detection of Bovine Herpesvirus Type 1 in Blood from Naturally Infected Cattle by Using a Sensitive PCR That Discriminates between Wild-Type Virus and Virus Lacking Glycoprotein E", *Journal of Clinical Microbiology*, Vol.37, No. 8, pp. 2498-2507, 1999.
31. F. Garbasi, M. Morra, L. Barino, E. Occhiello, *"Polymer surfaces, from physics to technology"*, pp. 345-397, New York, Wiley, 1994.
32. M.L. Hair, *Infrared Spectroscopy in Surface Chemistry*, pp. 240-290, Marcel Dekker, Inc. New York (1967)
33. H.A. Benesi, A.C. Jones, "An infrared study of the water-silica gel system," *Infrared Study of the Water-Silica Gel System,* Vol. 63, p179-182, 1959.
34. B. Lahlouh, J.A. Lubguban, G. Sivaraman, R. Gale, S. Gangopadhyay, "Silylation Using a Supercritical Carbon Dioxide Medium to Repair Plasma-Damaged Porous Organosilicate Films," *Electrochemical and Solid- State Letters*, Vol. **7**, No. 12, G338-341, 2004.
35. H. Hillborg, U.W. Gedde, "Hydrophobicity recovery of polydimethyl siloxane after exposure to corona discharges", *Polymer*, Vol. 39, No. 10, pp. 1991-1998, 1998.
36. "Hints from optimum elution of DNA from spin columns", Issue 4, 1998, www.qiagen.com.
37. L.R. Spott, Steve Wikse, Infectious Bovine Rhinotracheitis, Texas agriculture extension service, Texas A&M university, *Agricultural communications,* 2002.

3.9 Figures

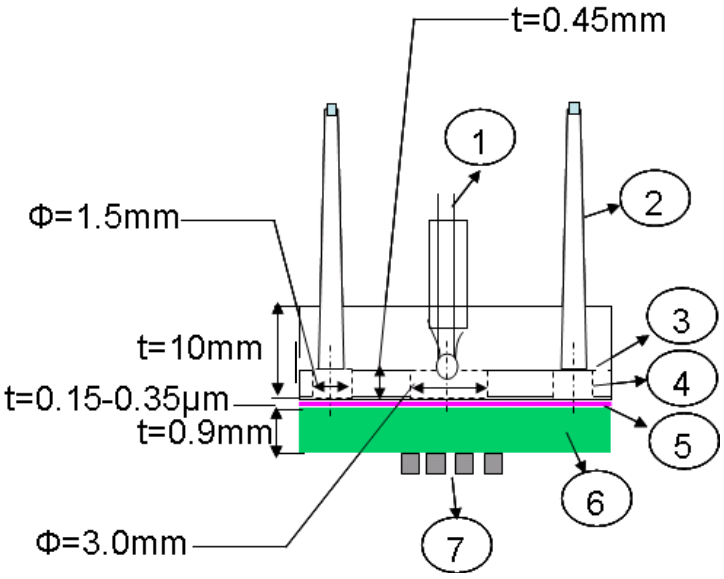

(a)

Component Name	Dimensions
Poly Dimethyl Siloxane (Channels)	(depth = 450 μm, width= 1mm, length =12mm)
Inlet outlet reservoirs	(diameter = 1.5mm, depth = 450 μm)
Poly Dimethyl Siloxane (Chamber)	(diameter=3mm, depth = 450 μm)

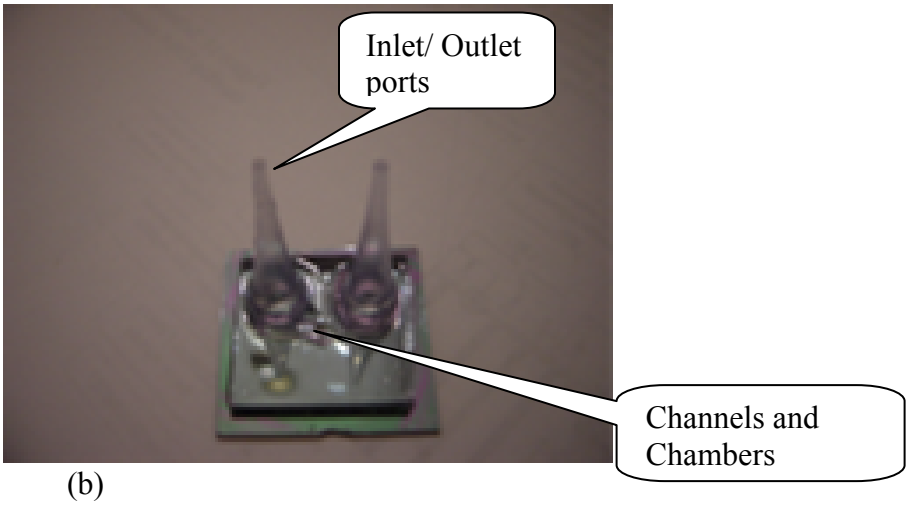

(b)

Figure 3.1: (a) Schematic of the Silicon PDMS cassette. (b) Image of a typical device.

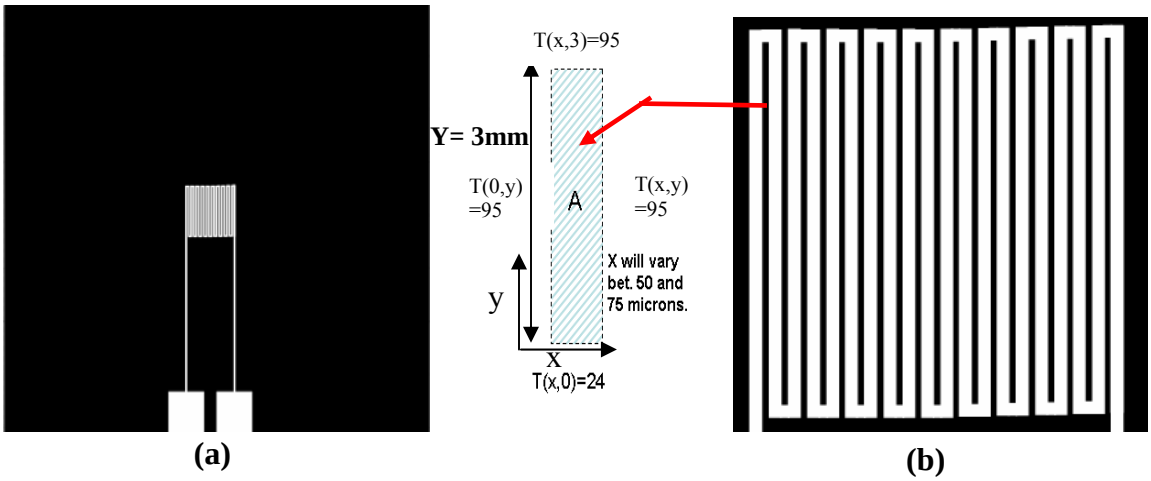

Figure 3.2: (a) Mask for Platinum heaters. (b) Magnified view of the heaters with description of the boundary condition and X-Y scale.

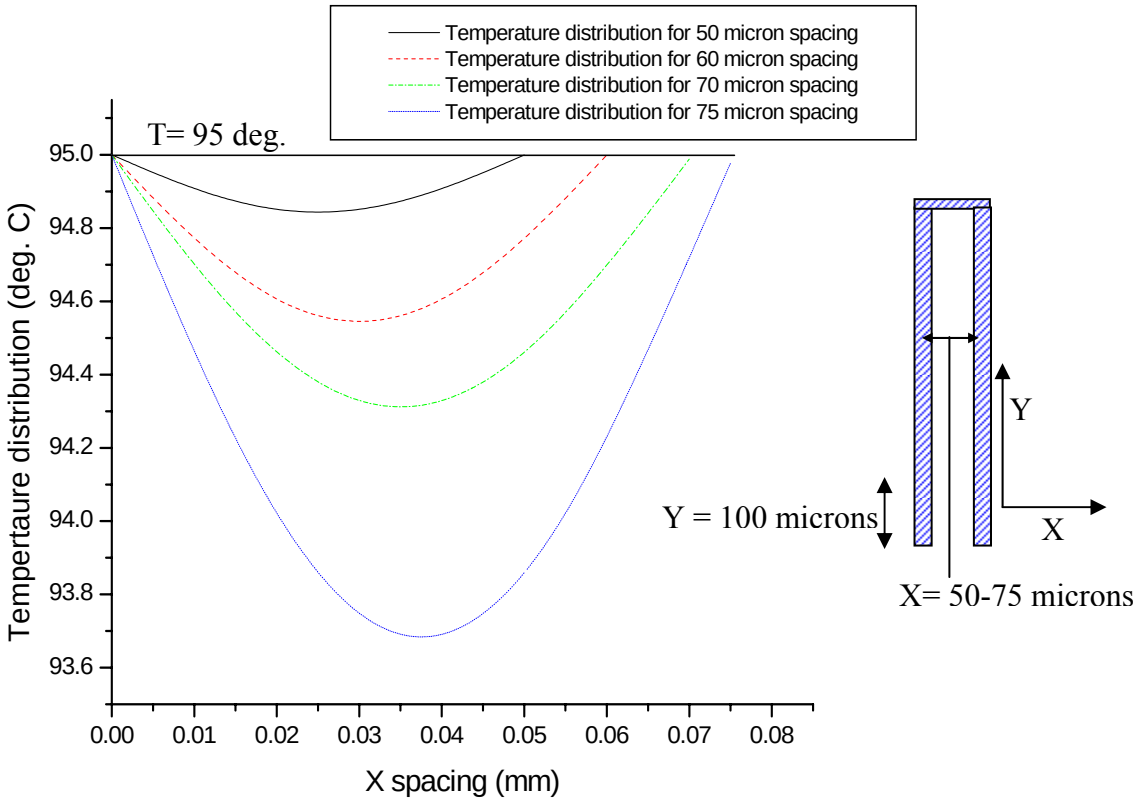

Figure 3.3: Temperature distribution with 'X' spacing varying from 0 to 75 microns.

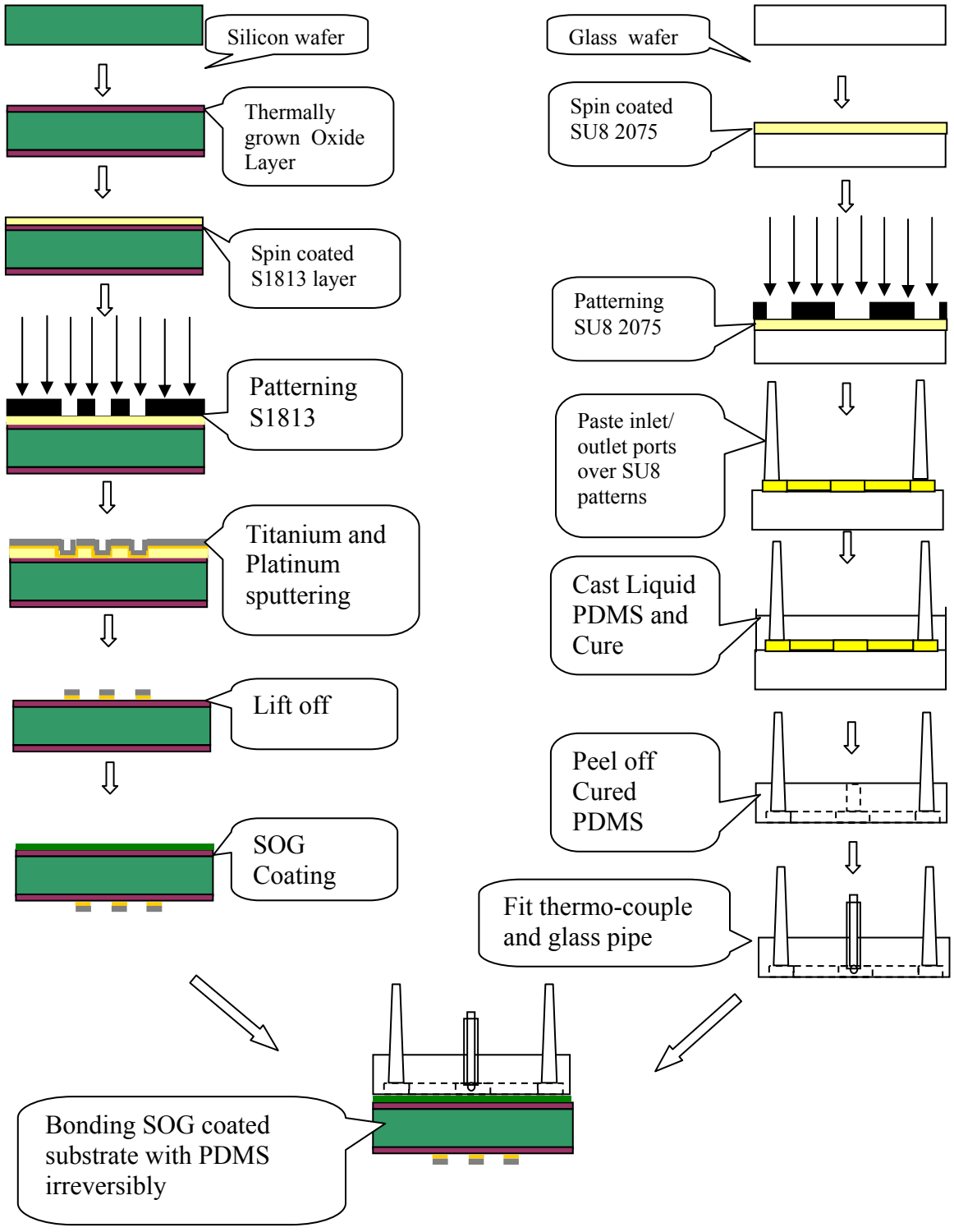

Figure 3.4: Fabrication process flow chart

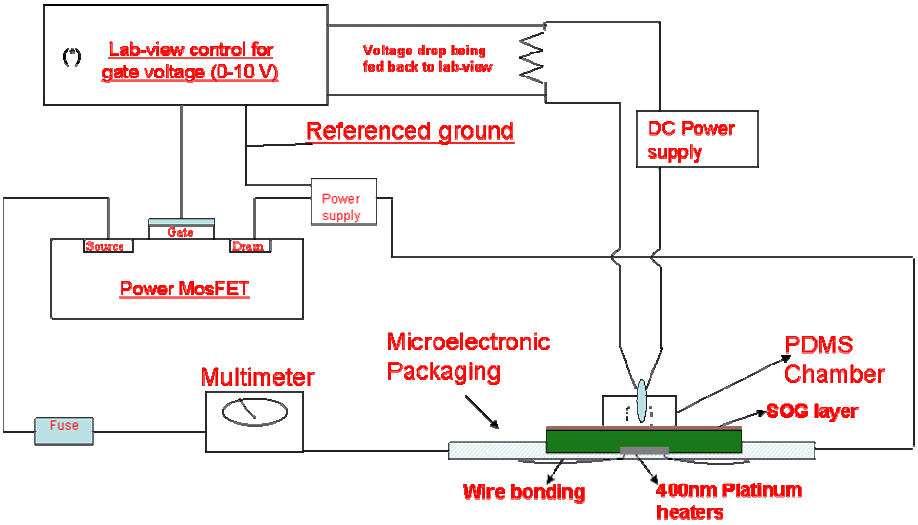

Figure 3.5: (a) Power MOSFET driven circuit acting as a current controller

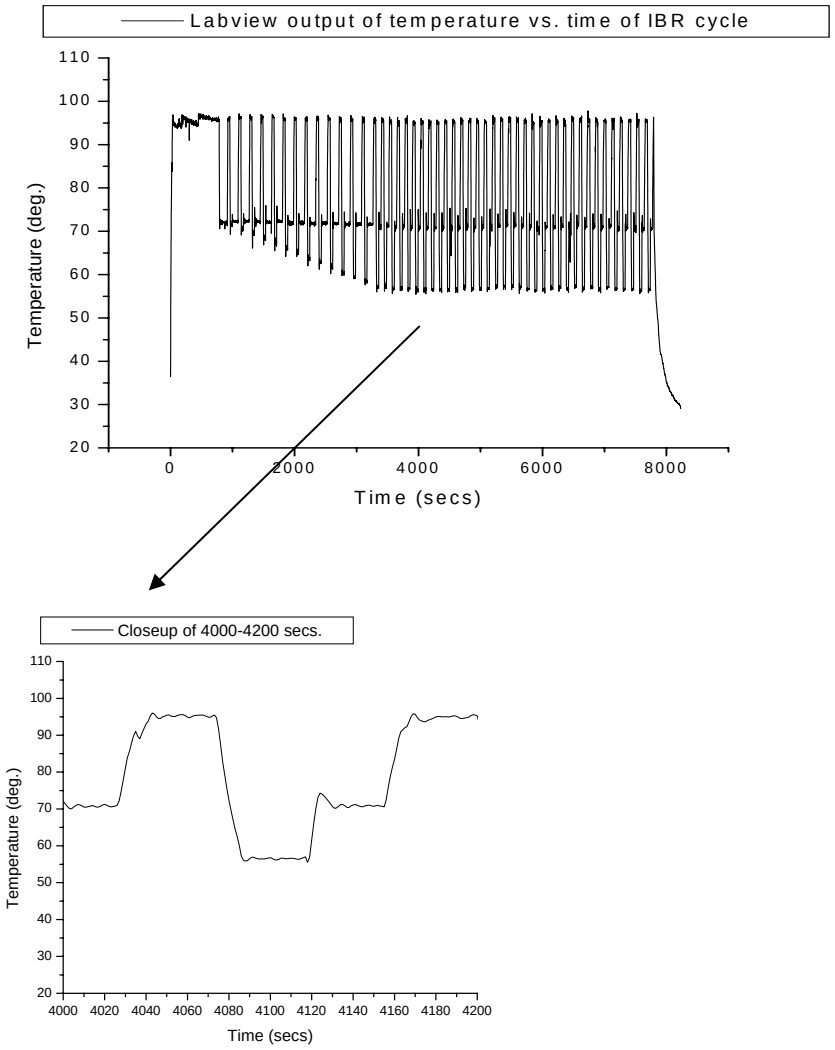

Figure 3.5: (b) Real time plot of temperature time data plotted by Lab-VIEW

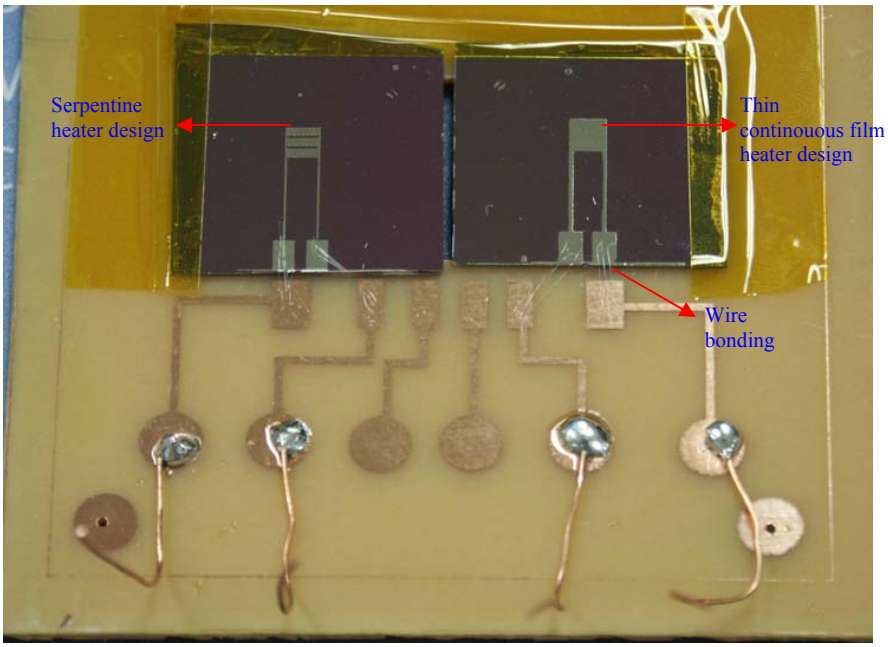

3.6: (a) Serpentine versus thin film continuous heaters wire bonded to copper connections on the Microelectronic packaging.

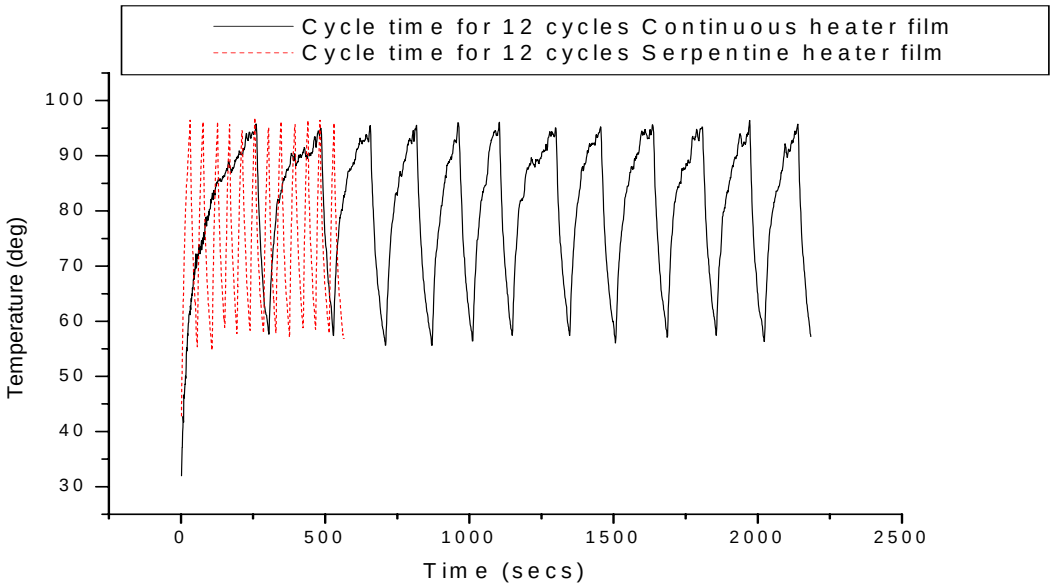

3.6: (b) Comparison of temperature ramp-up and ramp down time between continuous thin film heater and serpentine heater in a 3mm X 3mm area for 12 cycles.

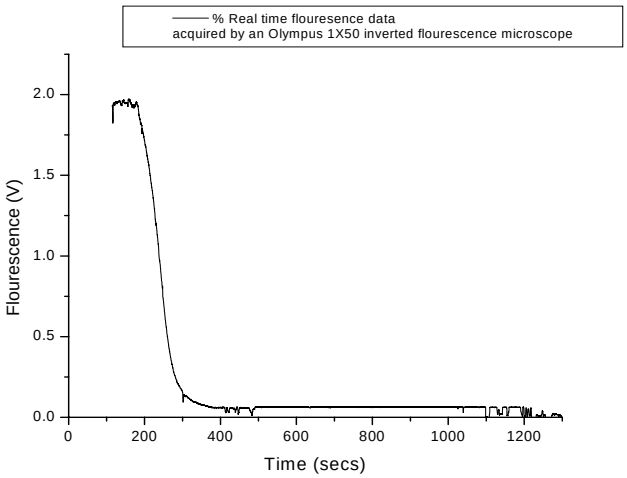

Figure 3.7: (a) Reduction in Fluorescence Intensity (Volts) with time (secs.)

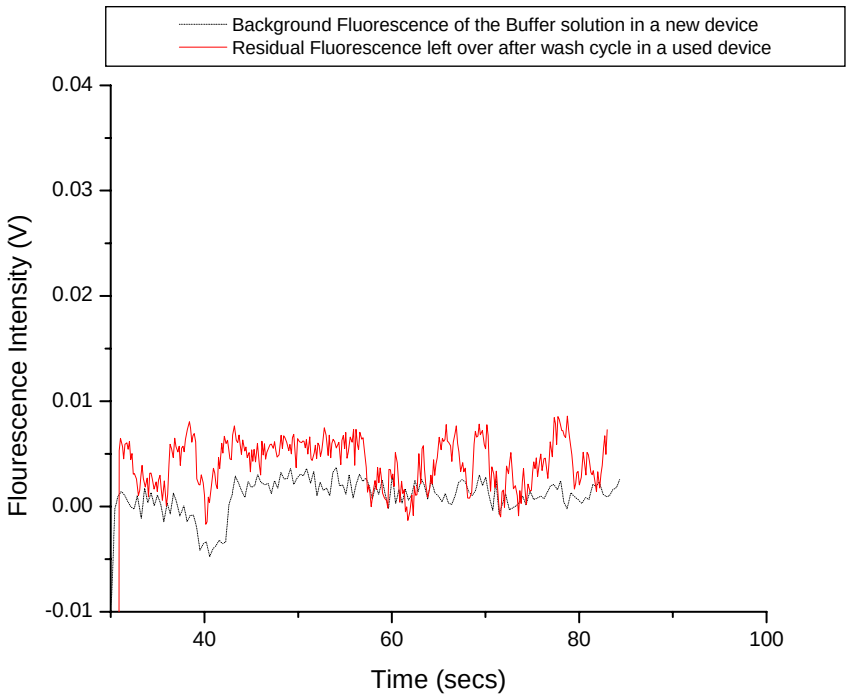

Figure 3.7: (b) Background fluorescence of the buffer solution and residual fluorescence left over in the micro-chamber.

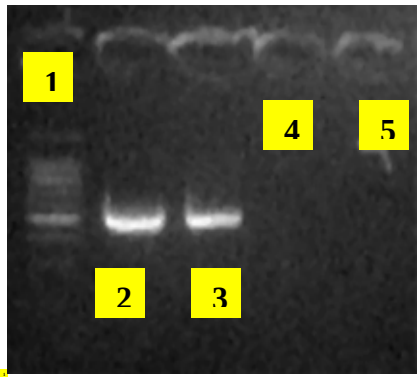

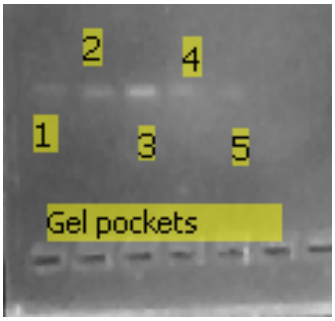

(a) (b)

Figure 3.8: (a) Slab gel image for the first on chip amplification (b) Slab gel image for the second on chip amplification

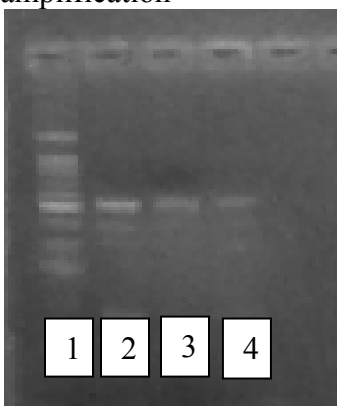

Figure 3.9: (a) Slab gel image of a 100000:1 dilution of initial template by amplifying on the on-chip device

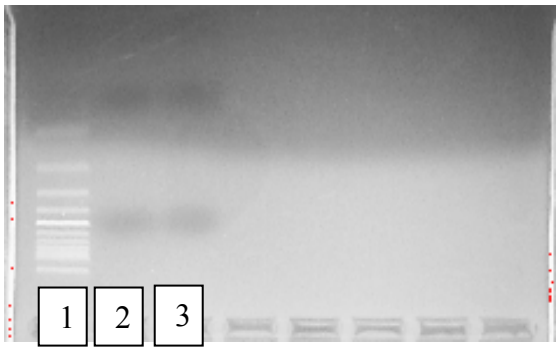

Figure 3.9: (b) Slab gel image of an amplified product without template DNA on a test chip after washing off the PCR products from the previous run

Chapter 4

HIGH CONDUCTIVITY AGAROSE NANO-PLATINUM COMPOSITE

4.1 Abstract

Micro-channel electro-phoretic separation systems have become an important part of gene sequencing and analysis. A significant amount of research has focused on the development of fast and high resolution separation systems as part of miniaturized genotyping platforms. These devices are not suitable for field deployment due to the high voltage needed for micro-channel based electrophoresis. In order to address this issue, we have developed a new doping technique of agarose gels with conducting platinum nano-particles which enhances the conductivity of agarose gels by five folds. We have observed a faster movement of DNA band in this novel gel material at lower operating voltages. We believe that the higher conductivity of the agarose and an associated faster movement of DNA arise from an increased dielectric constant of this doped material resulting in increased ionic mobilities.

4.2 Introduction

Technologies to enable miniaturized DNA electrophoresis within fused silica capillaries (50-75 microns ID) have been under development since last two decades [1]. The large surface area to volume ratio in micron-sized capillaries leads to an effective loss of the resistive Joule heat, allowing the voltage limitations that are imposed in slab gel electrophoresis to be surpassed greatly [2]. This also implies the necessity to use higher

electric fields (within the limits imposed by biased reptation [3]) to achieve higher DNA separation speeds in micro-channel systems. The development of DNA separation matrices for capillary electrophoresis systems remains an important endeavor, as the properties of the sieving polymers directly dictate the separation resolution and the migration behavior of DNA molecules, as well as the difficulty or ease of micro-channel loading of the matrix [4,5]. Some of the commonly used matrices include agarose, polyacrylamide, hydroxyalkylcellulose [6], polyvinyl alcohol and its copolymers [7] etc. Currently, a tremendous research emphasis is provided to micro-fluidic integrated gene analysis systems with sample preparation and analysis process on a single micro-fabricated substrate [8-10]. Such systems demonstrate an overall reduction in size, reduced use of reagents, increased speed and accuracy of analysis, and increased portability for field use etc. The field applications of such devices, however, are limited by power requirements imposed by the highly resistive capillary columns. The typically applied DC voltages to gel filled micro-fabricated capillaries in order to execute electrophoresis run in several kilovolts (10-30 KV) which can be only achieved in a laboratory setup [11]. Since speed and resolution of DNA separation have been the main focus of research in previous work, the ability to electrophorese at a lower voltage using conducting gel matrices has not been accomplished so far. Metal nano-particles, owing to their extremely small sizes and higher percentage of surface atoms (in comparison to bulk particles), posses totally different characteristics than their macro counterparts [12] and thereby, can induce significant changes in composites[13]. These characteristics can be successfully tailored to change electrical, optical, chemical, magnetic , catalytic or a variety of other properties of materials[14].

In this work, we have developed a novel gel material by doping agarose matrices with externally synthesized platinum nano-particles [15]. The platinum particles are chemically synthesized using a reduction process and mixed with agarose matrix forming an uniformly distributed array. The dielectric constant is found to significantly increase due to doping with Platinum nano-particles. The doped agarose films show a conductivity increase by a factor of five which increases approximately in a proportional manner with the platinum concentration. A probe station (M/s Micromanipulator) is used to perform IV measurements of agarose films using two disjointed sputtered thin film (160nm) platinum electrodes. The platinum doped agarose gel slabs, tested by physically translating a 527 bp DNA stain, show increase in mobility of the fluorescent bands. The increase in mobility and the higher conductivity is attributed to the enhanced dielectric constant. A 100-1000 bp gene marker has been successfully electrophoresced in this new gel material indicating that the gel resolution remains unaffected due to the doping process.

4.3 Experimental

4.3.1 Preparation of Platinum Colloids by Reduction with Sodium Boro-hydride

Platinum hydrosol was prepared by using a method reported earlier by Chen et. al. [15].

A typical procedure for obtaining the hydrosol is described as follows. A 10 ml of 5.8×10^{-3} M Potassium platinum (II) tetrachloride (K_2PtCl_4) was mixed in a schlenk flask under inert argon environment with 1.0ml of 2.67×10^{-2} M MSA (mercapto-succinic acid, M/s Sigma Aldrich). A magnetic stirrer was used for 5mins. and 5ml of 13.72 ×

10^{-2} M sodium boro-hydride (M/s Alfa Aesar) solution was added drop by drop to this mix. The solution color immediately changed indicating the formation of platinum [16]. The stirring was continued for another 30mins before the solution was taken out from the inert atmosphere. The molar ratio between MSA and K_2PtCl_4 was obtained as 0.46 (S/Pt), which is the same as reported by Chen et. al.[15]. Keeping the S/Pt ratio identical, the concentration of each component of this solution was doubled.

4.3.2 Preparation of Agarose Platinum Mix

Each platinum hydrosol solution was separately mixed with 1X TAE (Triacetate buffer) (pH=8.4)(M/S Fisher BioReagents) buffer sample in 1:4 volume ratio. Molecular biology grade low EEO (electro-endosmotic flow) agarose was mixed 2% (weight/ vol.) with this solution and the agarose was melted by heating to 80 deg. C in a microwave oven. A thin film of this material was spun on a plain silicon substrate and heated in a vacuum oven (at 60 deg. C overnight) for further characterization.

4.3.3 I-V Characterization for Measurement of Conductivity

Thoroughly cleaned laboratory 25.4mm ×25.4mm glass slides were sputter coated with two 1cm ×1cm square platinum electrodes separated by 1000microns (130nm thick) using standardized liftoff techniques [17]. A micromanipulator probe station was hooked to a Lab-VIEW based data acquisition system (DAQ, M/S National Instruments). A thin layer of the agarose melt with and without the nano-particle solution was spun bridging the two metal films and the I-V data was acquired by a computer (in 0-20 V range). Subsequently, a plot between the current density and electric field was obtained. The I-V

characteristics remain linear between 0-15V, after which the agarose starts melting. The corresponding field value at this melting point is recorded to be approximately 100-120 V/cm.

4.3.4 Characterization of the Nano-particles and Doped Films

A JEOL 1200 EX transmission electron microscope (TEM) was used to determine the size of the particles. The mean particle size and size distribution were obtained from the digitized photo images using Adobe Photoshop software. The silicon substrate with a dried film of the composite material was characterized using a S-4700 Hitachi scanning electron microscope (SEM) after a layer of carbon coating. The energy dispersive spectroscopy (EDS) was performed on these carbon coated agarose films using 10KeV accelerating voltage.

4.3.5 Measurement of Dielectric Constant of the Films

The plain and doped agarose films were spun coated on a p+ (0.0030-0.0070 Ω-cm) silicon substrate and Titanium metal was thermally evaporated in an electron beam system and patterned using a shadow mask. The CV measurements were performed on this film using a HP 4284A LCR meter. The dielectric constants of the films were calculated using a parallel plate capacitor model.

4.3.6 DNA Mobility Studies

The agarose melt with and without platinum hydrosol were poured as slabs and a PCR (Polymerase chain reaction) amplified 527bp viral DNA was electrophoresced through

these gels at identical voltages. A digital image was acquired on a Kodak inverted camera after 10, 15, 20 and 25min. intervals at voltages ranging from 200 V -50 V and a comparison of DNA mobility in both gel materials was performed.

4.4 Results and Discussion

4.4.1 Preparation of the Platinum Hydrosol

The platinum hydrosols of two different platinum concentrations were prepared by a reduction of potassium platinum (II) chlorate by sodium boro-hydride in surfactant (mercapto-succinic acid) micelles. Figure 4.1 (a) shows a TEM image of the spherical platinum nano-particles on a copper grid. The digital images were analyzed for particle size and distribution. Figure 4.1(b) shows a histogram for the particle size distribution on a count of 550 as the total number of particles. The mean diameter of the particles is calculated to be 13.16 ± 3.93nm. The sizes of these particles can be varied by changing concentration of the reducing agent (sodium boro-hydride) with respect to the chloro-platinate solution [16].

4.4.2 Agarose Platinum Mix

The agarose platinum mix was prepared by microwave heating of 2% (by weight) agarose powder in a solution of 1×TAE buffer and the nano-platinum dispersion mixed in a 1:4 volumetric ratio. A thin 1 micron film of this composite was spun on a silicon substrate and dehydrated overnight by heating at 60 deg. C under vacuum. This film was carbon coated and visualized further with a field emission scanning electron

microscope.(SEM) [Fig. 4.2(a)]. We found a well arranged array of platinum nano-particles of sizes in the range of 200-250 nm buried in the agarose matrix . The platinum agarose composite film was further analyzed using electron dispersive spectroscopy (EDS). An appreciably high peak around 2.09 KeV [Fig. 4.2(b)] resulting from the "Mα platinum lines" was observed. This indicates a strong presence of metallic platinum within the agarose matrix. There is no PtCl peak at 2.62 KeV indicating the complete reduction of the chloro-platinate salt. The particle aggregation observed in the agarose platinum films is a result of the microwave heating process. On performing a TEM of the platinized agarose we found a wide range of particle sizes buried in the agarose matrix. [Fig. 4.3]

4.4.3 IV- Characteristics

Two disjointed thin film platinum electrodes (thickness = 130nm, measured with a profilometer) were deposited on a well cleaned glass slide using sputtering and liftoff techniques. The two films are separated by a distance of 1000 microns. Agarose and its nano-platinum doped composite were selectively spin coated over this structure bridging the two disjointed electrodes and leaving end points for electrical contact. A Micromanipulator probe station connected to a Lab-VIEW operated data acquisition system and a Keithley 2400 source-meter was used to perform the IV measurements. Figure 4.4 shows a plot between the electric field (V/cm) and current density (amp/sq.cm). We have used high electric field values (maximum = 120 V/cm) for all our measurements with a future consideration of investigating their behavior in micro-capillaries. The ohmic conductivities in agarose gels have been reported earlier to be a

function of buffer pH, ionic strength and temperature (dependent on electric field) [21]. The average bulk conductivity of a plain agarose film using this method is found as 3.152 ± 0.103 S cm^{-1}. On doping with the lower concentration platinum hydrosol, the average conductivity is calculated as 7.206±0.144 S cm^{-1}. The conductivity changes to 14.07 ± 1.24 S cm^{-1} as the hydrosol with double the platinum content is used. We have found an approximately linear increase in the conductivity with change in platinum concentration. The ohmic conductivity increase obtained as result of doping with the higher platinum concentration is found to be almost five folds.

4.4.4 Measurements of Dielectric Constant

The CV measurements were performed on the different films spun coated on p+ (0.0030-0.0070 Ω-cm) Si substrates using a HP 4284A LCR meter. The Ti top contacts were electron beam evaporated and patterned using a shadow mask. The film thicknesses were measured with an alpha-step 200 profilo-meter (M/s Tencor Instruments). The dielectric constants were determined for the fully dried and wetted films for both doped and plain agarose. Figure 4.5 shows the frequency vs. dielectric constant (ε) comparison for the agarose (open squares) and the platinum agarose composite (open circles). The difference between the two curves is more prominent at lower frequencies. Nano-particles of noble metals have been used for increasing ε of polymer films in previous work [22]. The isolated metal nano-particles become polarized due to the presence of an applied electric field, thus enhancing the ε value of the medium. The constant nature of the difference at higher frequencies can be attributed to the inability of the dipoles to align with the changing electric field [23]. The higher ε value can be attributed to an overall change in

the background dielectric constant (real part of ε) due to the effective medium theory [23]. A comparison of the ε values was made at 1KHz as suggested earlier by Kundu et. al.[22]. For the plain agarose this was obtained as 2.4 whereas after doping with the highest conc. platinum solution, this changes to 19.2 which is about 8 times higher. As we see here that the ε value of the composite material is higher than either of the constituents which may be coming from quantum effect introduced by the dispersed phase. We used the Bergemen model to calculate the volume fraction of the dispersed platinum nano-particles using the following equation:

$$\varepsilon = \phi^2 \varepsilon_m + (1-\phi)^2 \varepsilon_g + 2\phi(1-\phi)(\frac{1}{\varepsilon_g} - \frac{1}{\varepsilon_m}) \ln(\frac{\varepsilon_m}{\varepsilon_g}) \qquad (1)$$

Where, ε_m is the magnitude of the dielectric constant of the dispersed platinum phase, ε_g is the dielectric constant of the agarose, ϕ is the volume fraction of the dispersed phase and ε is the dielectric constant of the composite. We tried to estimate the volume fraction by plugging in the values of the dielectric constant of platinum (13.4) [24], agarose (2.4) and the composite material (19.2)(obtained experimentally). The volume fraction is calculated to be above unity which explains that the composite does not behave as a bulk material. We performed an UV-Vis absorbance spectra of the platinum dispersed agarose material [Figure 4.6] and found a sharp peak in 220nm which can be attributed to the Pt nano-particles [25]. Another smaller peak near 300nm is observed due to the presence of platinum particle aggregates [26]. The absorbance at 220nm is around 20 times higher than that at 300nm which demonstrates a higher mono-dispersity of the

nanoparticles in agarose matrix. A similar feature can be observed in the TEM image of the agarose platinum films which demonstrates a much smaller presence of platinum aggregates over the mono-dispersed phase. We could not perform dielectric measurements of the wet samples because of thickness variability of the films

4.4.5 Increased DNA Mobility in the New Material

We have successfully electrophoresed a 527 bp DNA segment and observed an enhancement in its mobility with addition of platinum nanoparticles. The figure 4.7 shows images of agarose and platinum doped agarose taken at 10, 15, 20 and 25mins. at a DC potential of 200 V. We have used the higher concentration of platinum for this experiment. Similar images taken at 150, 100 and 50 volts were also analyzed. The mobility of the DNA stains was calculated using the one dimensional mobility equation [27].

$$\mu = v/ E \qquad (2)$$

where , μ = mobility of the stain, v= Velocity (cm/ sec.), E= Electric Field (V/cm)

The mobility values are calculated from the various images and these are plotted with the voltage values [Fig.4.8]. We have observed an increase in the mobility of the DNA stain at lower electric fields (8 V/cm) from 6.6E-5 cm^2/ V.sec to 9.3E-5 cm^2/ V.sec(1.5 times). No substantial difference was observed in mobility values below this electric field.

4.5 Discussion

We have observed a 1.5 fold increase in the DNA mobility at 8 V/cm electric field and a five fold enhancement in the conductivity as described earlier due to the inclusion of the platinum nano-particles in the gel matrix. At electric fields below this, the mobility of different DNA strands do not show any remarkable difference in both doped and plain agarose gels. The difference in mobility increases at higher field values as the field is increased to 16 V/cm. Hanna et. al. has reported the formation of NaCl salt in the hydrosol as a result of the reduction process of hexachloroplatinic acid [28]. A similar reaction mechanism in our case points to the formulation of NaCl and KCl salts in the platinum hydrosols, resulting as byproducts of the reduction process. This should increase the overall ionic strength which might be a cause of increased conductivity [21], although the enhancement in sample (527 bp DNA) mobility cannot be explained from this hypothesis. Stelwagen et. al. have reported the reduced mobility of DNA strands owing to the inclusion of low concentrations of NaCl in TAE buffer solution earlier [29]. The decrease in mobility with increasing conductivity appears to be due to the screening of the DNA molecules by the counter-ions in the surrounding ion atmosphere. However, we have observed the opposite behavior in the platinum-agarose composite. The SEM images show an ordered array or arrangement of these particles within the agarose. The dielectric constant of the medium enhances by a factor of 8 on doping this with platinum nano-particles. The DNA molecules being electrophoresed through both gels are larger in size compared to the surrounding ionic species. Therefore, their electrophoretic mobility in the medium is determined by the following equation:

$$u = \varepsilon\varepsilon_0\zeta / \eta \qquad (3)$$

where, u= mobility of the ion, ε is the dielectric constant of the medium, ζ is the zeta-potential of the ion and η is the viscosity of the medium [30]. The viscosity of the medium typically depends on the agarose % which remains unaltered in our case in both plain and doped agarose. We hypothesize that the enhanced DNA mobility in case of the new composite material arises from an enhancement in the dielectric constant due to presence of the dispersant phase in the agarose medium. The slope of the mobility versus electric field curve doubles in case of the doped agarose showing possibility of capillary electrophoresis at lower electric field values. We have demonstrated capillary electrophoresis in plain agarose capillaries in an earlier work [31] by using field values in the range of 70-80 V/cm (applied voltage =300 V). We have successfully electrophoresed a 100-1000 bp gene marker [Fig. 4.9] by using this gel material with a high resolution indicating no association of the fixed platinum phase with the sample. In our future work we plan to study the capillary electrophoresis with agarose platinum composites injected into micro-channels at field-deployable low voltages.

4.6 Conclusion

We have been able to develop a new Platinum Agarose composite material with enhanced sample mobility and increased conductivity. The sample mobility in the composite increases from 6.6E-5 cm^2/ V.sec to 9.3E-5 cm^2/ V.sec(1.5 times) at low (8V/cm) field values. The slope of the mobility versus electric field characteristics increase by a factor of 2. The conductivity of the new composite is found to increase five

folds. We believe this mobility increase comes from an enhancement of dielectric constant of the medium. We further plan to investigate this gel material further by injecting into micro-channels and capillaries for low voltage capillary electrophoresis.

4.7 Acknowledgements

The authors gratefully acknowledge the financial support from the National Pork Board and National Institute of Health to carry out this research. They also acknowledge the ellipsometry expertise provided by M. Othaman is analyzing film thicknesses.

4.8 References

1. A.S. Cohen, A.R. Najarian, A. Paulus, J.A. Guttman, B.L. Smith, B.L. Karger, "Rapid Separation and Purification of Oligonucleotides by High-Performance Capillary Gel Electrophoresis", *Proceedings of the national academy of science*, Vol. 85, pp. 9660-9663, 1988.
2. C.W. Kan, C.P. Fredlake, E.A.S. Doherty, A.E. Barron, " DNA sequencing and genotyping in miniaturized electrophoresis systems", *Electrophoresis*, Vol. 25, pp. 3564-3588, 2004.
3. C.R. Canter, C.L. Smith, "*Genomics: The science and technology behind the human genome project*", pp.120-125, John Wiley and Sons Inc., New York, 1999.
4. M.N. Albarghouthi, B.A. Buchholz, E.A.S. Doherty, F.M. Bogdan, H. Zhou, A.E. Barron, "Impact of polymer hydrophobicity on the properties and performance of DNA sequencing matrices for capillary electrophoresis", *Electrophoresis*, Vol. 22, pp. 737-747, 2001.
5. A.E. Barron, W.M. Sunada, H.W. Blanch, "Impact of polymer hydro-phobicity on the properties and performance of DNA sequencing matrices for capillary electrophoresis", *Biotechnology and Bioengineering*, Vol. 52, pp.259-270, 1996.
6. H.J. Tian, J.P. Landers, "Hydroxyethylcellulose as an effective polymer network for DNA analysis in uncoated glass microchips: optimization and application to mutation detection via heteroduplex analysis", *Analytical Biochemistry*, Vol. 309, pp. 212-223, 2002.
7. T. Moritani, K. Yoon, B. Chu, "DNA capillary electrophoresis using poly(vinyl alcohol). II. Separation media", *Electrophoresis*, Vol. 24, pp. 2772-2778, 2003.

8. A. Manz, H. Minhas, " The full potential, Editorial Article", *Lab on Chip*, Vol. 1, 1N-2N, 2001.
9. A. Manz, J.C.T. Eijkel, " Miniaturization and chip technology. What can we expect?", *Pure Applied Chemistry*, Vol. 72, pp. 1555-1561, 2001.
10. D.R. Reyes, D. Iossifidis, P.A. Auroux, A. Manz "Micro Total Analysis Systems. 1. Introduction, Theory, and Technology, 2. Analytical Standard Operations and Applications", *Analytical Chemistry*, Vol. 74, pp.2637-2652, 2002.
11. P. Camilleri, *" Capillary electrophoresis, theory and practice"*, pp. 300-310, CRC press Inc., Florida 2000.
12. M.C. Daniel, D. Astruc, " Gold Nano-particles: Assembly, Supra-molecular Chemistry. Quantum size related properties, and applications toward biology, catalysis and nanotechnology", Chemical Review, Vol. 104, pp. 293-346, 2004.
13. G.C. Righini, A. Verciani, S. Pelli, M. Guglielmi, A. Martucci, J. Fick, G. Vitrant, " Sol gel glasses for nonlinear optics", Pure applied optics, Vol. 5, pp. 655-666, 1996.
14. S.Y. Zhao, S.H. Chen, S.Y. Wang, D.G. Li, H.Y. Ma, " Preparation, phase transfer, and self assembled mono-layers of cubic Pt Nano-particles", Langmuir, Vol. 18, pp. 3315-3318, 2002.
15. S. Chen, K. Kimura, " Synthesis of Thiolate stabilized platinum nano-particles in protolytic solvents as isolable colloids", Journal of Physical Chemistry B., Vol. 105, pp. 5397-5403, 2001.

16. J. Yang, J.Y. Lee, T.C. Deivaraj, H.P. Too, " An improved procedure for preparing smaller and nearly mono-dispersed thiol stabilized platinum nano-particles", *Langmuir*, Vol. 19, pp. 10361-10365, 2003.

17. J.Y. Cheng, C.J. Hseih, Y.C. Chuang and J.R. Hsieh, "Performing micro-channel temperature cycling reactions using reciprocating reagent shuttling along a radial temperature gradient", *The Analyst,* Vol. 130, pp.931-940, 2005.

18. F. Gaboriaud, J.J. Ehrhardt, "Effects of different crystal faces on the surface charge of colloidal goethite particles: An experimental and modeling study", *Geochimica et Cosmochimica Acta*, Vol. 67, pp.967-983, 2003.

19. P. Hesleitner, D. Babic, N. Kalay, E. Matijevic, " Adsorption at solid/ solution interfaces, Surface charge and potential of colloidal Hematite", *Langmuir*, Vol. 3, pp. 815-820, 1987.

20. Personal communication with Lou Ross, Electron microscopy core, University of Missouri, Columbia, MO.

21. B.W. Janicki, S.A. Aron, A.S. Berson, "Technical factors affecting an immunoelectrophoretic reference system for analysis of mycobacterial antigens", *Applied Microbiology*, Vol. 25, pp. 130-134, 1973.

22. T.K. Kundu, D. Chakravorty, " Nano-composites of lead-zirconate-titanate glass ceramics and metallic silver", *Applied Physics Letters*, Vol. 67, pp. 2732-2734, 1995.

23. T. Kempa, D. Carnahan, M. Olek, M. Correa, M. Giersig, M. Cross, G. Benham, M. Senett, Z. Ren, K. Kempa, "Dielectric media based on isolated metallic nanostructures", *Journal of applied physics*, Vol. 98, pp. 034310/1-4, 2005.

24. S. Roberts, " Interpretation of the optical properties of metal surfaces", *Physical Review*, Vol. 100, pp. 1667- 1671, 1955.

25. H.H. Ingelsten, R. Bagwe, A. Palmqvist, M. Skoglundh, C. Svanberg, K. Holmberg, D.O.Shah, " Kinetics of the formation of nano-sized platinum particles in water-in-oil micro-emulsions", *Journal of colloid and interface science*, Vol. 241, pp.104-111, 2001.

26. J.F. Rivadulla, M.C. Vergara, M.C. Blanco, M.A.L. Quintela, J. Rivas, " Optical properties of platinum particles synthesized in micro-emulsions", *Journal of Physical Chemistry B*, Vol. 101, pp. 8997- 9004, 1997.g

27. D.M. Hawcroft, *" Electrophoresis: The Basics"*, pp. 53-70, Oxford University Press, New York, 1997.

28. H.H. Ingelsten, R. Bagwe, A. Palmqvist, M. Skoghlund, C. Svanberg, K. Holmberg, D.O. Shah, " Kinetics of the formation of Nano-sized platinum particles in water oil micro-emuslions", *Journal of Colloid and Interface science*, Vol. 241, pp. 104-111, 2001.

29. E. Stellwagen, N.C. Stellwagen, " The free solution mobility of DNA in Tris-acetate- EDTA buffers of different concentrations, with and without added NaCl", *Electrophoresis*, Vol. 23, pp.,1935-1941, 2003.

30. T.H. Rieger, "*Electrochemistry*", pp. 145-147, Prentice Hall, inc., New Jersey, 1987.

31. S. Bhattacharya, Y. Gao, V. Korampally, S.A. Grant, S.B. Kleiboeker, K. Gangopadhyay, S. Gangopadhyay, "*A novel on-chip platform for amplification of DNA*", Provisional patent filed.

4.9 Figures

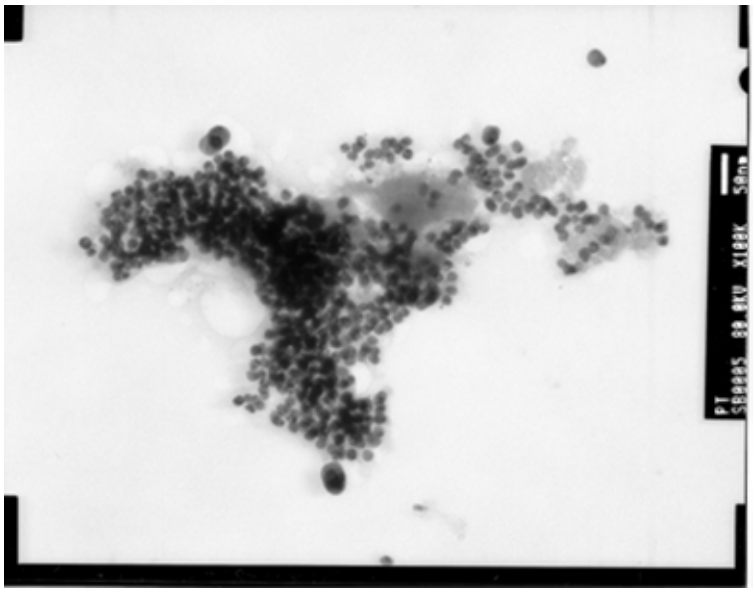

Figure 4.1: (a) TEM image of Platinum nano-particles

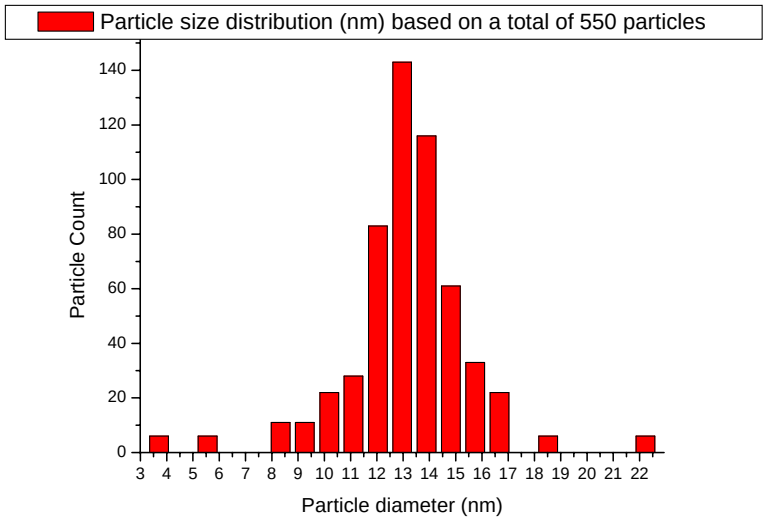

Figure 4.1: (b) Particle size distribution (average particle size= 13.16nm, Std. Dev. = $\pm$ 3.93nm)

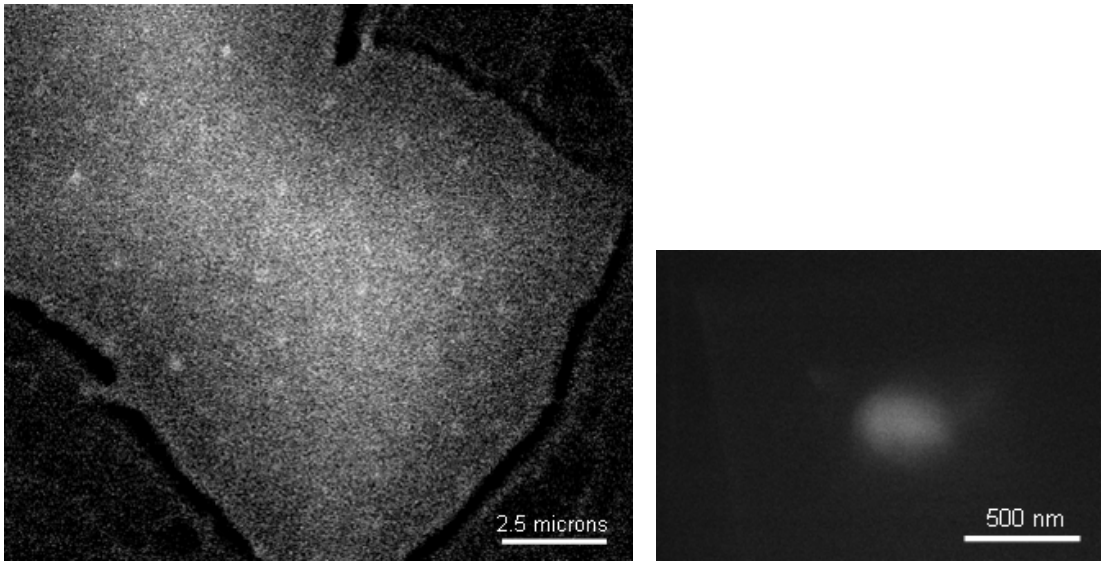

Figure 4.2: (a) Array of platinum nano-particles at 10K in agarose matrix and snapshot of a single particle at 60K magnification.

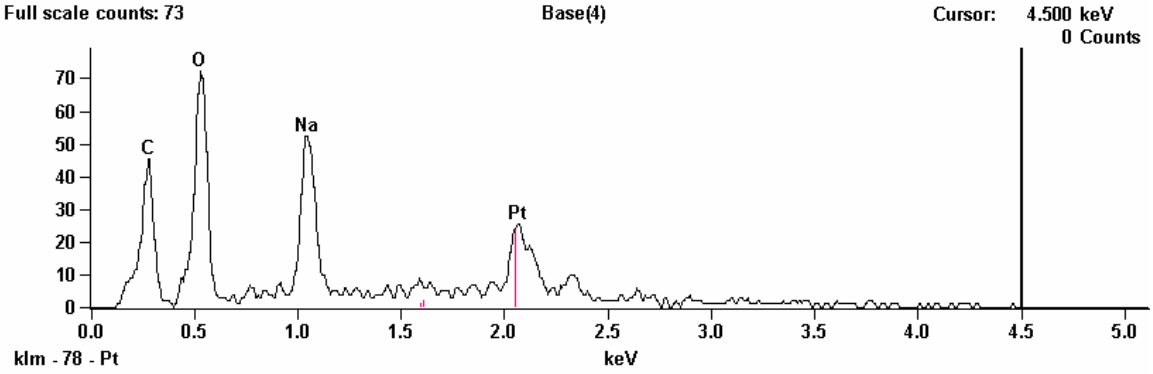

Figure 4.2: (b) EDS spectra of the platinum nano-particle taken at 30KV accelerating voltage (No PtCl peak at 2.62 indicating full reduction of chloro-platinate salt)

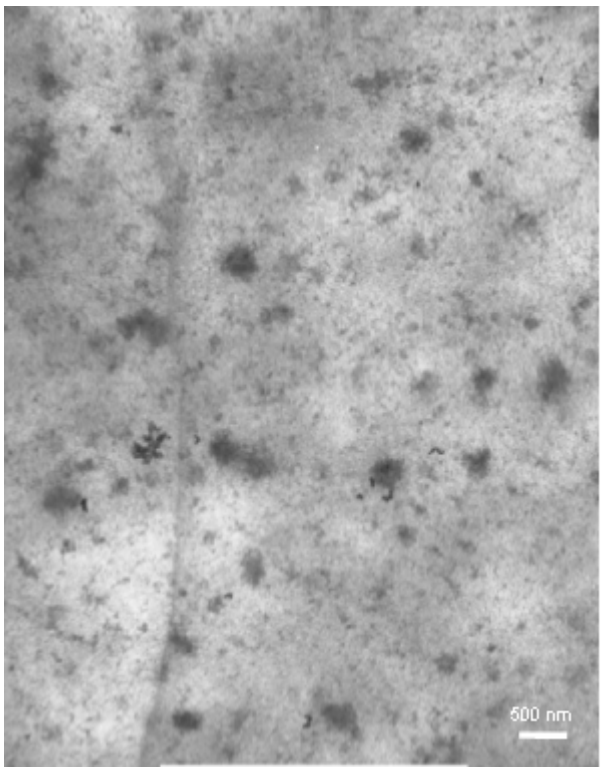

Figure 4.3: TEM image of an agarose membrane doped with Platinum nanoparticles.

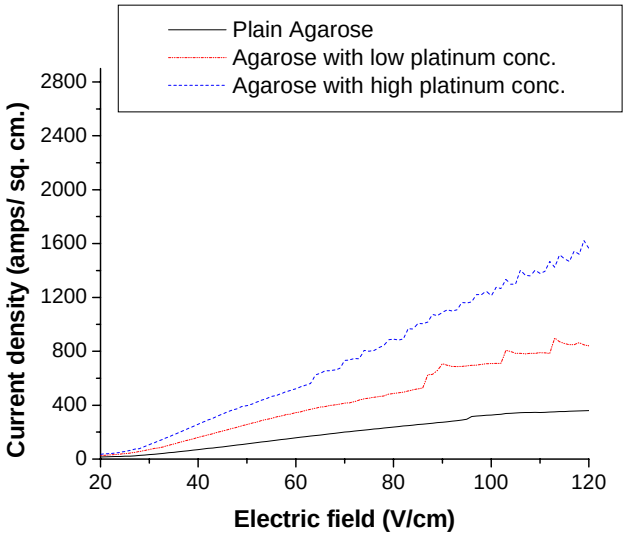

Figure 4.4: Plot between current density (amp/ sq.m.) and electric field (V/m)

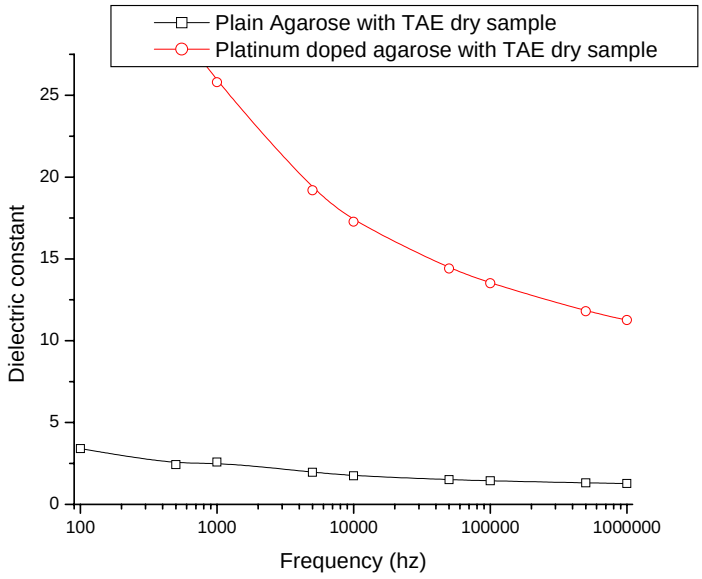

Figure 4.5: Comparison of dielectric constant of the agarose and platinum doped agarose.

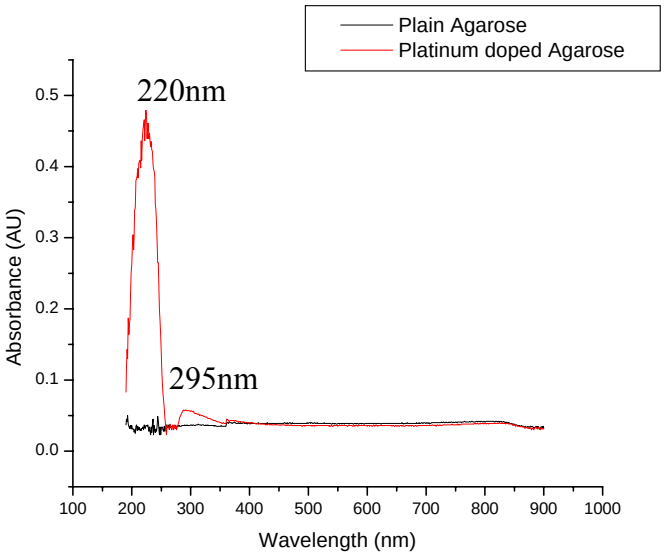

Figure 4.6: Absorption spectra of Platinized and plain agarose.

Applied Voltage	Type of agarose	Time =10mins	Time= 15mins.	Time= 20mins.	Time= 25mins.
200	Undoped	 7.8mm	 13.4mm	 18.7mm	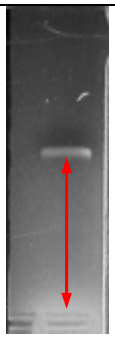 24.7mm
	Doped	 13.1mm	 19.4mm	 27.8mm	 36.6mm

Figure 4.7: Images of the fluorescent band in plain and platinum doped agarose taken at different times for 200V applied voltage

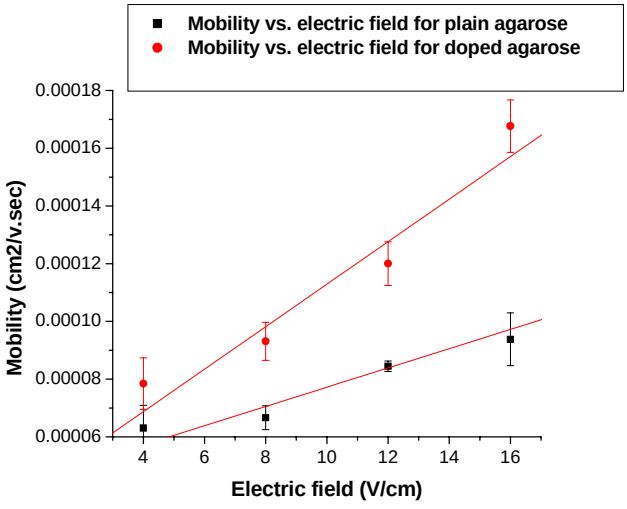

Figure 4.8: Mobility plots for plain and doped agarose.

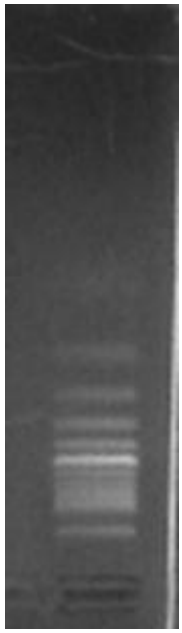

Figure 4.9: Image of a 100-1000 bp gene marker electrophoresed in a platinum doped agarose gel.

Chapter 5

A NOVEL MICRO-FABRICATED CAPILLARY BASED ELECTROPHORESIS SYSTEM

5.1 Abstract

A polydimethyl siloxane (PDMS) glass microchip for capillary electrophoresis that can separate different sizes of DNA molecules in a small experimental scale has been developed. We have used a thermo-responsive polymeric matrix for performing electrophoresis and optical fiber detection with an off chip spectrometer for detecting different molecular sizes.

5.2 Introduction

Capillary electrophoresis technology makes use of ultra-thin capillaries (50-100 microns diameter) filled with different sieving matrices which are mainly composed of non-crosslinked polymer solutions at concentrations above their entanglement threshold, yet dilute enough to get loaded into micro-channels and capillaries without application of excess pressure [1]. Although the resolving power of these gels is somewhat lower than highly cross linked slab gels, these effects can be offset by use of higher electric fields and longer electrophoresis lengths both of which can be achieved by using micro-fabrication techniques. Most micro-fabricated systems are scaled down versions of the conventional capillary electrophoresis technology and are realized by using production-friendly photolithographic techniques routinely employed by the microelectronic

industries. The scaling down in such devices is achieved using a compact design with a dense network of channels thus maintaining the overall free length available for electrophoresis within a very small area or by using shorter separation distance and high resolution matrices [2-5]. As majority of the detection systems associated with capillary electrophoresis are based on fluorescence measurements. Thus, it typically requires bulky optical sources and detectors that pose significant challenge in complete integration of all components on the same planar substrate. For example, the polymerase chain reaction (PCR)- capillary electrophoresis (CE) systems on microchips normally use laser diodes and photomultiplier tubes to perform confocal fluorescence detection. These accessories sometimes pose very tough challenges on the miniaturization process. As on date no complete integrated system is available on the market which points to some of these challenges. In order to address this bottleneck, many groups are investigating the fabrication of fluorescence detection optics directly onto the integrated micro-system that may allow precise positioning of the optical detection hardware in relation to the analyte of interest, removing the necessity for time-consuming alignment procedures as otherwise used in bulky off-chip detection setups.[6-10]. This work focuses on developing a micro-fabricated capillary electrophoresis system with integrated optical detection comprising of an embedded optical fiber and a light emitting diode source. One major concern in our miniaturized version of integrated CE-detector system is the high signal to noise ratio and very low background of the sieving matrix and capillary materials [11]. In order to address these issues, we have developed micro-capillaries using a transparent glass-PDMS micro-fabricated platform. We have found PDMS material to have peak absorption in the infrared region and is by and large optically clear

in the visible and ultra-violet region of the spectrum both of which are important for the intercalating dye Ethydium Bromide (EtBr) used for optical detection of DNA molecules. We have been able to successfully electrophoresce a 100-1000 bp gene marker in 225 micron-sized capillary with an electric field of 78 V/cm using agarose as the sieving matrix. However, there are several challenges of using agarose filled capillaries with on-chip integrated detection, such as the extremely high scattering and background fluorescence. The limit of resolution of slab gel electrophoresis using EtBr has been found as 10ng of sample [12]. The microchip can be easily produced by combination of a replica molding and clean bonding process using a SU8 master. The total time to electrophorese the gene marker on this chip is only 50 secs, which is $1/40^{th}$ the normal time taken in conventional slab gel electrophoresis systems. One limitation of using agarose is the huge scattering as observed by an absorption spectra, which severely affects the signal to noise ratio in case of agarose as the matrix material. As the principal goal of microchip electrophoresis is to reduce the limit of resolution, matrices like agarose would face severe challenges. Because of we have looked into alternate transparent gel matrices with an intention of lowering the limit of resolution. We have found a tri-co-block polymer (F127) which forms a reversible thermo-responsive gel system. This novel gel material possesses less DNA mobility as the agarose matrix; but, it is totally transparent with a extremely low background absorption and scattering. An additional advantage of this material is its lyotropic nature allowing the reusability of our platform.

5.3 Experimental

5.3.1 Fabrication of Micro-Capillaries with PDMS

Micro-capillaries were fabricated in PDMS using photolithography and replica molding techniques. The masks for selective patterning were designed by Adobe illustrator and printed by using a high-resolution printer [Figure 5.1]. The negative photo-resist SU8–2075 was spun onto a cleaned glass wafer of 63.5 mm diameter. The typical thickness of the resist in our experiment was about 225 micron after spinning. The SU8 was next patterned using the mask as shown in figure 5.1 and the inlet/ outlet ports were mounted over the mold with a thin layer of liquid PDMS. These were oven cured at 80 deg. for 5 mins for stability of the ports. This assembly was used to cast the PDMS (GE Silicones RTV 615) up to 2.5 mm thickness. After curing the PDMS cast, the thick edges were removed from the cast. These were then bonded to pieces of 500 microns thick precleaned glass slides (M/s Goldseal) of similar size by oxygen plasma treatment [Figure 5.2]. The blocking PDMS was cleared from the ports before bonding to make continuous channels.

5.3.2 Capillary Electrophoresis in Micro-Channels

Agarose powder was mixed 2% by weight in 5ml 1XTAE buffer solution and was micro-waved for 6secs until the agarose started boiling. The solution became clear on heating which was mixed with 0.1 micro-liter EtBr. A PCR amplified 527 bp product was mixed with a green loading dye and this was loaded at point 1 of the loading channel [see Figure 5.3]. The molten agarose solution was immediately injected into the micro-channel from

point 2(a) with the cross channel ports 1(a) and 1(b) pressurized. The agarose solution encapsulated a part of the loaded sample and before the agarose solidified, it was injected from port 2(b) and the channel was completely filled. The buried sample was moved to a desired location. The agarose in the channel with the buried sample in a predetermined place was left to solidify. The complete solidification was observed by the change in its coloration from white to milky. Two thin platinum wires were put into both ports 2(a) and 2(b) and a DC voltage source was used to establish an electric field. The loaded micro-channel was further characterized by using an inverted fluorescence source and a Kodak digital camera connected to a data acquisition system.

5.3.3 Synthesis of Pluronic Gels

We mixed 22gms of pluronic powder (M/s Sigma Aldrich) in 100ml of 1X Tri-borate (TBE) buffer and cooled this mix in a refrigerator (approx. 4 deg. C). in a large surface area container. The powder started to slowly diffuse into the solution after 30 mins. This could be visualized by the swirls running into the solution from its interface with the floating solid powder (similar to soap powder on water). The solid was allowed to dissolve in the solution at similar conditions for 10 hours until all powder transformed into a single phase and there was no visible un-dissolved F127. We mixed 0.5 micro-liter of EtBr and poured this solution over a gel tray at room temperature and waited for 30mins till it thickened and became immobile. This provided a transparent gel which was used for electrophoresis of DNA at 200V DC voltage. A similar UV set up was used for characterization of the movement of stains through this gel. The stain mobility was calculated and compared with that of agarose.

5.3.4 Fluorescence and Absorption Studies of Different Gels

Three different gel materials plain agarose, synergel and sea plaque (low melting point) agarose powders were dissolved 2% by weight in 100 ml 1X Tri-acetate (TAE) buffer and micro-waved for 3 mins. until all the powder state was dissolved resulting in a homogenous mix. We also found the emission and excitation wavelengths of the EtBr at different concentrations using a JASCO spectro-fluorometer.. We used 0.5 micro-liter of EtBr in these solution and characterized these on the spectro-fluorometer and a Shimadzu UV-Vis spectrometer for obtaining various spectra of these materials and also compared them with the new F127 polymer gel.

5.4 Results and Discussion

5.4.1 Capillary Electrophoresis Using Agarose

The devices were first loaded with 100-1000 bp DNA ladder (Promega, Madison, WI, USA) marked with the green loading dye using the cross channel and a procedure that has been described earlier. After loading the ladder through the cross channel the agarose was pushed through the port 2(a) and 2(b) using agarose solution and the sample was positioned as a plug in main channel [Figure 5.4]. We used several different agarose concentrations ranging from 1.0 to 2.5% and found that the agarose took excess curing times at lower concentrations and had a greater chance of bubble formation. [Figure 5.5] At higher concentrations (2 and 2.5 %) it cured too fast in comparison to the time taken by the twin port loading process, thus blocking the capillary and making discontinuously filled channels which did not show any electrophoretic behavior. Also, bubbles and other

inclusions changed the electric field within the capillaries drastically and there was no observable electrophoretic effect and the DNA ladder effectively moved as a plug.

Thus at lower percentage of agarose the capillary was not able to resolve the ladder properly. We investigated various operating voltages in the successfully loaded capillaries and found 300 V (Electric field= 78 V/cm) to be sufficient for electrophorescing the sample in the capillary. We observed a plug like movement of a 100-1000 bp gene marker [Figure 5.6(a)] for approx. 45 secs. The separation was completed at the end of 50 secs [Figure 5.6(b)]. Conventional slab gel techniques are able to electrophorese gene markers of similar size ranges in around 35 mins at 16 V/cm. Thus, we have obtained a reduction in the time of electrophoresis by a factor of 40 by using a 225 micron capillary. We have further investigated the electrophoresis in a nano-platinum doped agarose matrix [14] by using a lower voltage as detailed is Chapter 4.

5.4.2 Limit of Resolution of Agarose Gels Using Slab Gel Electrophoresis

A DNA solution with 527 bp was electrophoresced using agarose slabs. The portion of the slab containing the 527 bp band was dissolved in a membrane solution and passed through silica filters [15]. The DNA was separated from the dissolved agarose by centrifugation through the silica filters. An elution buffer was used to extract the DNA from the silica membrane. Absorbance studies were performed on this solution to get the DNA concentration and purity of solution and a solution of double stranded (ds) DNA in elution buffer was prepared with 50 ng/ micro-liter concentration. This master sample was diluted to 10^{th}, 100^{th}, 1000^{th}, 10000^{th} and 100000^{th} dilution and thus the resulting concentrations were 0.5, 0.05, 0.005, 0.0005 and 0.00005. These known concentrations

were tested in standard agarose gel beds with known quantity of Ethidium Bromide to detect the limit of detection on the standard gel bed. This gel bed could detect upto 10ng of DNA sample [Figure 5.7]. However agarose, being milky in nature, possesses a huge background fluorescence and scattering. As two main requirements of our micro-fabricated capillaries are minimal background and a possibility of reusability, we chose thermo-responsive polymer pluronic (F127) for our micro-fabricated capillary studies [16].

5.4.3 Pluronic Gels

The pluronic gel was prepared by varying different weight % of F127 powder in 1X TBE buffer. The literature has widely reported pluronic to be a thermo-responsive polymer. The pluronic is a tri-co-block polymer which contains polyethylene oxide (PEO) and polypropylene oxide (PPO) in the following orientation $(EO)_{106}(PO)_{70}(EO)_{106}$ [17]. Above a critical concentration and temperature, the pluronic polymers associate into micelles [Figure 5.8] as the hydrophobic effect drives the (PO) segment of the molecule into the nearly water-free central core surrounded by hydrated (EO) tails. [18-20]. Liquid crystalline phases form at high solution concentrations to minimize the volume excluded by spherical or columnar micelles [21,22]. Figure 5.9 shows the sol-gel-sol phase transition curve for pluronic gels indicating the concentration versus temperature effects [23]. The curve indicates the formation of gels at room temperature above 21 wt. % concentration. The gels turn into solution phase at a temperature of approximately 65 deg. C at the higher side. We plan to install micro-heaters beneath the microchip to melt the gel phase back into sol phase and pump this out completely for refills with new

solution. We have also investigated the structural stability of these gels for the purpose of slab gel electrophoresis with an intention of carving gel pockets for sample loading and observed a very replicable shape retention above 22 wt. %. [Figure 5.10]. We used 22% for all our gel studies.

5.4.4 Fluorescence and Absorption Studies of Gels

The fluori-meter scans on a 0.002 volume % Ethidium Bromide (EtBr) solution in 1X TAE buffer indicated the absorption maxima of the dye at 280, 300 and 480 nm [Figure 5.11]. The corresponding emission maxima was observed at 620 nm [Figure 5.12]. The wavelength of 480nm was consequently chosen as the excitation maxima as this would result in a secondary peak from diffraction grating at 760nm not interfering with the emission peak of EtBr. We plan to use the same frequency for all on chip studies using LED's and an ocean optics bench-top spectro-fluorometer. We have investigated the fluorescence spectra of agarose doped with 0.001% EtBr by volume and found a huge background fluorescence causing a plateauing around the region 600nm to 700nm [Figure 5.13]. We hypothesize that this plateauing effect resulted from a background fluorescence from the agarose and/ or, due to a very weak signal to noise ratio because of huge scattering of light. The cured agarose sample was milky white. We cleared this gel by using Synergel which is an agarose additive and a clarifier and Seaplaque gel which is a low melting agarose. We also took absorption spectra of all these gels to find out the ability of the gel to resolve the 0.001% EtBr. Figure 5.11 shows the absorption spectra of EtBr in 1X TAE buffer solution. The scan was started from 400nm as the plastic cuvette used in this case showed strong absorption below 400nm. On performing the UV-Vis

spectroscopy we found this new gel to clearly resolve the 480nm absorption peak of the EtBr dye. We did not use the other excitation maximas because of variable absorption of plastic cuvette holder at lower wavelengths. Figure 5.14 shows a comparative plot of absorption vs. wave-number for different grades of agarose and F-127 (pluronic). The agarose, synergel and seaplaque have a very high absorption level in comparison to the F127 in the 480nm wavelength (absorption peak of EtBr). Thus the spectra was not able to resolve this absorption at 480nm for agarose, synergel and seaplaque agarose. The florescence data for all gels indicate an inability for all the agarose samples to resolve the 0.001% EtBr [Figure 5.15]. However, the F127 was able to resolve this low concentration of EtBr. In order to find out the absorption wavelengths we performed an excitation scan of the agarose, synergel, seaplaque and F127 samples loaded with EtBr. Table 5.1 indicates the various absorption wavelengths for all these samples. The best scans were found to be at 461nm for agarose, synergel and sea plaque and at 509nm for F127. Since EtBr has an emission peak at 622nm region therefore all other excitation wavelengths have a secondary peak very close to the EtBr range which explains the explains the best resolution at higher (461nm and 509nm) wavelengths respectively.

5.4.5 Comparative Mobility Studies of F127 and Agarose Gels

The comparative study of ds DNA mobility has been performed between the pluronic and agarose gels. Although the transparency of F127 slab gel results in excellent optical characterization, we have observed that the mobility (calculated using the one dimensional mobility model as illustrated in Chapter 3) of the stains reduce to 55% of that in cross-linked agarose [Figure 5.17, Table 5.2]. We plan to doped this new gel

material with platinum nano-particles to increase its mobility keeping the optical properties similar in a future endeavor.

5.5 Conclusions

We have demonstrated capillary electrophoresis on chip using cross-linked agarose. We have observed electrophoresis of a 100-1000 bp gene marker by applying a 78 V/cm DC voltage in 50 secs. There is a huge background fluorescence and scattering problem in all agarose gels due to its milky nature. We have investigated a thermo-responsive alternate completely transparent gel material. We plan to use the nano-particle doping technique developed in Chapter 3 to increase mobility at lower electrophorescing voltages using this new gel material. The reusability of this platform will be investigated in our future endeavors.

5.6 Acknowledgements

The authors gratefully acknowledge the financial support from the National Pork Board and National Institute of Health to carry out this research. The authors deeply acknowledge the help obtained from Darcy Lichlyter, Research Scientist, Biological Engineering Department and Rosalyn Manor, Graduate student, Biological Engineering Department for fluorescence characterization of gel materials.

5.7 References

1. V.M. Ugaz, R.D. Elms, R.C. Lo, F.A. Shaik, M.A.Burns, " Micro-fabricated electrophoresis systems for DNA sequencing and genotyping applications: current technology and future directions", *Phil. Trans. R. Soc. Lond. A*, Vol. 362, pp. 1105-1129, 2004.
2. C.T. Culbertson, S.C. Jacobson, J.M. Ramsey, "Dispersion sources for compact geometries on microchips", *Analytical Chemistry*, Vol.70, pp. 3781-3789, 1998.
3. S.K. Griffiths, R.H. Nilson, " Low dispersion turns and junctions for micro-channel systems", *Analytical Chemistry*, Vol. 73, pp.272-278, 2001.
4. T.J. Johnson, D. Ross, M. Gaitan, L.E. Locascio, " Laser modification of performed micro-channels: application to reduce band broadening around turn subject to electro-kinetic flow", *Analytical Chemistry*, Vol.73, pp.3656-3661, 2001.
5. J.I. Molho, A.E. Herr, B.P. Mosier, J.G. Santiago, T.W. Kenny, R.A. Brennen, G.B. Gordon, B. Mohammadi, "Optimization of turn geometries for microchip electrophoresis", *Analytical Chemistry*, Vol. 73, pp. 1350-1360, 2001.
6. J. C. Roulet, R. Volkel, H. P. Herzig, E. Verpoorte, N. F. de Rooij, R. Dandliker, "Performance of an integrated micro-optical system for fluorescence detection in micro-fluidic systems", *Analytical Chemistry*, Vol.74, pp.3400- , 2002.
7. M. L. Chabinyc, D. T. Chiu, J. C. McDonald, A. D. Stroock, J. F. Christian, A. M. Karger, G. M. Whitesides, An integrated fluorescence detection system in poly(dimethylsiloxane) for micro-fluidic applications, *Analytical Chemistry*, Vol. 73, pp. 4491- , 2001.

8. V. Namasivayam, R. S. Lin, B. Johnson, S. Brahmasandra, Z. Razzacki, D. T. Burke, M. A. Burns, "Advances in on-chip photo-detection for applications in miniaturized genetic analysis systems", *Journal of Micromechanics and Microengineering*, Vol. 14, pp. 81- , 2004.

9. E. Thrush, O. Levi, W. Ha, G. Carey, L. J. Cook, J. Deich, S. J. Smith, W. E. Moerner, J. S. Harris, "Integrated semiconductor vertical-cavity surface-emitting lasers and PIN photodetectors for biomedical fluorescence sensing", *IEEE Journal of Quantum Electronics*, Vol. 40, pp. 491-495 , 2004.

10. T. Kamei, B. M. Paegel, J. R. Scherer, A.M. Skelley, R. A. Street, R. A. Mathies, "Integrated hydrogenated amorphous Si photodiode detector for microfluidic bioanalytical devices", *Analytical Chemistry*, Vol. 75, pp.5300- ,2003.

11. J.W. Hong, K. Hozokawa, T. Fujii, M. Seki, I. Endo, " Micro-fabricated polymer chip for capillary gel electrophoresis", *Biotechnology Progress*, Vol. 17, pp. 958-962, 2001.

12. Application note, "Fluorescent DNA gel stain detection", www.amershambio sciences.com.

13. S. Bhattacharya , A. Datta, J.M. Berg, S. Gangopadhyay, "Studies on surface wettability of Poly dimethyl siloxane and glass under Oxygen plasma treatment and their correlation to bond strength", *Journal of Microelectromechanical systems*, Vol. 14, No.3, 2005.

14. S. Bhattacharya, N. Chanda, S.A. Grant, K. Gangopadhyay, S. Gangopadhyay, P.R. Sharp, "High conductivity agarose nano-platinum composites**",** (In preparation).

15. Personal communication with Dr. S.B. Kleiboeker, Veterinary Diagnostic Laboratory, College of Veterinary Medicine, University of Missouri, Columbia, MO.
16. C.W. Kan, C.P. Fredlake, E.A.S. Doherty, A.E. Barron, "DNA sequencing and genotyping in miniaturized electrophoresis systems", *Electrophoresis*, Vol. 25, pp. 3564-3588, 2004.
17. R.L. Rill, B.R.Locke, Y. Liu, D.H.V. Winkle, " Electrophoresis in lyotropic polymer liquid crystals", *Proc. Natl. Acad. Sci., USA.*, Vol.95, pp. 1534-1539, 1998.
18. K. Mortensen, W. Brown, B. Norden, "Inverse melting transition and evidence of 3-dimensional cubatic structure in a block copolymer micellar system", *Physical Review Letters*, Vol. 68, pp.2340-2343, 1992.
19. P. Linse, "Phase Behavior of Poly(ethylene oxide)-Poly (propylene oxide) Block Copolymers in Aqueous Solution", *Journal of Physical Chemistry*, Vol. 97, pp.13896-13902, 1993.
20. P. Linse, M. Malmsten, "Temperature-Dependent Micellization in Aqueous Block-Copolymer Solutions", *Macromolecules*, Vol. 25, pp. 5434-5439, 1992.
21. M. Malmsten, B. Lindman, "Self-Assembly in Aqueous Block Copolymer Solutions", *Macromolecules*, Vol. 25, pp. 5440-5445, 1992.
22. G. Wanka, H. Hoffmann, W. Ulbritch, "Phase Diagrams and Aggregation Behavior of Poly (ox yethy1ene)-Poly (oxypropylene) -Poly(oxyet hylene) Triblock Copolymers in Aqueous Solutions", Vol. 27, pp.4145-4149, 1994.

23. M.S. Shim, H.T. Lee, W.S. Shim, I. Park, H. Lee, T. Chang, S.W. Kim, D.S. Lee, "Poly(D,L-lactic acid-*co*-glycolic acid)-*b*-poly(ethylene glycol)-*b*-poly (D,L-lactic acid-*co*-glycolic acid) triblock copolymer and thermoreversible phase transition in water", *Triblock copolymers and thermoreversible phase transition in water*, Vol. 12, pp. 188-196, 2001

5.8 Figures

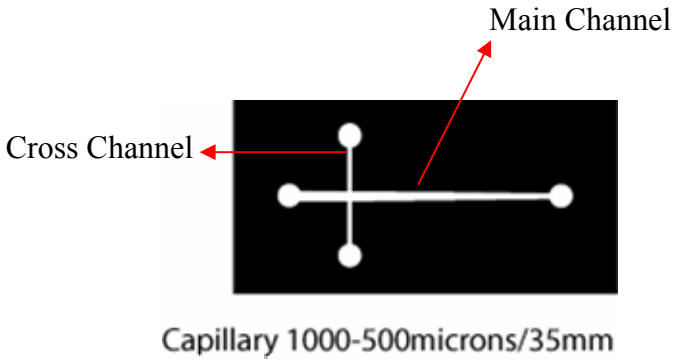

Fig. 5.1: Mask for micro channel electrophoresis

Fig. 5.2: Glass PDMS micro-channel structures for capillary electrophoresis.

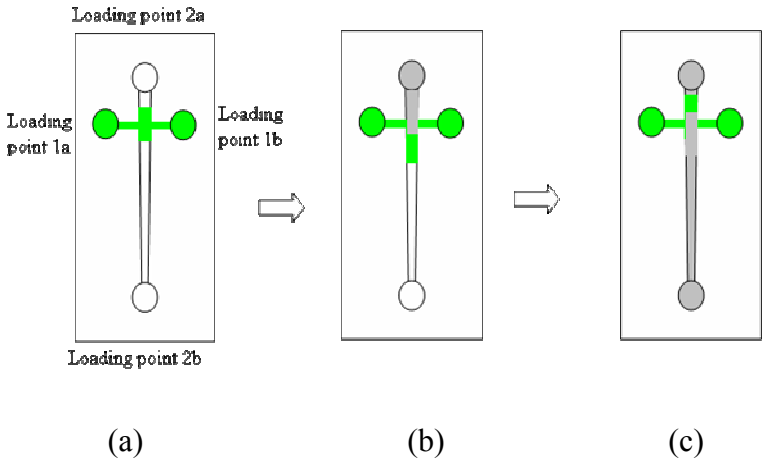

Fig. 5.3: (a) sample loading from port 1a. (b) port 1a and b pressurized and agarose melt loaded from 2a (c) agarose melt injected from port 2b and sample buried in the agarose by room cooling of the microchannel.

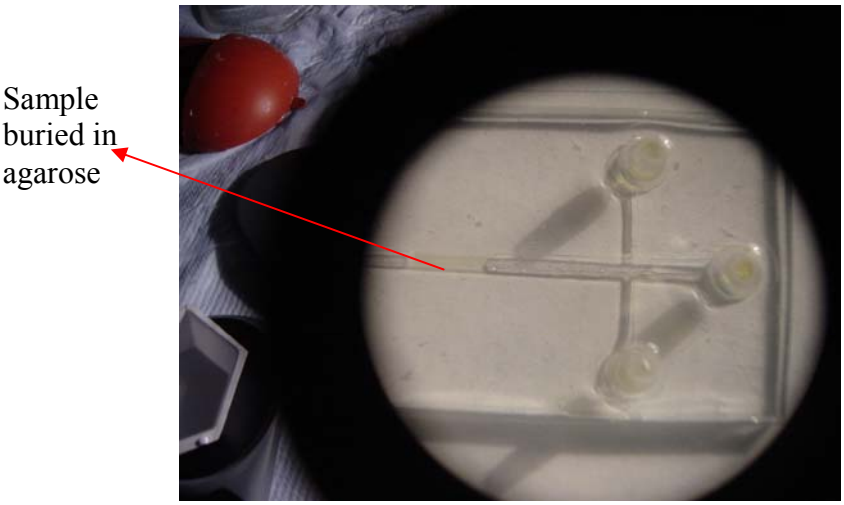

Fig. 5.4: Capillary loaded with agarose burying the sample

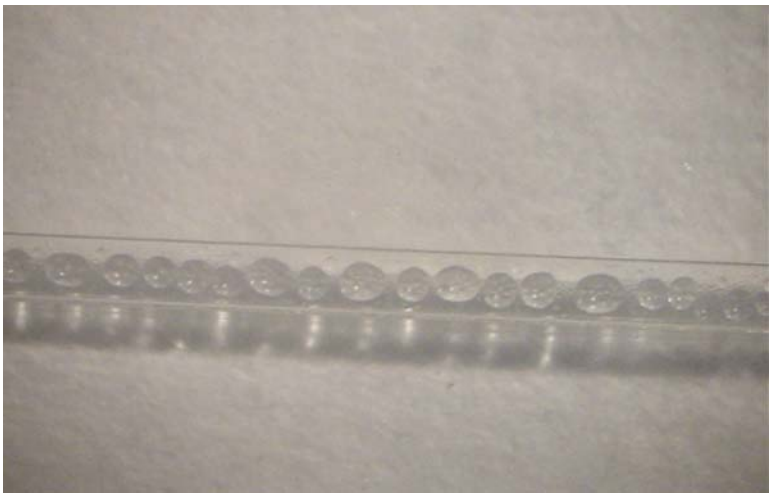

Fig.5.5: Bubbles entrapped in capillaries

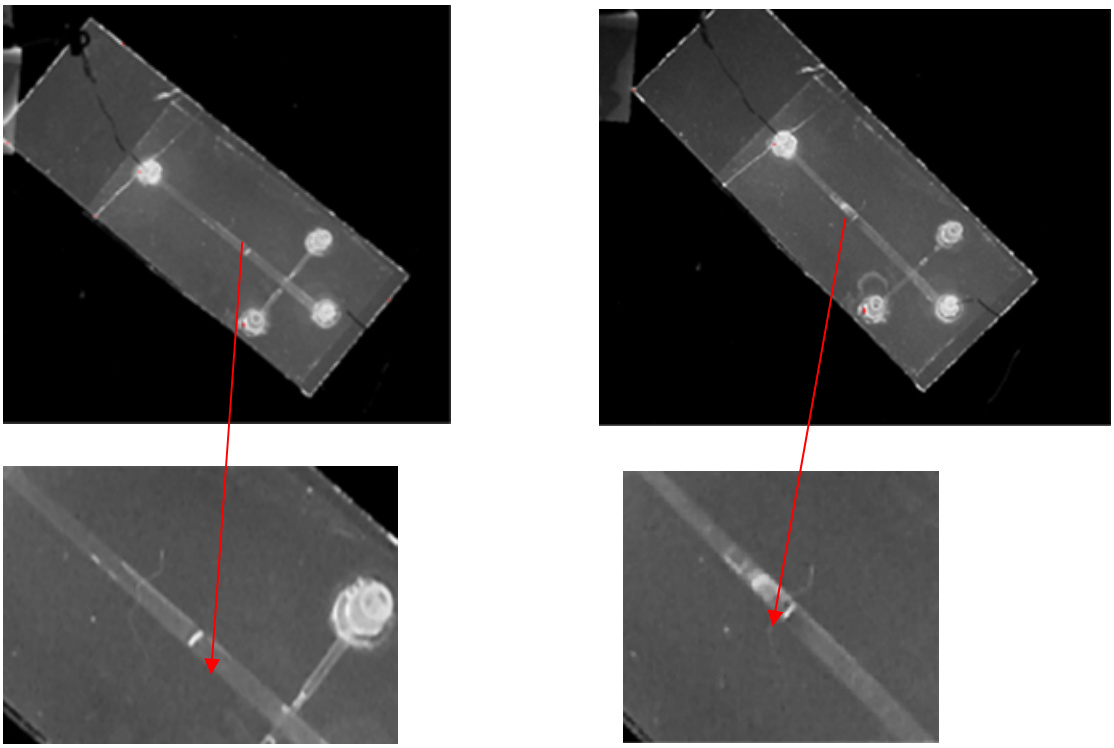

(a) (b)

Fig.5.6: (a) Movement of a 100-1000 bp gene marker captured in an UV detection setup after 25 secs.(b) electrophoresis of gene marker between 45 and 50 secs. (300 V DC is applied).

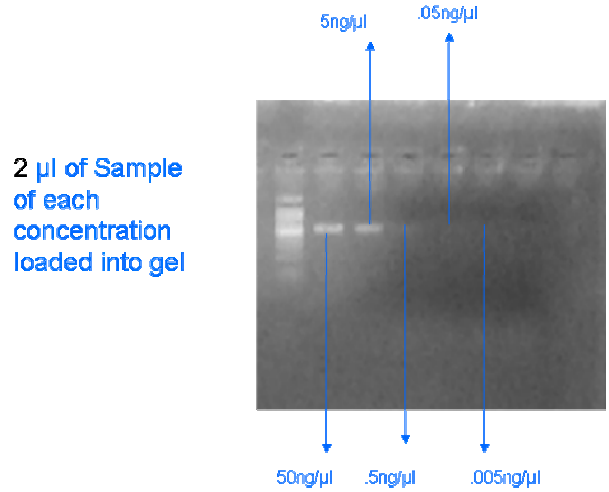

Figure 5.7: Limit of Detection of Agarose Gel using EtBr (10ng of DNA)

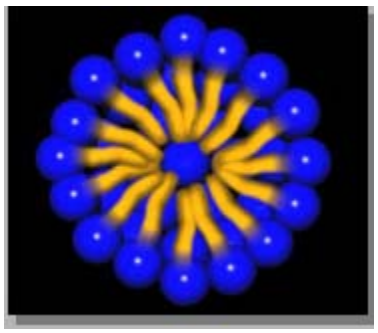

Fig. 5.8: Micelle formation of Pluronic molecules in 1X TBE buffer.

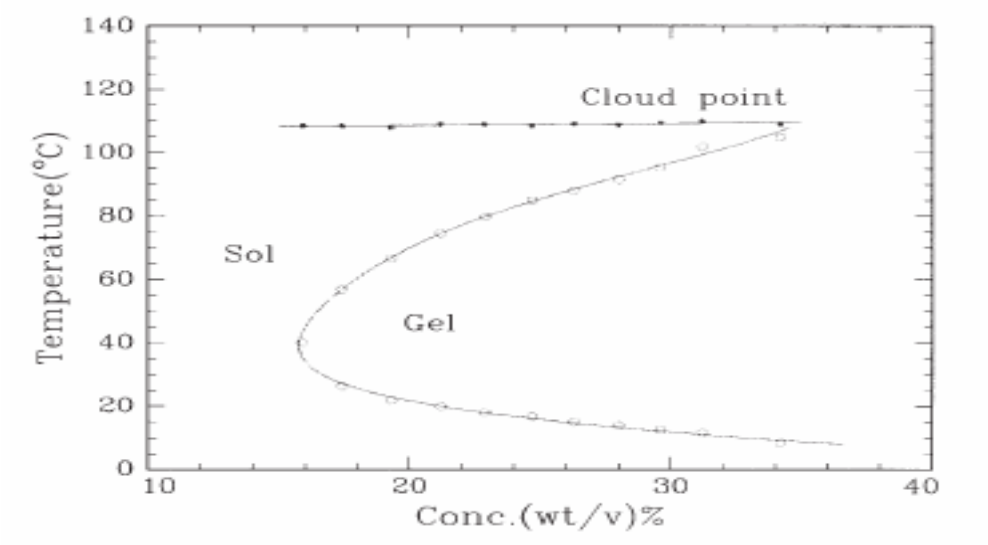

Fig. 5.9: Phase transition curve for F127 molecules.

No retention of carvings
and distortions

Fig. 5.10: Mechanical stability of F127 gels. (22% onwards the gel is able to retain its deformations)

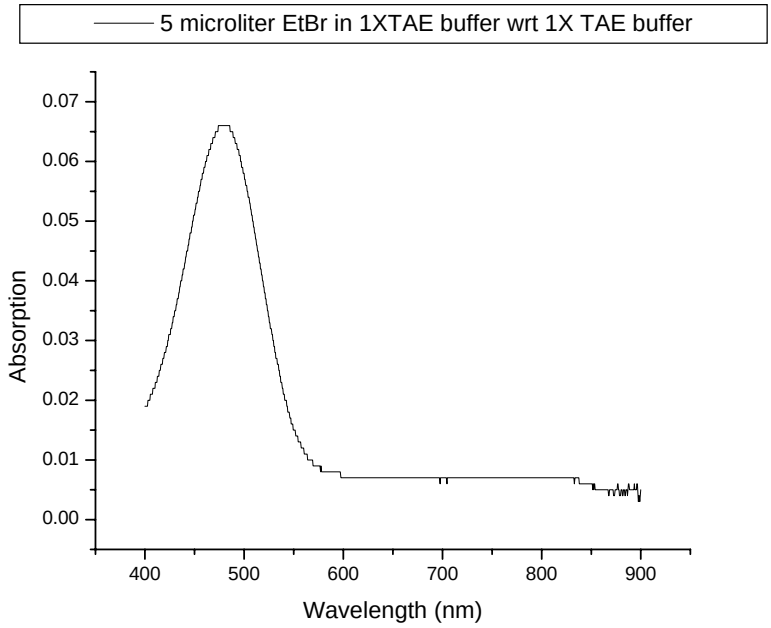

Fig. 5.11 Absorption spectra of EtBr in 1X TAE buffer (absorption peak at 480nm)

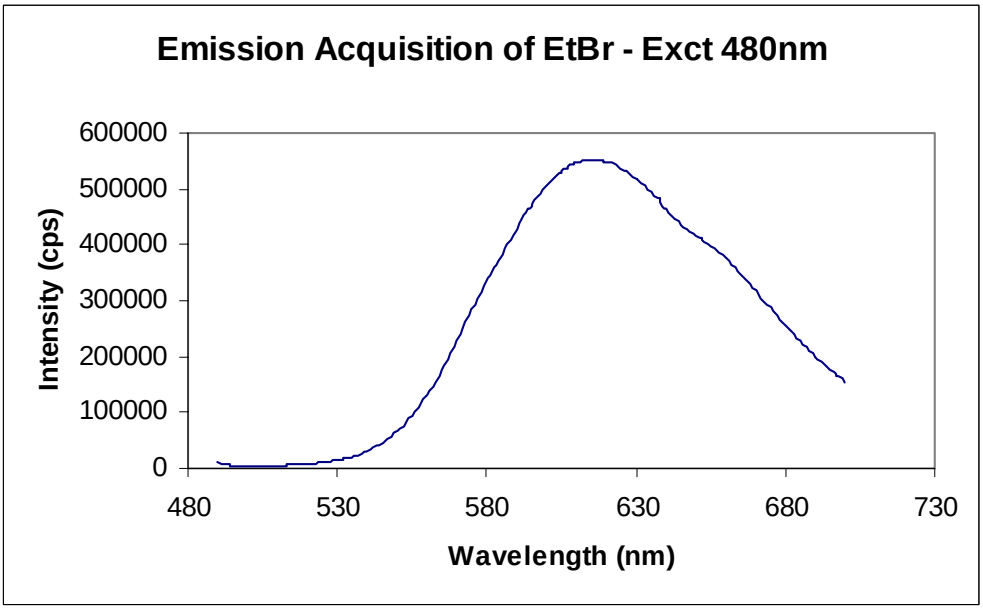

Fig. 5.12: Emission peak of EtBr (emission maxima at 620nm).

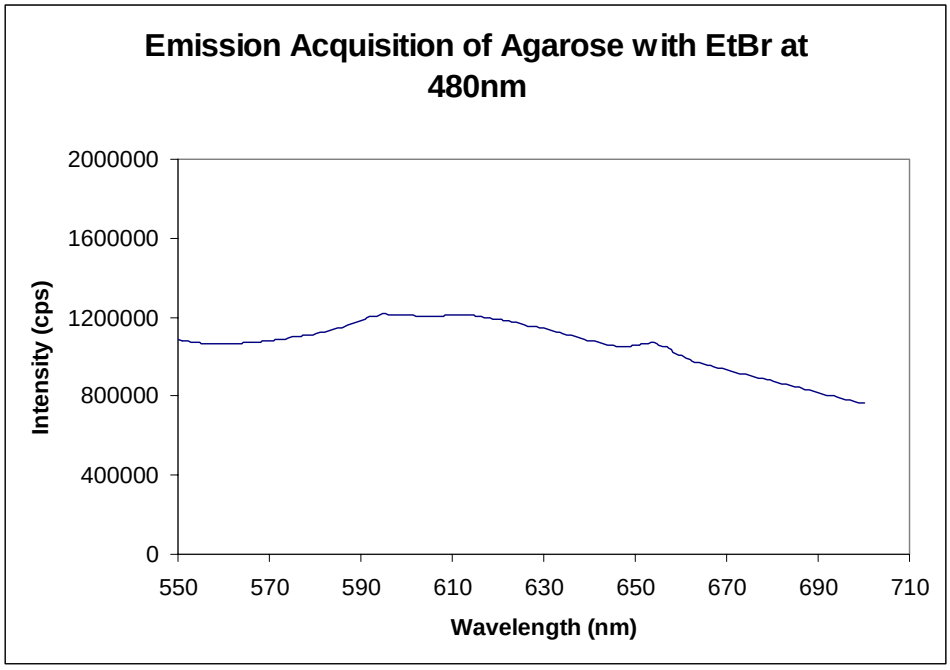

Fig. 5.13: Emission acquisition of agarose with EtBr at 480nm excitation (Plateauing observed due to high scattering and background fluorescence)

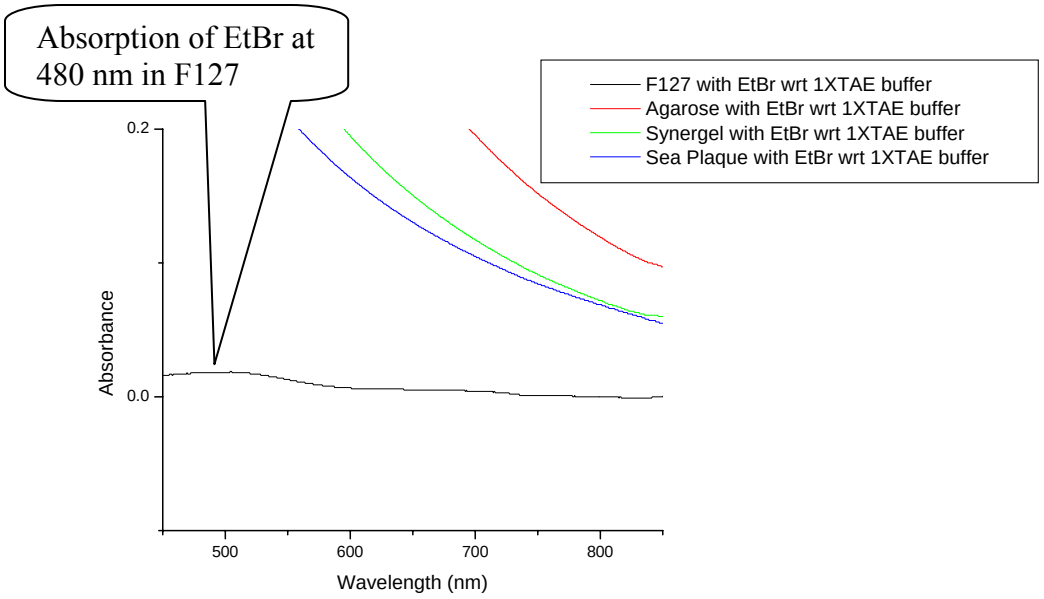

Fig. 5.14: Absorption spectra of EtBr doped Agarose, synergel, sea-plaque and F127 using UV-Vis. Note the high scattering of agarose and its versions in comparison to F127

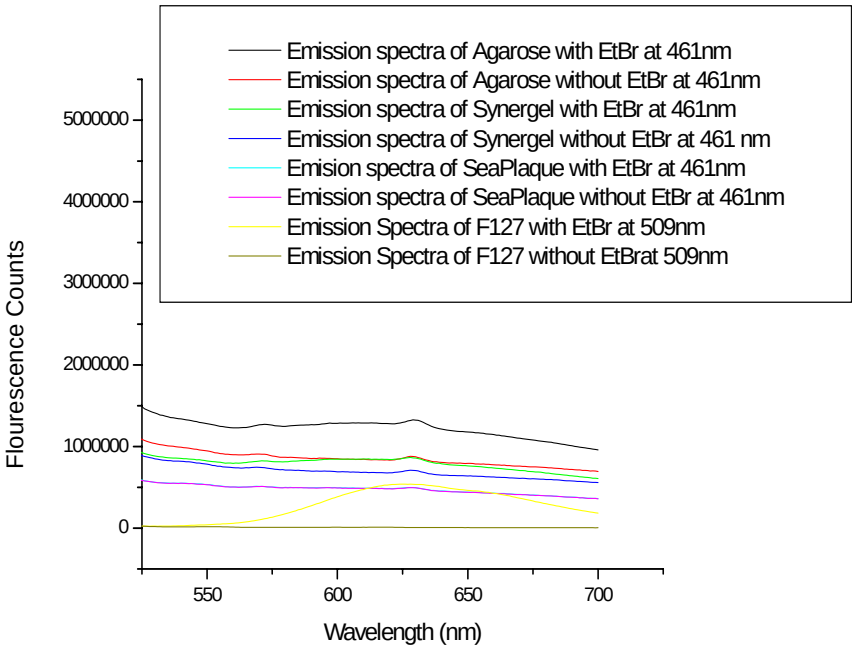

Fig. 5.15: Fluorescence spectra of EtBr in agarose, synergel, sea-plaque and F127.

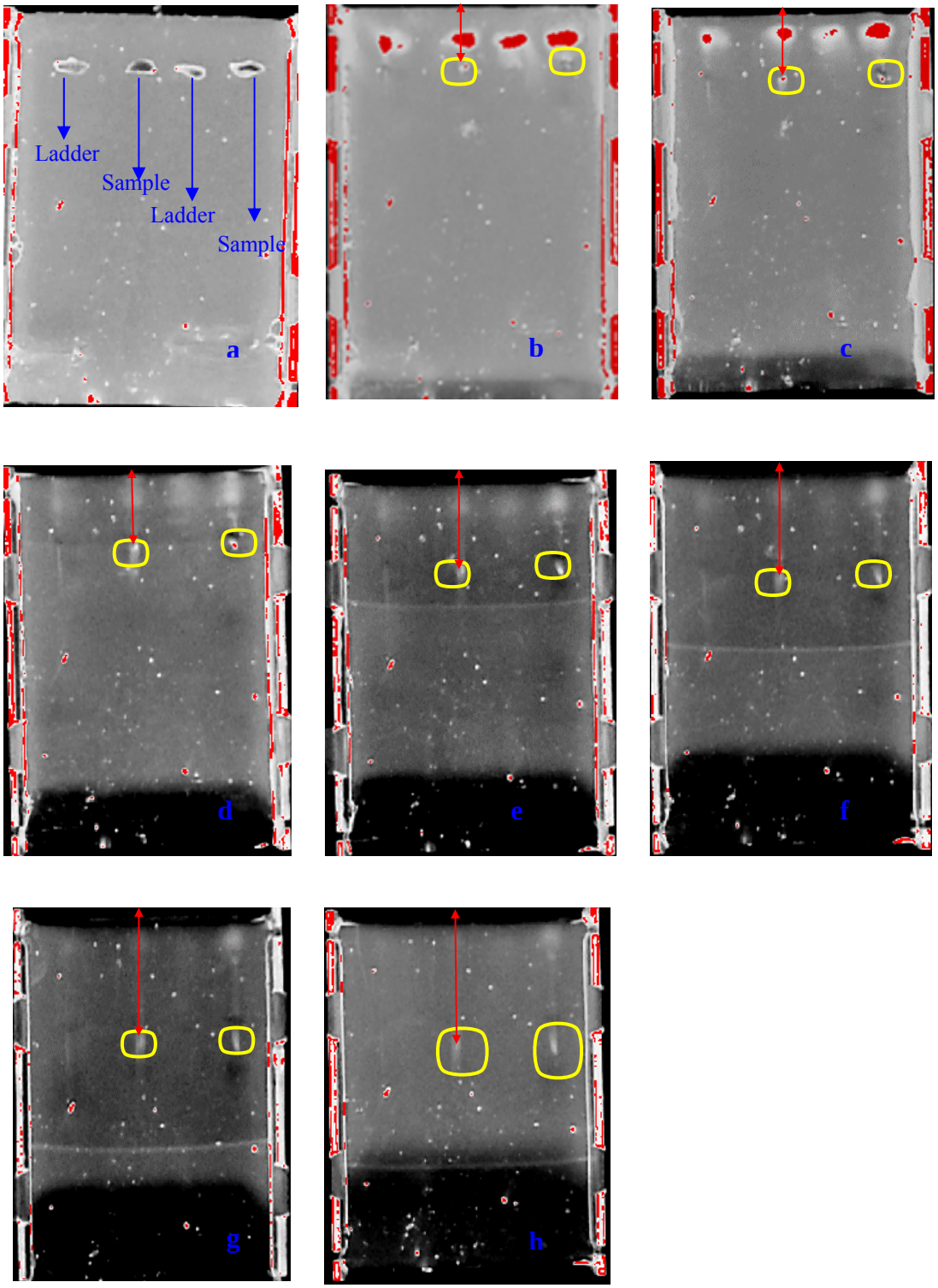

Fig. 5.16: Gel images at times(a)0, (b)15, (c)30, (d)45, (e)60, (f)75, (g)90, (h)105 minutes respectively using F127 as sieving media at an operating voltage of 200V.

Table 5.1: Absorption wavelengths of various gel materials:

Agarose Excitation	Synergel Excitation	Seaplaque Excitation	F127 Excitation
353nm	353nm	353nm	312nm
383nm	381nm	381nm	326nm
461nm	461nm	461nm	509nm

Table 5.2: Mobility calculations in agarose and F127 gels.

Gel Material	Distance Moved (mm)	Time of movement (secs.)	Velocity (cm/ sec)	Electric Field (V/cm)	Mobility (cm2/V.sec.)	Average Mobility	Std. Dev.
Agarose	7.82	600	.001302	16	8.13E-5	9.38E-5	9.15E-6
	13.43	900	.001493		9.33E-5		
	18.75	1200	.001562		9.76E-5		
	24.68	1500	.001645		.000102		
F127 (Pluronic gel)	5.81	900	.000647	14.4	4.48E-5	4.59E-5	5.67E-6
	9.84	1800	.000547		3.79E-5		
	20.57	2700	.000762		5.29E-5		
	27.28	3600	.000757		5.26E-5		
	30.86	4500	.000685		4.76E-5		
	34.89	5400	.000646		4.48E-5		
	36.68	6300	.000582		4.04E-5		

Ratio between mobilities in the two sieving media = .555

Chapter 6

CONCLUSION AND FUTURE DIRECTIONS

6.1 Conclusion and Future Directions

We have optimized the micro-fabrication and design process of a PDMS-SOG-Silicon on-chip DNA amplifier for amplification of a 527 fragment of the IBR virus genome using a 51 cycle PCR process. The chip is extremely durable and can be thermally cycled for a significant amount of time without any damaging thermal stresses, which is a main reason for failure of Glass PDMS micro-chambers. We have further developed a serpentine heater design by numerically solving a two dimensional steady state heat conduction equation. This new heater design has been compared to an equi-sized thin continuous film which has been used in many on chip PCR chamber designs in prior work. There is a considerable increase in the ramp up and down rate with the serpentine design over its continuous counterpart. We have also developed a new regime of PDMS to SOG bonding. We performed the contact angle, bond strength study for SOG-PDMS bonding leading to the development of a set of exposure parameters for maximum bond strength. This maximum bond strength is 83 psi using the standardized blister test, higher than glass-PDMS and PDMS-PDMS bonds. We have also investigated bonding of PDMS to silicon dioxide substrates using SOG as an intermediate layer. We have also traced a fast recovery of SOG surface with an increase in post exposure relaxation time, a condition which provides a hydrophobic surface so that the DNA does not stick to the chamber walls. ATR-FTIR results confirmed this temporal recovery as well. A similar behavior occurred in the PDMS surface. The recovery could be an effect of surface chain

scission reactions on the PDMS or SOG surface. The developed chip can be a multiple use type of platform for PCR runs as strengthened by fluorescence studies. We have future plans to carrying out sequential amplification of positive and negative samples on the same test chip with an inbetween thorough washing step. We reduced the ramping up and down time for the 51 cycle process to an order of magnitude less than that required in a conventional setup. The PDMS silicon chip developed in our work is a first step towards the fabrication of an inexpensive DNA microanalysis platform for fast and accurate identification of target molecules and will be able to provide an assay for field applications. We have further developed a novel doping technique of agarose gels with nano-platinum dispersions which results in a two fold mobility enhancement. The increased mobility is primarily due to the increase in the dielectric properties of the agarose platinum composite. We have further performed capillary electrophoresis on a chip using agarose matrix. The capillary is able to resolve a 100-1000 bp DNA ladder with a voltage of 300V at 50 secs. operating time. This time is $1/40^{th}$ the time of electrophoresis of a similar ladder taken by conventional slab gel electrophoresis. We have further developed a lyotropic gel material with lesser sample mobility but an enhanced signal to background ratio due to lower background fluorescence and scattering. We also plan to design a micro total analytical system by integrating micro-fluidic, optical and electronic parts to the same chip. Figure 6.1 shows a schematic of such a setup. It consists of a micro-PCR chamber, micropumps, and microheaters. Additional components of the device include gel electrophoresis micro-channels and solid core waveguide fluorescence collectors. The post PCR mix will be transported from the PCR chamber “A” into the gel channel “C” using peristaltic pump set “B”. A set

of sputtered platinum heaters will be used as electrodes across the gel channel, which will provide transportation of the amplified sample across fixed distances in the horizontal length scale. An array of waveguides, "D" , spatially located on the basis of the standardized distance traversed by the target base pairs will pick up the fluorescence response and transport it to an off-chip spectrometer, confirming the presence of the target. The successful development of this lab-on-a-chip device will have several advantages over conventional bench top systems, which primarily include an overall reduction in size, reduced use of reagents, decreased power requirements, increased speed and accuracy of analysis, and increased portability for field use. We envision this assay as a highly sensitive analyzer tool with a capability to detect trace samples with high accuracy.

6.2 Figures

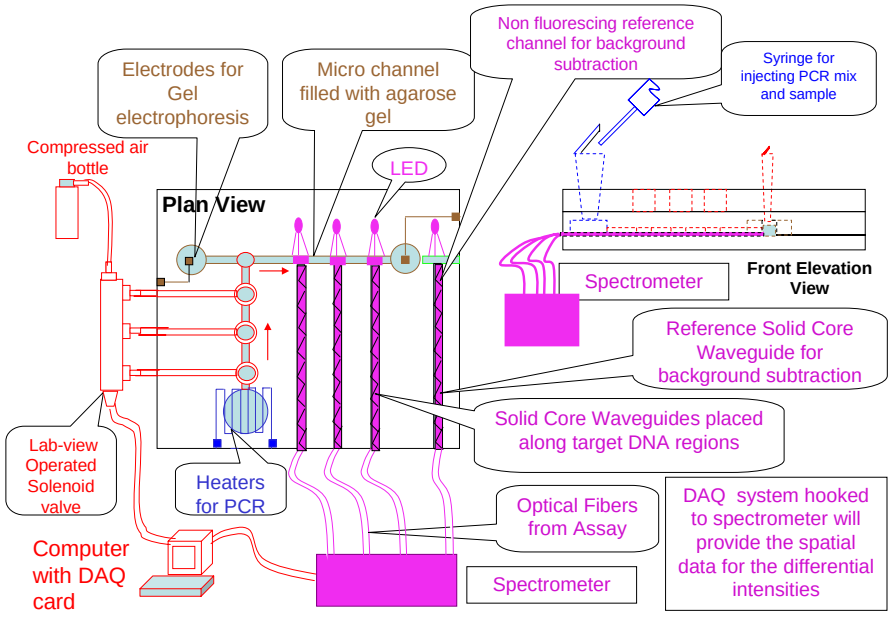

Fig. 6.1 Plan view and side elevation of DNA micro-analyzer.

VITA

Shantanu Bhattacharya was born March 23rd , 1974, in Krishangar , West Bengal, India. He received his B.S. degree in Industrial and Production Engineering from the University of Delhi, New Delhi, India, in 1996 and M.S. degree in Mechanical Engineering from Texas Tech University, Lubbock, in 2003. He has very recently completed his Ph.D. degree in Biological engineering with the University of Missouri at Columbia. He has been selected in the Chancellor's list in 2004 and 2006. Apart from this his research has also won him several accolades particularly in the Missouri Life-science Week 2004 and Research Creative Activities Forum 2006. Before joining the Masters programme, Shantanu, worked with Suzuki Motors Corporation as a Senior Engineer from 1996 to 2002 in various capacities and different areas. His current research interests include design and development of micro-fluidic platforms for biosensor applications, material science, nanotechnology and novel nano-energetic material synthesis and testing.